2009-01-01

Estimating Variation in Stiffness and Volume Change of Clays from Geochemical and Index Properties

Cynthia Roxanna Zuniga
University of Texas at El Paso, crzuniga@miners.utep.edu

ESTIMATING VARIATION IN STIFFNESS AND VOLUME CHANGE OF CLAYS FROM GEOCHEMICAL AND INDEX PROPERTIES

CYNTHIA R. ZUNIGA

Department of Civil Engineering

APPROVED:

Soheil Nazarian, Ph.D., Chair

Carlos Chang-Albitres Ph.D.

Peter Golding, Ph.D.

Patricia D. Witherspoon, Ph.D.
Dean of the Graduate School

ESTIMATING VARIATION IN STIFFNESS AND VOLUME CHANGE OF CLAYS FROM GEOCHEMICAL AND INDEX PROPERTIES

by

CYNTHIA R. ZUNIGA, BSCE, EIT

THESIS

Presented to the Faculty of the Graduate School of

The University of Texas at El Paso

in Partial Fulfillment

of the Requirements

for the Degree of

MASTER OF SCIENCE

Department of Civil Engineering

THE UNIVERSITY OF TEXAS AT EL PASO

December 2009

ACKNOWLEDGEMENTS

The successful progress of this project could not have happened without the help and input of Mr. Soheil Nazarian, PhD., PE. Special thanks are extended to Mr. Imad Abdallah, MSCE, EIT, who has been very supportive on this project and was very helpful in finalizing this report. The author also acknowledges Mr. Carlos Chang-Albitres, PhD., and Mr. Peter Golding, PhD. for providing valuable guidance and input.

ABSTRACT

Clayey soils from six different locations in Texas were analyzed and evaluated with respect to their expansion and shrinkage and change in stiffness associated with moisture content variation. These soils consist of five high plasticity-index (PI) clays (PI greater than 25) and one low-PI clay (PI = 17). The behavior of the clays changes dramatically with moisture content fluctuation, thus causing stiffness and volume changes throughout the year. Total or differential volume movements caused by swell or shrinkage strains of expansive soils and reduction in modulus can exert enough pressure to damage the pavements and cause maintenance problems.

The intent of this research project is to develop mathematical models capable of predicting the behavior of clays under different moisture conditioning processes. The variations in modulus and lateral and vertical strains were evaluated under three different moisture conditioning processes. In the first process, called Dry-from-Optimum (DFO), specimens were compacted at their corresponding optimum moisture contents and then subjected to drying. In the second process, Saturated-from-Optimum (SFO), specimens prepared at their optimum moisture contents were subjected to saturation. The third process, Dry-from-Saturated (DFS), consisted of moisture conditioning specimens prepared at their corresponding optimum moisture contents to saturation first and then drying the saturated specimens. The proposed models are based on two sets of geotechnical parameters of soils: index parameters and chemical-mineralogical parameters. The models were validated with one set of data not used in the development of the models.

Comparison between the model predictions and the measured data show that these models are able to reproduce the main features of stiffness and volume changes due soil moisture fluctuations. The developed models can be implemented in the assessment of the pavement performance of pavements subjected to moisture fluctuations.

TABLE OF CONTENTS

ACKNOWLEDGEMENTS iv

ABSTRACT v

TABLE OF CONTENTS vi

LIST OF TABLES xi

LIST OF FIGURES xiii

CHAPTER 1: INTRODUCTION 1

1.1 Background 1

1.2 Organization of Report 3

CHAPTER 2: LITERATURE REVIEW 5

2.1 Factors Influencing Shrink/Swell Potential 5

2.1.1 Index Properties 6

2.1.2 Chemical and Mineralogical Properties 8

2.1.2.1 Clay Mineralogy and Soil Chemistry 8

2.1.2.2 Cation Exchange Capacity 10

2.1.2.3 Soluble Sulfate Content 11

CHAPTER 3: TEST TO CHARACTERIZE EXPANSIVE SOILS 12

3.1 Introduction 12

3.2 Tests to Characterize Strength Properties 12

3.2.1 Triaxial Test 12

3.2.2 Indirect Tensile Test 13

3.2.3 Unconfined Compressive Strength (UCS) Test 14

3.3 Tests to Characterize Stiffness Properties 15

3.3.1 Cyclic Triaxial Test 15

3.3.2 Resilient Modulus Test 15

3.3.3 Free-Free Resonant Column Test 16

3.3.4 Permanent Deformation Test 18

3.3.5 Fixed Free Resonant Column Test 19

3.4 Tests to Characterize Swell Properties 20

3.4.1 Free Swell Test 20

3.4.2 Swell Pressure Test 21
3.4.3 Suction Measurement Tests – Filter Paper Method 22
3.5 Tests to Characterize Shrinkage Properties 23
3.5.1 Coefficient of Linear Extensibility (COLE) Test 24
3.5.2 Linear Shrinkage Bar Test 24
3.5.3 Shrinkage Strain Test 24
CHAPTER 4: DEVELOPMENT OF MODELS 26
4.1 Introduction 26
4.2 Testing Procedure 26
4.3 Test Results 27
4.4 Preparation and Conditioning of Specimens 29
4.4.1 Drying Phase 29
4.4.2 Saturation Phase 31
4.5 Development of Relationships 32
4.5.1 Dry from Optimum Process (DFO) 33
4.5.2 Saturated from Optimum Process (SFO) 34
4.5.3 Dry from Saturation Process (DFS) 35
4.6 Moisture Conditioning Process 35
4.7 Normalization Process 36
4.8 Prediction Model 38
4.9 Presentation of Results 40
CHAPTER 5: IMPACT OF INDEX PROPERTIES 43
5.1 Introduction 43
5.2 Estimation of Fit Parameters 43
5.2.1 Combined DFO and SFO Process 44
5.2.2 DFS Process 47
5.3 Estimation of Maximum and Minimum Strains 47
5.3.1 Combined DFO and SFO Process 48
5.3.2 DFS Process 51
CHAPTER 6: IMPACT OF SOIL CHEMISTRY 53
6.1 Introduction 53
6.2 Estimation of Fit Parameters 54
6.2.1 Combined DFO and SFO Process 54

6.2.2 DFS Process 57
6.3 Estimation of Minimum and Maximum Strains 58
6.3.1 Combined DFO and SFO Process 58
6.3.2 DFS Process 58
CHAPTER 7: CASE STUDY – VALIDATION OF MODELS 63
7.1 Prediction Process 63
7.2 Validation using Index Properties 66
7.3 Validation using Chemical-Mineralogical Properties 69
CHAPTER 8: SUMMARY AND CONCLUSIONS 72
REFERENCES 75
APPENDIX A: LATERAL STRAIN PREDICTION MODELS 78
A.1: Lateral Strain Paris Prediction Model 78
A.2: Lateral Strain San Antonio Prediction Model 78
A.3: Lateral Strain Bryan Prediction Model 79
A.4: Lateral Strain El Paso Prediction Model 79
APPENDIX B: VERTICAL STRAIN PREDICTION MODELS 80
B.1: Vertical Strain Houston Prediction Model 80
B.2: Vertical Strain Paris Prediction Model 80
B.3: Vertical Strain San Antonio Prediction Model 80
B.4: Vertical Strain Bryan Prediction Model 81
B.5: Vertical Strain El Paso Prediction Model 81
APPENDIX C: MODULUS PREDICTION MODELS 82
C.1: Modulus Houston Prediction Model 82
C.2: Modulus Bryan Prediction Model 82
C.3: Modulus Paris Prediction Model 82
C.4: Modulus San Antonio Prediction Model 83
C.5: Modulus El Paso Prediction Model 83
APPENDIX D: SUMMARY OF FIT PARAMETERS AND INDEX PROPERTIES RELATIONSHIPS – LATERAL AND VERTICAL STRAINS 84
D.1: Correlations between Index Properties of Soils and Parameter B 84
(Lateral Strain, DFS Process) 84
D.2: Correlations between Index Properties of Soils and Parameter C 85

(Vertical Strain, Combined DFO and SFO Process) 85
D.3: Correlations between Index Properties of Soils and Parameter B 86
(Vertical Strain, DFS Process) 86
APPENDIX E: SUMMARY OF FIT PARAMETERS AND INDEX PROPERTIES RELATIONSHIPS - MODULUS 87
E.1: Correlations between Index Properties of Soils and Parameter A 87
(Modulus, Combined DFO and SFO Process) 87
E.2: Correlations between Index Properties of Soils and Parameter B 88
(Modulus, Combined DFO and SFO Process) 88
E.3: Correlations between Index Properties of Soils and Parameter A 89
(Modulus, DFS Process) 89
E.4: Correlations between Index Properties of Soils and Parameter B 90
(Modulus, DFS Process) 90
APPENDIX F: SUMMARY OF FIT PARAMETERS AND CHEMICAL-MINERALOGICAL PROPERTIES RELATIONSHIPS-STRAINS 91
F.1 Correlations between Chemical-Mineralogical Properties and Parameter B 91
(Lateral Strain, DFS Process) 91
F.2: Correlations between Chemical-Mineralogical Properties and Parameter C 92
(Vertical Strain, Combined DFO and SFO Process) 92
F.3: Correlations between Chemical-Mineralogical Properties of Soils and Parameter B 93
(Vertical Strain, DFS Process) 93
APPENDIX G: SUMMARY OF FIT PARAMETERS AND CHEMICAL-MINERALOGICAL PROPERTIES RELATIONSHIPS - MODULUS 94
G.1: Correlations between Chemical-Mineralogical Properties of Soils and Parameter A 94
(Modulus, Combined DFO and SFO Process) 94
G.2: Correlations between Chemical-Mineralogical Properties and Parameter B 95
(Modulus, Combined DFO and SFO Process) 95
G.3: Correlations between Chemical-Mineralogical Properties and Parameter A 96
(Modulus, DFS Process) 96
G.4: Correlations between Chemical-Mineralogical Properties and Parameter B 97
(Modulus, DFS Process) 97
APPENDIX H: SUMMARY OF MINIMUM AND MAXIMUM STRAINS AND INDEX PROPERTIES RELATIONSHIPS 98
H.1: Summary of Correlations between Index Properties of Soils and Minimum Lateral Strain 98

(DFS Process) 98
H.2: Summary of Correlations between Index Properties of Soils and Minimum Vertical Strain .. 99
(Combined DFO and SFO Process) 99
H.3: Summary of Correlations between Index Properties of Soils and Maximum Vertical Strain 100
(Combined DFO and SFO Process, DFS Process) 100
H.4: Summary of Correlations between Index Properties of Soils and Minimum Vertical Strain 101
(DFS Process) 101
APPENDIX I: SUMMARY OF MINIMUM AND MAXIMUM STRAINS AND CHEMICAL-MINERALOGICAL PROPERTIES RELATIONSHIPS 102
I.1: Summary of Correlations between Chemical-Mineralogical Properties and Minimum Strain 102
(Lateral Strain, DFS Process) 102
I.2: Summary of Correlations between Chemical-Mineralogical Properties and Minimum Vertical Strain 103
(Combined DFO and SFO Process) 103
I.3: Summary of Correlations between Chemical-Mineralogical Properties and Maximum Vertical Strain 104
(Combined DFO and SFO Process, DFS Process) 104
I.4: Summary of Correlations between Chemical-Mineralogical Properties and Minimum Vertical Strain 105
(DFS Process) 105
VITA 106

LIST OF TABLES

Table 2.1: Soil Properties that Influence Shrink-Swell Potential (Nelson and Miller 1992) 6
Table 2.2: Expansive Soil Classification based on Colloid Content, Plasticity Index and Shrinkage Limit (after Holtz and Gibbs, 1956) 7
Table 2.3: Expansive Soil Classification based on Shrinkage Limit or Linear Shrinkage.....7
(after Altmeyer, 1955) 7
Table 2.4: Expansive Soil Classification based on Percent Passing No. 200 Sieve, Liquid Limit and Standard Penetration Resistance (after Chen, 1965) 7
Table 2.5: Expansive Soil Classification based on Plasticity Index (after Chen, 1988) 7
Table 2.6: Expansive Soil Classification based on Plasticity and Shrinkage Limit (after Raman, 1967)...8
Table 2.7: Laboratory Tests used in Identification of Expansive Soils (Nelson and Miller 1992) 9
Table 2.8: Particle features and Engineering Properties of Clay Minerals.....10
(Nelson and Miller 1992).....10
Table 2.9: Typical values of CEC for the three basic Clay Minerals (Mitchell, 1976).....10
Table 4.1: Index Properties of Soils 27
Table 4.2: Moisture-Density Test Results 27
Table 4.3: Chemical and Mineralogical Properties of Soils 28
Table 4.4: Seismic Modulus Test Results.....28
Table 4.5: Maximum and Minimum Strain Values 36
Table 4.6: Best Fit Parameters - Normalized Shrinkage Strains vs. Normalized Moisture Content (Combined DFO and SFO Process).....39
Table 4.7: Modified Best Fit Parameters - Normalized Shrinkage Strains vs. Normalized Moisture Content (Combined DFO and SFO Process) 40
Table 4.8: Best Fit Parameters - Normalized Shrinkage Strains vs. Normalized Moisture Content.....40
(DFS Process) 40
Table 4.9: Best Fit Parameters - Normalized Modulus vs. Normalized Moisture Content.....40
Table 5.1: Correlation Analysis between Parameter C and Index Properties.....46
(Combined DFO and SFO Process).....46
Table 5.2: Correlation Analysis between Modulus and Index Properties 46
(Combined DFO and SFO Process).....46
Table 5.3: Correlation Analysis between Parameter B and Index Properties (DFS Process) 47

Table 5.4: Correlation Analysis between Modulus and Index Properties (DFS Process) 48
Table 5.5: Correlation Analysis between Minimum Strain and Index Properties 51
(Combined DFO and SFO Process) 51
Table 5.6: Correlation Analysis between Maximum Strain and Index Properties 51
(Combined DFO and SFO Process and DFS Process) 51
Table 5.7: Correlation Analysis between Minimum Strain and Index Properties 52
Table 6.1: Correlation Analysis between Parameter C and Chemical-Mineralogical Properties 56
(Combined DFO and SFO Process) 56
Table 6.2: Correlation Analysis between Modulus and Chemical-Mineralogical Properties
(Combined DFO and SFO Process) 56
Table 6.3: Correlation Analysis between Parameter B and Chemical-Mineralogical Properties 57
(DFS Process) 57
Table 6.4: Correlation Analysis between Modulus and Chemical-Mineralogical Properties 57
(DFS Process) 57
Table 6.5: Correlation Analysis between Minimum Strain and Chemical-Mineralogical Properties 61
(Combined DFO and SFO Process) 61
Table 6.6: Correlation Analysis between Maximum Strain and Chemical-Mineralogical Properties 61
(Combined DFO and SFO Process and DFS Process) 61
Table 6.7: Correlation Analysis between Minimum Strain and Chemical-Mineralogical Properties 62
Table 8.1: Best Fit Parameters Predictors 73
Table 8.2: Best Minimum and Maximum Strain Predictors 74

LIST OF FIGURES

Figure 1.1: Map of Texas showing Shrink-Swell Potential of Expansive Soils....2
Figure 3.1: Triaxial Test Apparatus....13
Figure 3.2: Indirect Tensile Strength Test....14
Figure 3.3: Unconfined Compressive Test Apparatus....14
Figure 3.4: Typical Resilient Modulus Test....16
Figure 3.5: Free-Free Resonant Column Test....17
Figure 3.6: Typical Deformation Response in Permanent Deformation Test....19
Figure 3.7: Free Swell Test Apparatus....21
Figure 3.8: Swell Pressure Test Apparatus....22
Figure 3.9: Total and Matric Suction Measurements....23
Figure 4.1: Change in Shrinkage Strain vs. Time during Drying....30
Figure 4.2: Change in Seismic Modulus and Moisture Content vs. Time during Drying....30
Figure 4.3: Change in Expansion Strain vs. Time during Saturation....31
Figure 4.4: Change in Seismic Modulus and Moisture Content vs. Time during Saturation....31
Figure 4.5: Conditioning Process Model....32
Figure 4.6: Change in Shrinkage Strain vs. Moisture Content (Fort Worth)....33
Figure 4.7: Change in Seismic Modulus vs. Moisture Content (Fort Worth)....33
Figure 4.8: Typical Variations in Expansion Strains with Moisture Content (Fort Worth)....34
Figure 4.9: Typical Variations in Seismic Modulus with Moisture Content (Fort Worth)....34
Figure 4.10: Typical Variations in Shrinkage Strains with Moisture Content (Fort Worth)....35
Figure 4.11: Typical Variations in Seismic Modulus with Moisture Content (Fort Worth)....35
Figure 4.12: Typical Variations in Normalized Lateral and Vertical Strains with Normalized Moisture Content (Combined DFO and SFO Process)....37
Figure 4.13: Typical Variations in Normalized Lateral and Vertical Strains with Normalized Moisture Content (DFS Process)....37
Figure 4.14: Typical Variation in Normalized Modulus with Normalized Moisture Content (Combined DFO and SFO Process)....38
Figure 4.15: Typical Variation in Normalized Modulus with Normalized Moisture Content (DFS Process)....38
Figure 4.16: Strain Prediction Model (Fort Worth)....41

Figure 4.17: Modulus Prediction Model (Fort Worth) 42
Figure 5.1: Flowchart of Strain or Modulus Prediction Based on Index Properties....44
Figure 5.2: Example of Correlations between Index Properties of Soils and Parameter C....45
(Lateral Strain, Combined DFO and SFO Process)....45
Figure 5.3: Summary of Correlations between Index Properties of Soils and Minimum Lateral Strain ..49
(Combined DFO and SFO Process)....49
Figure 5.4: Summary of Correlations between Index Properties of Soils and Maximum Lateral Strain..50
(Combined DFO and SFO Process and DFS Process) 50
Figure 6.1: Flowchart of Strain or Modulus Prediction Based on Chemical-Mineralogical Properties....53
Figure 6.2: Example of Correlations between Chemical-Mineralogical Properties of Soils and Parameter
C (Lateral Strain, Combined DFO and SFO Process) 55
Figure 6.3: Summary of Correlations between Chemical-Mineralogical Properties of Soils and Minimum
Lateral Strain (Combined DFO and SFO Process)....59
Figure 6.4: Summary of Correlations between Chemical-Mineralogical Properties and Maximum Lateral
Strain (Combined DFO and SFO Process and DFS Process)....60
Figure 7.1: Flowchart of Strain and Modulus Prediction Relationship Based on Index and/or Chemical-
Mineralogical Properties of Soils. 63
Figure 7.2: Comparison of Measured and Predicted Lateral and Vertical Strains and Normalized
Moisture Content for the Houston Clay Material using Index Properties....68
Figure 7.3: Comparison of Measured and Predicted Normalized Modulus and Normalized Moisture
Content for the Houston Clay Material using Index Properties 68
Figure 7.4 Measured and Predicted Lateral and Vertical Strains and Normalized Moisture Content for
the Houston Clay using Chemical-Mineralogical Properties 70
Figure 7.5: Comparison of Measured and Predicted Normalized Modulus and Normalized Moisture
Content for the Houston Clay Material using Chemical-Mineralogical Properties 71

CHAPTER 1: INTRODUCTION

1.1 Background

Expansive clay soils are defined as soils that exhibit significant volume change when subjected to moisture variation. These problem soils typically include high plasticity index (PI) clays, highly overconsolidated clays rich in Montmorillonite minerals, and weathered shales. Expansive soils that may swell enough to cause pavement problems are generally clays falling into the American Association of State Highway and Transportation Officials Method (AASHTO) A-6 or A-7 groups, or classified as CH or CL by the Unified Soil Classification System (USCS), and with a Plasticity Index greater than 25 by ASTM D4318.

Pavements are particularly susceptible to damage by expansive soils because they are lightweight and extend over large areas. Worldwide experience has shown that pavements constructed on expansive soils often require costly rehabilitation well before the end of their design life. Although the estimation of pavement damage is somewhat subjective, even the most conservative estimates show that expansive soils are a major contributor to the frequent road maintenance problems (Nelson and Miller 1992).

Moisture content variation is one of the most significant factors that affect the engineering and physical properties of the subgrade soils, and thus, the pavement performance. Depending on the supply of moisture in the subgrade, expansive soils might experience changes in volume of up to 30% or more. Clayey soils swell when they absorb water and shrink as they dry. During periods of high moisture, excess water penetrates into cracks and diffuses into the soil mass, and thus, clay exhibits exceptionally low strength and tends to expand. The low strength of the subgrade contributes to the structural damage of the road (Thompson and Elliot 1985). Conversely, during periods of low moisture, expansive soils exhibit a significant increase in strength and stiffness (modulus), thus contributing to a positive impact on the life of the pavement. However, the increase in stiffness results in the increase in the brittleness of the clay. The loss of moisture also contributes to the shrinkage of the clay. This tendency to shrink along with the increase in the brittleness leads to the formation of surface cracks. Finally, in the saturated stage, the subgrade is so weak that the pavement would fail under much smaller loads than when the same subgrade is at its optimum state.

According to Nelson and Miller (1992), the expansive soil problems in eastern Texas are primarily related to both shrinking and swelling. In those areas, moisture fluctuations over the different seasons cause shrinking during dry periods and swelling when they are wetted again. Volume change can take place over relatively short periods of time ranging from a few hours to a few years. In central and western Texas, the problems include both swelling of overconsolidated, desiccated soils as well as shrinking. (See Figure 1.1)

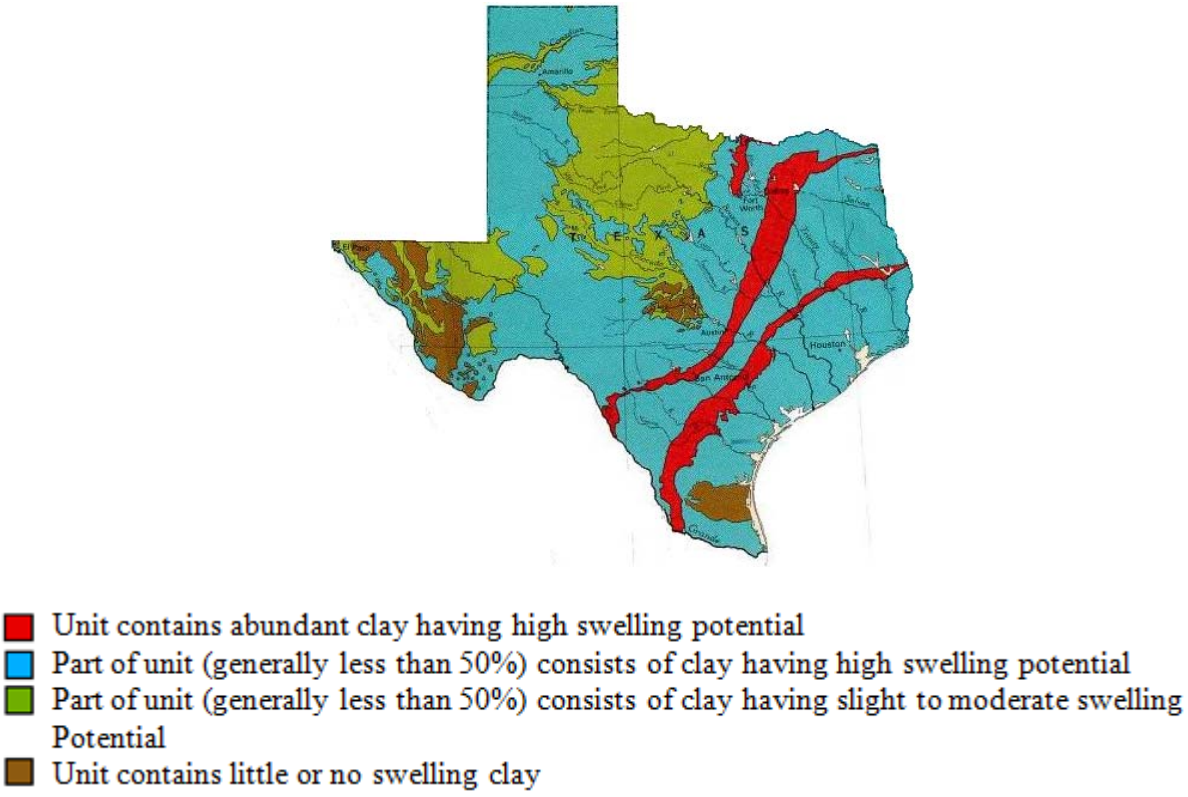

Figure 1.1: Map of Texas showing Shrink-Swell Potential of Expansive Soils

Besides the strength and stiffness changes throughout the year, total or differential volume movements caused by swell or shrinkage strains of expansive soils can exert enough pressure to damage the pavements and cause maintenance problems. Damages sustained by pavements include distortion of pavements. This distortion may be caused by swelling of expansive subgrade soils, which in turn, leads to cracking. Longitudinal cracking is mainly attributed to shrinkage of underlying layers which may also

be accelerated by repeated traffic loads (Engineering Manual 1110, 3-138, US Army Corps of Engineers 1984).

The main focus of this report is to develop mathematical models capable of predicting strains (shrinkage and expansion) and modulus under different moisture conditioning processes that can be used in pavement design. The proposed models are based on two geotechnical parameters of soils: index parameters and chemical and mineralogical parameters. The models were validated with data that were not used in the development of the models. Six different clay materials, consisting of one low PI clay and five high PI clays, were analyzed as part of a testing procedure to cover soil conditions often encountered in different parts of Texas.

1.2 Organization of Report

Chapter 2 contains a thorough literature review of recent studies addressing the behavior of expansive soils with respect to change in moisture content. The factors influencing soil volume changes are discussed in relation to soil index properties and chemical-mineralogical properties of soils.

Chapter 3 addresses commonly used laboratory tests to describe expansive subgrade properties. This includes tests to characterize strength/stiffness properties and tests to characterize swell/shrink properties.

Chapter 4 describes the overall research approach. It describes the preparation and moisture conditioning implemented on the subject soils. Also discussed is the test program carried out to determine the strength/stiffness and volume change properties of these soils. The results collected from different laboratory tests will be presented. This chapter ends by presenting mathematical models for quantitatively predicting strains (lateral and vertical) and modulus under different moisture conditioning processes. Methods used for normalizing data are discussed, and curve fitting process as well as the best prediction models are presented.

Use of laboratory test data to develop prediction relationships between index properties and the different fit parameters measured after dry and wet conditioning processes are documented in Chapter 5, while the different fit parameters of the models and their correlation to the chemical-mineralogical properties are summarized in Chapter 6.

Chapter 7 presents the validation of the results. Prediction models, as validated with one set of data not used in the analysis, are discussed and an explanation on how the model prediction is able to reproduce the main features of stiffness and volume changes is summarized.

Finally, summary and conclusions for future research are given in Chapter 8.

CHAPTER 2: LITERATURE REVIEW

2.1 Factors Influencing Shrink/Swell Potential

Factors influencing swelling potential of any particular expansive soil are determined by the percentage of clay and the type of clay in the soil, initial placement condition, stress history, nature of pore fluid, temperature, volume change permitted during swelling, shape size and thickness of sample as well as time (Nayak and Christensen, 1971). According to Holtz and Kovacs (1981), swelling depends on the clay minerals present in the soil, the soil structure and fabric and several physicochemical aspects of the soil such as cation valance, salt concentration, cementation and presence of organic matter (see Table 2.1).

The relationships among the index properties and physical state of expansive clay soils to their swelling characteristics have been the topic of extensive research. Komornik and David (1969) developed an equation in which the logarithm of swelling pressure was related to both the liquid limit and dry unit weight. El-Sohby and Mazen (1987) concluded that these two parameters are significant in the determination of swelling pressure.

Several regression equations were developed by Hossain et al. (1997) relating swelling to initial dry unit weight, initial water content, liquidity index, liquid limit or plasticity index. But none of the above equations incorporated the effects of physico-chemical factors on swelling properties of soils.

Nwaiwu and Nuhu (2006) carried out laboratory tests to evaluate the pH, electrical conductivity, loss on ignition of the soils, grain size distribution (Hydrometer test) and percentage free swell of expansive clay materials. They concluded that the swelling behavior can be predicted from a combination of physico-chemical/physico-mineralogical and index properties of clays. According to Nwaiwu and Nuhu, the specific gravity and electrical conductivity can be used to predict the swell potential, while the same factors along with clay content and plasticity index can be used to predict the free swell, swelling strain and swelling pressure of the clay.

Table 2.1: Soil Properties that Influence Shrink-Swell Potential (Nelson and Miller 1992)

Factor	Description	Reference
Clay Mineralogy	Clay minerals which tipically cause soil volume changes are montmorillonites, vermiculites and some mixed layer minerals. Illites and kaolinites are infrequently expansive, but can cause volume changes when particle sizes are extremely fine (less than a few tenths of a micron).	Grim (1968); Mitchell (1973, 1976); Snethen et al. (1977)
Soil Water Chemistry	Swelling is repressed by increased cation concentration and increase cation valence. For example, Mg^{2+} cations in the soil water would result in less swelling than Na^{+} cations.	Mitchell (1976)
Soil Suction	Soil suction is an independent effective stress variable, represented by the negative pore pressure in unsaturated soils. Soil suction is related to saturation, gravity, pore size and shape, surface tension, and electrical and chemical characteristics of the soil particles and water.	Snethen (1980); Fredlund and Morgenstern (1977); Johnson (1973); Olsen and Langfelder (1965); Aitchison et al. (1965)
Platicity	In general, soils that exhibit plastic behavior over wide ranges of moisture content and have high liquid limits have greater potential for swelling and shrinking. Plasticity is an indicator of swell potential.	
Soil Structure and Fabric	Flocculated clays tend to be more expansive than dispersed clays. Cemented particles reduce swell. Fabric and structure are altered by compaction at higher water contents or remolding. Kneading compaction has been shown to create dispersed structures with lower swell potential than soils statically compacted at lower water contents.	Johnson and Snethen (1978); Seed et al. (1962a)
Dry Density	Higher densities usually indicate closer particle spacings, which may mean greater repulsive forces between particles and larger swelling potential.	Chen (1973); Komomik and David (1969); Uppal (1965)

2.1.1 Index Properties

Index properties are primary indicators of swelling behavior. Commonly determined properties such as soil plasticity and density can provide a great deal of insight regarding the expansive potential of soils. According to Nelson and Miller (1992), the use of Atterberg limits is definitely the most popular approach to predict swell potential. Holtz and Gibbs (1956) presented the criteria shown in Table 2.2 based on undisturbed soil samples.

However, Altmeyer (1955) eliminated the use of percent clay because many laboratories do not include hydrometer analysis in their testing programs. Instead, he suggested the use of shrinkage limit or linear shrinkage, as shown in Table 2.3. Chen (1965) developed a correlation between percent finer than the No. 200 sieve size, liquid limit, and standard penetration blow counts to predict potential expansion, as shown in Table 2.4. Chen also presented a single index method for identifying expansive soils solely by plasticity index, as shown in Table 2.5 (Chen, 1988). Raman (1967) presented the degree of expansion as a function of plasticity index and shrinkage index (Table 2.6).

Table 2.2: Expansive Soil Classification based on Colloid Content, Plasticity Index and Shrinkage Limit (after Holtz and Gibbs, 1956)

Data from Index Tests[a]			Probable Expansion (% Total Volume Change)	Degree of Expansion
Colloid Content (% minus 0.0001 mm)	Plasticity Index	Shrinkage Limit		
>28	>35	<11	>30	Very High
20-31	25-41	7-12	20-30	High
13-23	15-28	10-16	10-20	Medium
<15	<18	>15	<10	Low

[a] based on Vertical Loading of 1.0 psi

Table 2.3: Expansive Soil Classification based on Shrinkage Limit or Linear Shrinkage (after Altmeyer, 1955)

Linear Shrinkage	Shrinkage Limit (%)	Probable Swell (%)	Degree of Expansion
<5	>12	<0.5	Noncritical
5-8	10-12	0.5-1.5	Marginal
>8	<10	<1.5	Critical

Table 2.4: Expansive Soil Classification based on Percent Passing No. 200 Sieve, Liquid Limit and Standard Penetration Resistance (after Chen, 1965)

Laboratory and Field Data			Probable Expansion (% Total Volume Change)	Degree of Expansion
Percentage Passing No. 200 Sieve	Liquid Limit (%)	Standard Penetration Resistance (Blows/ft)		
>95	>60	<30	>10	Very High
60-95	40-60	20-30	3-10	High
30-60	30-40	10-20	1-5	Medium
<30	<30	<10	<1	Low

Table 2.5: Expansive Soil Classification based on Plasticity Index (after Chen, 1988)

Swelling Potential	Plasticity Index
Low	0-15
Medium	10-35
High	20-55
Very High	35 and above

Table 2.6: Expansive Soil Classification based on Plasticity and Shrinkage Limit (after Raman, 1967)

PI (%)	SI (%)	Degree of Expansion
<12	<15	Low
12-23	15-30	Medium
23-32	30-40	High
>32	>40	Very High

Snethen et al. (1977) evaluated numerous published criteria for predicting potential swell. The results of their evaluation showed that liquid limit and plasticity index are the best indicators of potential swell along with natural and environmental conditions.

2.1.2 Chemical and Mineralogical Properties

Soils characteristics may be considered either as microscale or macroscale factors. Microscale factors include the mineralogical and chemical properties of the soil. Macroscale factors include the index properties of soils, which in turn are dictated by the microscale factors. (Nelson and Miller 1992).

2.1.2.1 Clay Mineralogy and Soil Chemistry

Clay mineralogy is a fundamental factor controlling expansive soil behavior. Clay minerals can be identified using a variety of techniques, the more common of which are listed in Table 2.7. Clay minerals of different types typically exhibit different swelling potentials because of variations in the electrical field associated with each mineral. The swelling capacity of an entire soil mass depends on the amount and type of clay minerals in the soil, the arrangement and specific surface area of the clay particles, and the chemistry of the soil water surrounding those particles. Particle features and engineering properties of the important clay minerals are summarized in Table 2.8.

An important characteristic of clay minerals is the small size of their crystals. Typical thicknesses can be as small as 15 basal spacing (Å) and lateral dimensions are on the order of microns. This makes visual or standard microscopic examination impossible. X-Ray diffraction methods and electron microscopy have been then used for identification on the basis of crystal structure.

Table 2.7: Laboratory Tests used in Identification of Expansive Soils (Nelson and Miller 1992)

Test	Reference	Properties Investigated	Parameters Determined
Atterberg Limits:	ASTM Standards 1991	Plasticity, consistency	
Liquid Limit (LL)	ASTM D-4318	Upper limit water content of plasticity	PI = LL - PL = Plasticity Index
Plastic Limit (PL)	ASTM D-4309	Lower limit water content of plasticity	LI = $\frac{w - LL}{LL - PL}$ = Liquidity Index
Shrinkage Limit (SL)	ASTM D-427	Lower limit water content of soil shrinkage	R = Shrinkage Ratio
Clay Content	ASTM D-422	Distribution of fine-grained particle sizes	Percent finer than 2μm
Mineralogical Tests:	Whittig (1964)	Mineralogy of clay particles	
X-Ray Diffraction	ASTM STP 479 (1970)	Characteristic crystal dimensions	Basal spacings
Differential Thermal Analysis	Barshad (1965)	Characteristic reactions to heat treatments	Area and amplitude of reaction peaks on thermograms
Electron Microscopy	McCrone and Delly (1973)	Size and shape of clay particles	Visual record of particles
Cation-Exchange Capacity	Chapman (1965)	Charge deficiency and surface activity of clay particles	CEC (meq/100 g)

Different clay minerals also may be identified using chemical analyses. However, because each group has somewhat similar engineering properties, structural grouping are more convenient. Three important structural groups of clay minerals are described for engineering purposes as follows: (Nelson and Miller 1992)

- Kaolinite Group: Generally non-expansive.
- Mica-like Group: Includes illites and vermiculites, which can be expansive, but generally do not pose significant problems.
- Smectite Group: Includes montmorillonites, which are highly expansive and are the most troublesome clay minerals.

Table 2.8: Particle features and Engineering Properties of Clay Minerals
(Nelson and Miller 1992)

Mineral Group	Basal Spacing (Å)	Particle Features	Interlayer Bonding	Specific Surface (mg^2/g)	Atterberg Limits[a]			Activity[b] (PI/% Clay)
					LL (%)	PL (%)	SL (%)	
Kaolinites	14.4	Thick, stiff 6-sided flakes 0.1 to 4 x 0.05 to 2µm	Strong hydrogen bonds	10-20	30-100	25-40	25-29	0.38
Illites	10.0	Thin, stacked flakes 0.0003 to 0.1 x 1.0 to 10 µm	Strong potassium bonds	65-100	60-120	35-60	15-17	0.9
Montmorillonites	9.6	Thin, filmy flakes >10Å x 1.0 to 10 µm	Very weak van der Waals bonds	700-840	100-900	50-100	8.5-15	7.2

[a] LL, PL and SL, liquid, plastic and shrinkage limits, respectively
[b] From Skempton (1953)
Summarized from Mitchell (1976)

2.1.2.2 Cation Exchange Capacity

The CEC is the quantity of exchangeable cations required to balance the negative charge on the surface of the clay particles. CEC is expressed in milliequivalents per 100 grams of dry clay. In the test procedure, excess salts in the soil are first removed and absorbed cations are replaced by saturating the soil exchange sites with a know species. The amount of the known cation needed to saturate the exchange sites is determined analytically. The composition of the original cation complex can be determined by chemical analysis of the original extract (Nelson and Miller 1992). CEC is related to clay mineralogy. High CEC values indicate a high surface activity. In general, swell potential increases as the CEC increases. Typical values of CEC for the three basic clay minerals are shown in Table 2.9.

Table 2.9: Typical values of CEC for the three basic Clay Minerals (Mitchell, 1976)

Clay Mineral	CEC (meq/100 g)
Kaolinite	14.4
Illite	10.0
Montmorillonite	9.6

The measurement of CEC requires detailed and precise testing procedures that are not commonly done in most soil mechanics laboratories. However, this test is routinely performed in many agricultural soils laboratories and is inexpensive (Nelson and Miller 1992).

2.1.2.3 Soluble Sulfate Content

Despite the advances in geotechnical engineering, a need continues to exist for a method for improving the characteristics of soils, particularly those soils which have a high sulfate content making them subject to undesirable swell or expansion.

Sulfate-induced heave in lime-stabilized soils is a serious problem that can cause costly infrastructure damage if not addressed and occurs when lime is added to soil containing sulfate. Lime, a common soil stabilizer, is mixed with expansive soils to make them non-expansive. However, when a certain amount of sulfate is present naturally in the soil, in the form of gypsum, a common rock forming mineral, the addition of lime and water will form a highly expansive mineral, ettringite, and cause excessive swelling. When exposed to water, ettringite can expand up to 250% and the resulting lime/soil mixture becomes more expansive than the natural soil (Adams et al., 2008).

Expansion due to the growth of ettringite in lime stabilized sulfate soils often produces severe problems, for instance, in the construction and performance of pavement foundation systems. The amount and type of sulfates present in the soil, namely sodium sulfate and/or calcium sulfate, and the amount and type of clay material present are properties which play key roles in the post-stabilization expansion developed over time in lime treated sulfate soils. The formation of ettringite is also known to be responsible for the deterioration of concrete by sulfate attack. Because the quantity of sulfates present generally dictates the extent to which ettringite will form, it is important to evaluate sulfate content in soils intended for construction purposes. Simply stated, the greater the content of soluble sulfates in a soil, the greater the potential for the growth of ettringite and therefore, the greater the potential for excessive swelling (Walker and Daniel 1992).

CHAPTER 3: TEST TO CHARACTERIZE EXPANSIVE SOILS

3.1 Introduction

Subgrade materials are typically characterized by their resistance to deformation under an applied load, which can be either a measure of their strength, which is the greatest stress they can sustain, or stiffness, which is how well a material is able to return to its original shape and size after being stressed. Stiffness of pavement layers defines their efficiency to distribute load-induced stresses within the pavement system. Many studies have demonstrated that roads build on expansive soil fails prematurely primarily because of the highly variable properties of expansive clays due to moisture fluctuations throughout the year. Failures occur as a result of variations in strength and stiffness or subgrade volumetric change or both. It is, therefore, of great importance to characterize these variations and predict their effects on pavement performance.

Strength and stiffness properties of subgrade soils are often determined by conducting appropriate strength/stiffness tests at compacted moisture levels. Ways to characterize strength and stiffness properties include both laboratory testing and field testing. On the other hand, swell and shrinkage properties are mainly characterized based on swell characterization tests.

3.2 Tests to Characterize Strength Properties

Most strength measurements are performed in the laboratory. These include the triaxial test with static or cyclic loading, direct shear test, unconfined compression tests, and others.

3.2.1 Triaxial Test

The purpose of the triaxial compression test is to determine the shear strength of soils to and determine the relationships between stresses and strains. A cylindrical soil specimen surrounded by a waterproof membrane is enclosed and tested in a pressure chamber known as a cell, as shown in Figure 3.1. The pressure in the cell is raised to the desired value and the sample is then brought to failure by applying an additional vertical load, which is slowly introduced through a rod extending through the top of the cell. To obtain the shear strength parameters of the soil, a number of specimens (normally at least three) are tested at different cell pressures (typically 0, 5, 10, and 15 psi). For each test, the deviatoric

stress at failure is determined and used to plot a Mohr circle. The tangential envelope to touch these circles then defines the shear strength parameters.

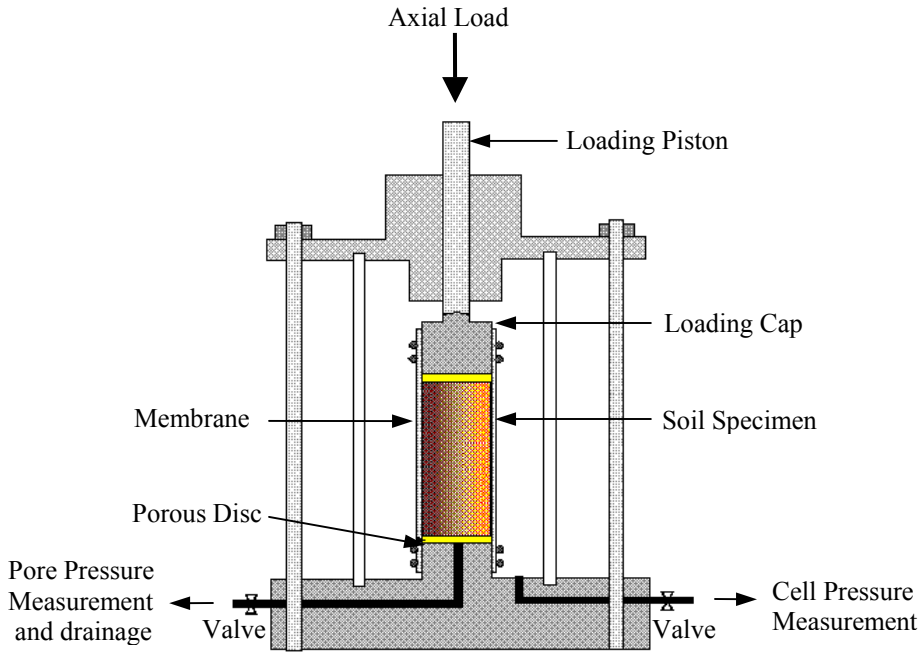

Figure 3.1: Triaxial Test Apparatus

The triaxial strength parameters obtained from triaxial tests include cohesion, angle of internal friction and the classification of materials. These parameters can be utilized to predict pavement performance in many pavement design and modeling programs.

3.2.2 Indirect Tensile Test

In the indirect tensile strength test (ASTM D-3967), a cylindrical specimen is loaded diametrically across the circular cross section (see Figure 3.2a) at a controlled deformation rate of 51 mm (2 in.) per minute. The loading causes a tensile deformation perpendicular to the plane of loading ultimately resulting into a tensile failure. By knowing the load at failure and the dimensions of the test specimen, the indirect tensile strength can be calculated. Figure 3.2b shows the load fixture and a principal picture of the loading for an indirect tensile strength test.

a) Apparatus

b) Loading Situation

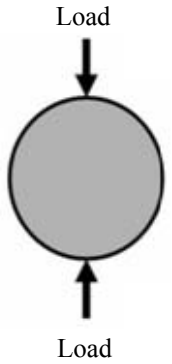

Figure 3.2: Indirect Tensile Strength Test

3.2.3 Unconfined Compressive Strength (UCS) Test

In the unconfined compressive strength test (ASTM D-2166), a cylindrical soil sample with dimensions of 4 in. by 8 in and with no lateral confinement is placed in a triaxial chamber. An axial compressive load is then gradually applied to the soil until it fails (the load reaches its peak value). The load is applied fairly rapidly (typically about 1 minute to failure), thus producing undrained conditions. The maximum stress at which the specimen fails is called the unconfined compressive strength of the material. As the sample compresses, the center part bulges, so the area increases (Coduto 1998). The unconfined compressive strength test has the advantage of being simple and inexpensive. A typical unconfined compressive test apparatus is shown in Figure 3.3.

Figure 3.3: Unconfined Compressive Test Apparatus

3.3 Tests to Characterize Stiffness Properties

The stiffness of subgrade soils is an important indicator of soil performance and a required input for a pavement design. Stiffness properties of subgrade soils are often determined and measured by conducting appropriate tests at compacted moisture levels. Stiffness tests can be carried out in the laboratory as well as in the field. Laboratory stiffness measurement methods include the cyclic triaxial test, resilient modulus test, permanent deformation test, free- free resonant column test, and fixed-free resonant column test.

3.3.1 Cyclic Triaxial Test

Cyclic Triaxial test is widely used to investigate changes in strength and stiffness under cyclic loading conditions. The cyclic triaxial test apparatus applies cyclic or dynamic loading to the soil specimen. This form of loading can simulate traffic loading conditions. The test system controls three parameters, axial stress, confining pressure and back pressure. The cylindrical specimen is prepared at optimum moisture content and tested to study pore water pressure, deformation response and effect of repeated loading conditions.

Cyclic loading on saturated undrained clays induces a decrease in effective stress as well as a rearrangement of the soil particle structure, which may lead to degradation in strength and stiffness. This phenomenon of high PI subgrade having low strength during rainy season contributes to the structural damage of the road. Miller et al. (2000) reported that for highly plastic clay, the cyclic shear strength was sensitive to the initial degree of saturation. The cyclic strength may decrease by approximately 80% as the initial degree of saturation is increased from 90 to 100%. Shahu and Yudhbir (1999) proposed cyclic triaxial tests on samples prepared at optimum moisture content and at saturated condition to better evaluate the strength and stiffness variations of subgrade materials. In their study, significant degradation of the subgrade soil under saturated condition was observed.

3.3.2 Resilient Modulus Test

The resilient modulus (M_R) is a measurement of the soil response when subjected to repeated loading, and is the most important characteristic of subgrades used in pavement design. All pavement designs are based on the resilient modulus of the supporting subgrade soils.

In a resilient modulus test, a repeated axial cyclic stress of fixed magnitude, load duration and cyclic duration is applied to a cylindrical test specimen. While the specimen is subjected to this dynamic cyclic stress, it is also subjected to a static confining stress provided by a triaxial pressure chamber. The total resilient (recoverable) axial deformation response of the specimen is measured (see Figure 3.4) and used to calculate the resilient modulus. Under repeated loads, the modulus becomes nearly constant after a number of loading cycles and the response can be assumed to be approximately elastic. This steady value of modulus is defined as the resilient modulus and is assumed to occur after about 200 cycles of loading. (AASHTO 1993). Therefore, it can be understood that a material's resilient modulus is actually an estimate of its modulus of elasticity (E). While the modulus of elasticity is stress divided by strain for a slowly applied load, resilient modulus is stress divided by strain for rapidly applied loads – like those experienced by pavements. Typically, the resilient modulus is determined in the laboratory in accordance with AASHTO T307 under conditions of maximum dry density and optimum water content (Drumm and Madgett 1997).

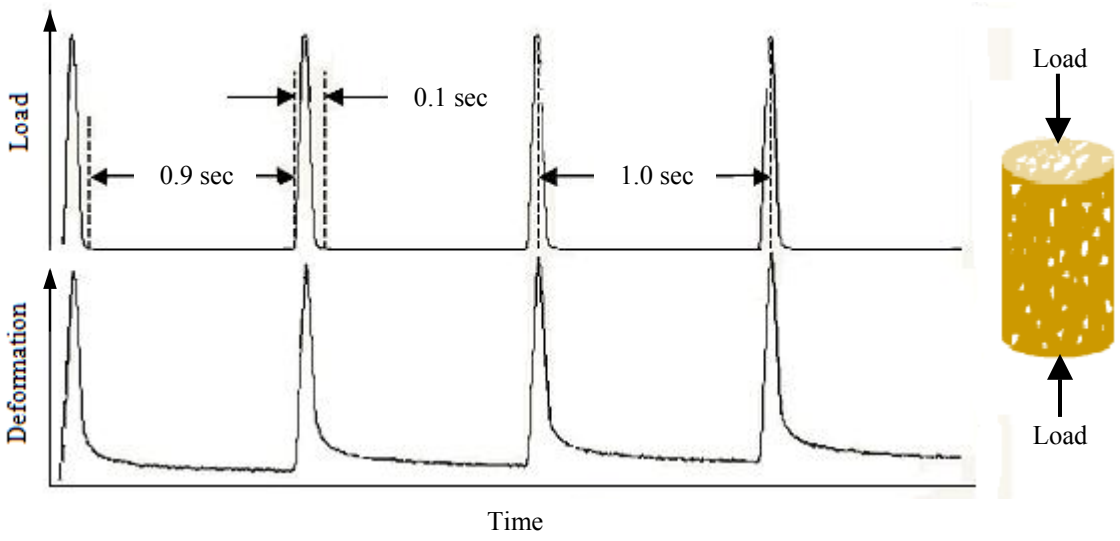

Figure 3.4: Typical Resilient Modulus Test

3.3.3 Free-Free Resonant Column Test

In a free-free resonant column (FFRC) test, a cylindrical specimen is subjected to an impulse load at one end while seismic energy over a large range of frequencies propagates within the specimen. Depending on the dimensions and the stiffness of the specimen, energy associated with one or more frequencies is trapped and resonate as they propagate within the specimen. The purpose of this test is to

determine these resonant frequencies. Since the dimensions of the specimen are known and if one can determine the resonant frequencies, then one can readily determine the modulus of the specimen using principles of wave propagation in a solid rod.

The FFRC device is a reasonably low cost device that has been successfully utilized by some TxDOT personnel. Due to the nondestructive nature of this test, one specimen can be tested repeatedly to obtain the variation in modulus with moisture (Yuan and Nazarian 2002). Also, the same specimen can be used to measure the change in length and diameter of the specimen during saturation and drying. Test results have shown that the modulus from the FFRC device is reasonably well-correlated to the modulus from the resilient modulus tests and the angle of internal friction from the triaxial tests (Nazarian and Yuan, 2003). The schematic of the device is shown in Figure 3.5.

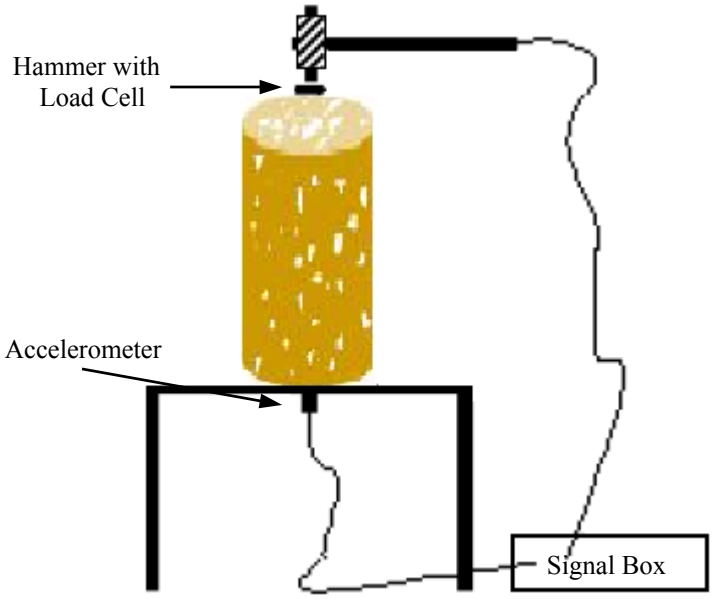

Figure 3.5: Free-Free Resonant Column Test

As the specimen is dried, the modulus significantly increases and the moisture content decreases. However, as soon as the water is introduced, the modulus significantly decreases and the moisture content increases. A number of moisture patterns have to be studied to determine the most appropriate test protocol. However, this method has the potential for providing relevant information for the design at a minimal cost.

3.3.4 Permanent Deformation Test

The major function of subgrade soils is to provide support to pavement structures. Under heavy traffic loads, subgrade soils may deform and contribute to distress in the overlying pavement structure. In asphalt pavements this distress normally takes the form of cracking and rutting. It has been well documented that the subgrade soil plays a critical role in the initiation and propagation of permanent deformation of pavement structures and directly influences pavement performance (Huang 1993).

Although the deforming behavior of subgrade soils is relatively difficult to identify and define, it is an essential factor in determining pavement structural performance. A scientific hypothesis supported by some researchers' work (Elliott and Thompson 1985) suggests that subgrade deformation not only directly governs rutting, but may have a strong relationship with cracking of the pavement's surface as well. Thus, subgrade soils contribute to the two main pavement distresses: rutting and cracking.

Majority of rutting or the vertical permanent deformation of the pavement structure is assumed to be contributed by the pavement layers such as base, sub-base and subgrade. In subsoils, 'subgrade' being the weakest, contributes maximum (approximately 40%) of the total permanent deformation. Hence it is very important to consider the permanent deformation aspects of the subgrade while estimating the total rutting magnitudes in a pavement section (Puppala et al., 1999).

Earlier studies regarding rut depth determination considered only top few layers such as asphalt base and subbase for analysis but later it was recognized the need to include permanent deformation caused by subgrade to calculate total rut depth. Thompson and Smith (1990) concluded that shear strength properties provide a better characterization of permanent deformation aspects of soils than the stiffness related properties. To characterize any subsoil, it is important to understand the soil's plastic strain response along with the resilient response.

Repeated load triaxial test is used to calculate permanent deformation of subgrade specimens. To minimize the imperfect contacts between the end platens and specimen, testing is started with the conditioning at prescribed confining and deviatory stress level for 1,000 cycles. Actual testing is then followed by subjecting the sample at a particular combination of confining and deviatory stress levels. The vertical deformation from linear variable displacement transformers (LVDTs) is monitored and

recorded continuously during testing. Figure 3.6 shows the typical deformation response monitored during testing.

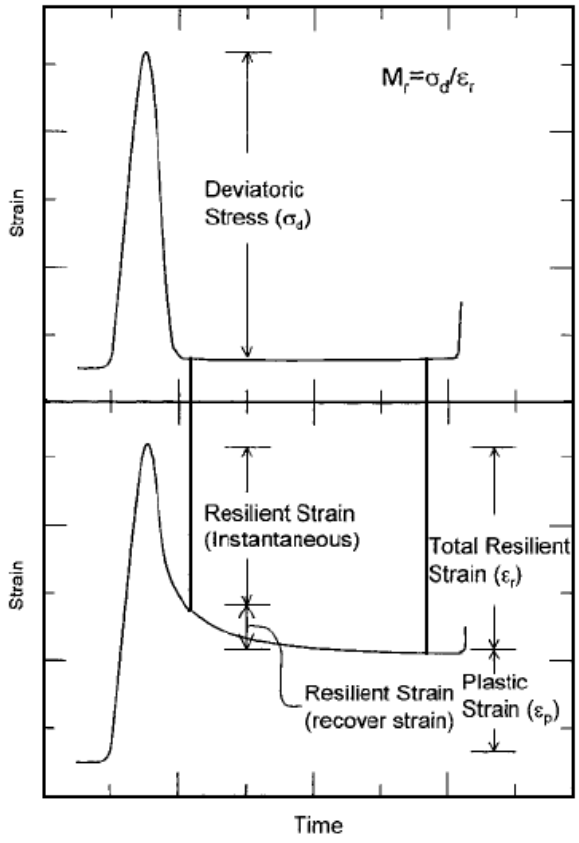

Figure 3.6: Typical Deformation Response in Permanent Deformation Test

The elastic deformation recorded is used to determine the resilient modulus values while as plastic deformation is used to determine the permanent deformation values. Initially, as the number of cycles increases, the permanent deformation accumulates rapidly. At higher cycles, the permanent deformation accumulates much slower (Sabnis et al. 2008).

3.3.5 Fixed Free Resonant Column Test

The fixed-free resonant column device has traditionally been used to measure low-strain properties in laboratory soil and rock specimens. The resonant column equipment is used to determine shear wave velocity, shear modulus and damping ratio of soil under different confining pressure, void ratios, shear strain amplitude, number of cycles and time of confinement (Xiaoming and Jing, 2002).

The test subjects solid or hollow cylindrical specimens to torsion or axial loading by an electromagnetic loading system. The soil specimen in fixed-free end conditions is either put to torsion simple shear or in a fundamental torsion mode of vibration. From theory of elasticity and geometric properties of specimen, the shear modulus can be determined. Damping ratio is determined from decaying vibration or hysteresis loop characteristics (Xiaoming and Jing, 2002).

3.4 Tests to Characterize Swell Properties

Swelling of materials which are relevant in civil and underground engineering are counted among the most alarming phenomena in geotechnics. The volume increasing of clay by absorption of water is a physical effect (osmosis), whereas the volume increasing during the hydration of anhydrite into gypsum is a chemical effect. Nevertheless, the consequences for the constructions are always the same: destructive stresses, deformations and loss of strength, often occurring and recognized months or even years later. In conventional engineering practice, the majority of laboratory swell tests are conducted in the oedometer type apparatus with low seating pressures. A brief description of the free swell tests, swell pressure test and suction measurement test is provided below.

3.4.1 Free Swell Test

The free swell test measures the amount of swell potentials of a soil sample in an oedometer. This test can be conducted to measure swell potentials in a vertical direction only or three dimensionally. The free swell of the soil is determined as the ratio of the change in volume to the initial volume, expressed as a percentage. Figure 3.7 illustrates the schematic of free swell test apparatus. Compacted soil specimens prepared at three different compaction moisture contents – dry, optimum, and saturated conditions are placed between two porous stones at the top and bottom, covered by a rubber membrane, fully inundated with water at both ends and monitored for the vertical and diametric swell movement until there was no further significant swell over a twelve-hour period. For vertical free swell test, a linear variable displacement transformer (LVDT) is placed on top of the soil specimen to monitor and record free vertical swell movements. The three-dimensional free swell test setup is the same except a LVDT and a dial gauge are used to monitor both vertical and diametric swell movements. All tests

should be conducted at room temperature and three identical soil specimens should be used for each variable condition.

Holtz and Gibbs (1956) stated that soils having free swell values as low as 100% may exhibit considerable expansion in the field when wetted under light loading. Although soils with free swell values below 50% are not considered to exhibit appreciable volume change, Dawson (1953) reported that several Texas clays with free swell values in the range of 50% have caused considerable damage through expansion. It is believed that this is due to extreme climatic conditions in combination with the expansion characteristics of the soil (Nelson and Miller 1992).

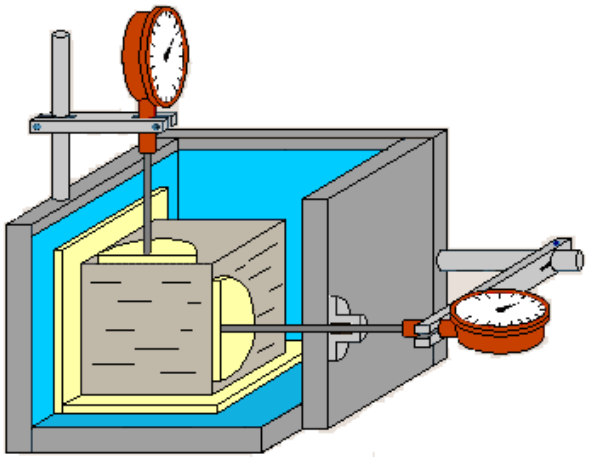

Figure 3.7: Free Swell Test Apparatus

3.4.2 Swell Pressure Test

The swell pressure test measures the amount of overburden pressures necessary for preventing the expansion of soils. The swell pressure of expansive soils is commonly determined by restraining the soil specimen from undergoing any volume change under fully soaked conditions. Several types of swell pressure tests are reported in the literature including: (1) conventional consolidation test procedure which yields an upper bond value; (2) method of equilibrium void ratio at different consolidation pressures, which gives the least swell pressure; and, (3) constant volume method, which yields an intermediate value. Further details on these test methods are available in Ohri (2003). Among them, constant volume test is the one most frequently used (Wanyan et al. 2008).

The same oedometer test setup as for free swell test is used to conduct the swell pressure test. The soil specimen placed in the test setup exhibits swell behavior within an hour after full submersion. The free swell recorded will be zeroed by adding loads to the consolidation frame.

When the sample does not undergo any swell movement for more than two days, the test is discontinued. Figure 3.8 depicts a swell pressure test apparatus. Water is supplied from the bottom while the specimen is confined. The final total load applied along with the surcharge load is used to determine swell pressures. Ramamurthy (1971) suggested the use of low height cylindrical specimen and a rubber membrane to overcome laboratory test errors caused by side friction and non-uniform distribution of moisture over the soil specimen during saturation.

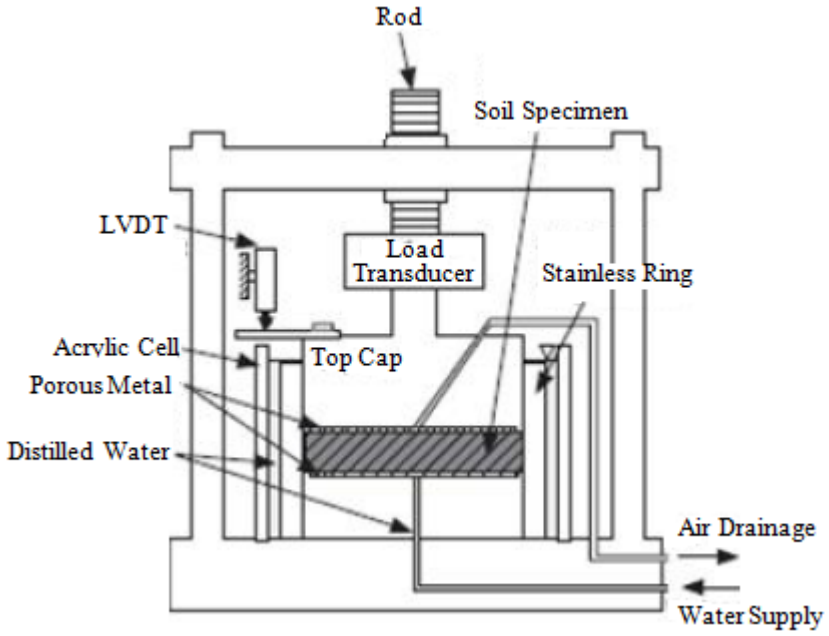

Figure 3.8: Swell Pressure Test Apparatus

3.4.3 Suction Measurement Tests – Filter Paper Method

Suction measurements have been recently used to characterize the heave potentials of expansive soils. Suction tests at low applied load are simple and do not require specialized equipment. The total suction in a soil consists of two parts, osmotic suction and matric suction. The suction changes associated with the movement of water in the liquid and vapor phases are called matric suction and osmotic suction, respectively.

The filter paper suction test method evaluates the total and matric suction of the soil specimen in the laboratory (Tsai and Petry, 1995). Quantitative ash-free filter papers exhibit a consistent and predictable relationship between water content and suction (Nelson and Miller 1992).

A soil specimen is first cut into two halves and smoothened for establishing a close contact with the filter paper. A single filter paper is used along with two larger diameter protective filter papers to collect the moisture from the test specimen (almost any brand of high permeability and larger diameter filter paper can be used as protective filter papers for matric suction measurements). The other half of the soil sample is put on top and the two pieces are taped together and inserted into a glass jar. A clean PVC O-ring is inserted on top of the soil sample. Figure 3.9 shows the procedure schematic. The glass jar is then inserted into a well-insulated container for suction equilibrium with a temperature-controlled environment. Finally, the moisture contents of the filter papers are calculated to measure both total and matric suctions. Detailed procedural steps are presented in Bulut et al., (2001).

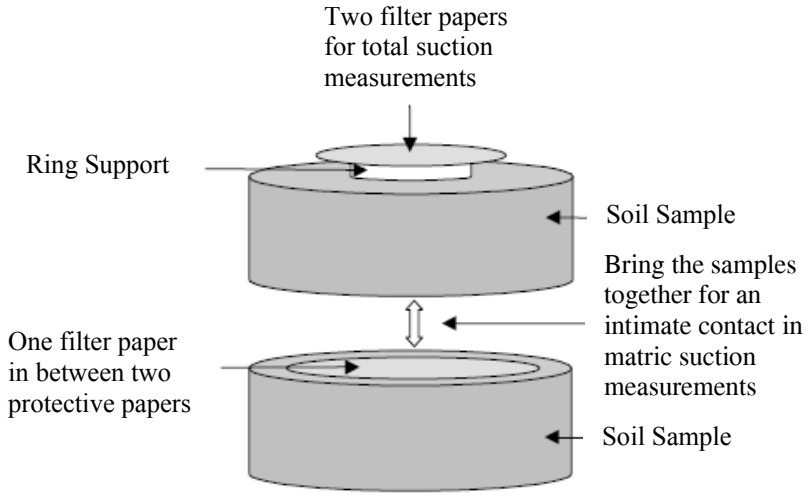

Figure 3.9: Total and Matric Suction Measurements

3.5 Tests to Characterize Shrinkage Properties

Use of shrinkage tests is limited in practice. However, it is equally important to understand both swelling and shrinkage variations to address related pavement distress issues. Descriptions of three shrinkage tests are provided in the following paragraphs.

3.5.1 Coefficient of Linear Extensibility (COLE) Test

The COLE test is a shrinkage test used routinely by the U.S. Soil Conservation Service and National Soil Survey Laboratory, for characterizing expansive clays. The COLE test determines the linear strain of an undisturbed, unconfined sample on drying from 5 psi suction to oven dry suction. The procedure involves coating undisturbed soil samples with a flexible plastic resin. The resin is impermeable to liquid water, but permeable to water vapor. Natural clods of soil are brought to a soil suction of 5 psi in a pressure vessel. They are weighed in air and water to obtain their volumes. The samples are then oven dried and another volume measurement is performed in the same manner. The value of COLE is given by:

$$COLE = \frac{\Delta L}{\Delta L_D} = \left(\frac{\gamma_{dB}}{\gamma_{dM}}\right)^{0.33} - 1 \tag{3.1}$$

where $\Delta L/\Delta L_D$ = linear strain relative to dry dimensions; γ_{dB} = dry density of oven dry sample and γ_{dM} = dry density of sample at 5 psi suction.

3.5.2 Linear Shrinkage Bar Test

The linear shrinkage bar test gives an indication of the plasticity index of the soil, since the shrinkage ratio of the soil when dried in its plastic state is related to its plasticity index. Linear shrinkage bar test can be used to complement the volumetric shrinkage properties and develop correlations between linear and volumetric shrinkage strains. To perform the test, a wooden or metal box without a top and with a square cross section is filled with soil sample and left to air dry at room temperature until color changes slightly or oven dry at 230°F (110°C). The shrinkage ratio can be measured by pushing the dried sample to one end of the box and calculate the length of the gap as a percentage of the length of the box. Shrinkage ratio is calculated using:

$$LS = \frac{100\,(L_W - L_D)}{L_W} \tag{3.2}$$

where LW = length of the wet soil bar, and LD = length of the dry soil bar.

3.5.3 Shrinkage Strain Test

The linear shrinkage strain test uses small amounts of soils and the rigid wall boxes restrain warping movements in soils observed under field conditions. Puppala et al. (2004b) developed 3-D

volumetric shrinkage strain test method to overcome these limitations. Soil is first crushed in a pulverizer and then oven-dried for 24 hours. The dried soil is then passed through Sieve No. 40 and the fine fraction of soil is collected and used for soil specimen preparation. The fine soil fraction is mixed with water at target moisture contents. For each moisture condition, soil is compacted in a volumetric shrinkage mold (5.0 in. height and 2.3 in. diameter) and the surface is flattened with a straight edge. For liquid limit state, since the clay is in slurry form, it is poured into the cylindrical molds. The mold with either compacted soil specimen or soil slurry is air dried for 12 hours and then transferred to an oven (set at 160ºF) for 24 hours. After the 24 hours, the average height and diameter of the specimen are measured using vernier calipers to determine the volumetric shrinkage strains. To determine the volumetric shrinkage strain, the digital images of surface and area pictures of cylindrical soil specimen before and after the shrinkage test are captured by digital camera and analyzed (Wanyan et al. 2008). The parameters extracted are used in Equation 2.3 to determine volumetric shrinkage strains.

$$V.S. = \frac{V_i - V_f}{V_i} = 1 - \frac{V}{V_i} = 1 - \left(\frac{A_{sf}}{A_{si}} \times \frac{A_{cf}}{A_{ci}} \times \frac{P_{ci}}{P_{cf}} - \right) = 1 - (R_s \times R_c \times R_p) \tag{3.3}$$

where V_i, V_f = initial and final volume of the cylindrical specimen, respectively; A_{si}, A_{sf} = initial and final surface area of specimen after shrinkage in pixels; A_{ci}, A_{cf} = initial and final circular area of specimen after shrinkage in pixels; P_{ci}, P_{cf} = perimeter of the initial and final circular area after shrinkage in pixels; R_s = ratio of surface area of the soil specimen $= \frac{A_{sf}}{A_{si}}$; R_c = ratio of circular cross-section area of soil specimen $= \frac{A_{cf}}{A_{ci}}$ and R_p = ratio of the circular perimeter of the soil specimen, which is given by $\frac{P_{ci}}{P_{cf}}$.

Puppala et al. (2004b) concluded that the new method provided higher strains compared to the manual test since irregular and hairline cracks were taken into account.

Based on these stiffness/volume change characterization properties, the next section will present the development of models to predict lateral and vertical strains and modulus with time.

CHAPTER 4: DEVELOPMENT OF MODELS

4.1 Introduction

Soils from six different sites in Texas were analyzed and evaluated. These soils, ranging from A-6 to A-7-6 in accordance with AASHTO or CL to CH in accordance with the USCS System, consist of five high-PI clays (PI greater than 25) and one low-PI clay (PI = 17). The high PI clays were brought from Fort Worth, Houston, San Antonio, Paris and Bryan Districts, whereas the low PI-clay was from El Paso.

This chapter starts by describing the preparation and moisture conditioning implemented on these soils. Also discussed is the test program carried out to determine the strength/stiffness and volume change properties of these soils at different moisture conditions. The results collected from different tests are presented. The different processes followed in the development of mathematical models used in the prediction of lateral/vertical strains and modulus with moisture is also discussed. The curve fitting process carried out to find the best prediction models are explained and results in the form of best fit curves will be presented. The resemblance between the predicted values and the measured data are presented through an example using the test data of the clay material from Fort Worth. Detailed results for all soils can be found in Appendix A for lateral strain, Appendix B for vertical strain and Appendix C for modulus.

4.2 Testing Procedure

Several index tests, consisting of particle size analysis of soils (ASTM D-422) and Atterberg limits (ASTM D-4318) were carried out on clay materials. Moisture-density tests were performed on all materials to obtain their optimum moisture contents and maximum dry densities following ASTM D-698. Several chemical and mineralogical tests were also carried out to better understand the properties of the clays. These include dominant clay mineralogy, cation exchange capacity and soluble sulfate content. Free-free resonant column (FFRC), tests were carried out to quantify the stiffness of each clay material.

Specimens were prepared and tested at three different moisture conditions. In the first set of tests, the specimens were prepared and tested at their corresponding optimum moisture contents. The

second moisture conditioning involved drying specimens prepared at their optimum moisture contents to constant weights. The third set of specimens were again prepared at their optimum moisture contents and saturated.

4.3 Test Results

Table 4.1 presents a summary of various index properties of all soils. Generally, soils that exhibit plastic behavior over wide ranges of moisture content and that have high liquid limits have greater potential for swelling and shrinking. Therefore, clay materials from Houston, Bryan and Paris are considered to exhibit very high swelling potential, whereas Fort Worth soil is considered as exhibiting high swelling potential. These soils are classified as A-7-6 as per ASSHTO Soil Classification System and CH as per USCS System. El Paso clay material is considered as exhibiting low swelling potential.

Table 4.1: Index Properties of Soils

Property	Site Location					
	Fort Worth	Houston	Bryan	Paris	San Antonio	El Paso
Passing #40 (%)	100	100	100	100	100	100
Passing #200 (%)	85	87	78	81	83	88
Specific Gravity	2.7	2.7	2.7	2.7	2.7	2.7
Liquid Limit (LL, %)	61	54	45	60	58	30
Plastic Limit (PL, %)	32	19	14	24	32	14
Plasticity Index (PI, %)	29	35	31	36	26	16
AASHTO Classification	A-7-6	A-7-6	A-7-6	A-7-6	A-7-6	A-6
USCS Classification	CH	CH	CH	CH	CH	CL

The moisture-density properties of the soils are shown in Table 4.2. Clay material from El Paso exhibits the highest dry density, whereas the Bryan clayey soil exhibits the highest value among the high PI clay group.

Table 4.2: Moisture-Density Test Results

Property	Site Location					
	Fort Worth	Houston	Bryan	Paris	San Antonio	El Paso
Moisture Content (%)	24	20.1	19.5	23	21.7	16.5
Maximum Dry Density (pcf)	91.5	99.1	108	92.1	91.5	112

Table 4.3 presents a summary of various chemical and mineralogical properties of all soils. Generally, soluble sulfates less than 2,000 ppm are considered to be a low value, therefore, all clay materials present low soluble sulfate content. A method formulated by Puppala et al. (1999), which is a modified standard gravimetric procedure, was used for measuring the amount of soluble sulfates along with a calorimetric based TxDOT method.

Regarding the clay mineralogy, X-Ray diffraction, the most popular method, has been utilized for this research. Fort Worth, San Antonio, Bryan and Paris clays predominantly contain montmorillonite, signifying the potential for greater volume change in the field. Although the Houston clay contains less montmorillonite, the value is still considerable. El Paso clay contains noticeably low amount of montmorillonite.

Table 4.3: Chemical and Mineralogical Properties of Soils

Property	Site Location					
	Fort Worth	Houston	Bryan	Paris	San Antonio	El Paso
Organic Content (%)	5.6	3.2	N/A	3.2	3.4	1.6
Soluble Sulfates (ppm)	358	247	498	136	82	1202
Cation Exchange Capacity (meq/100 g)	117	76	77	133	96	57
Specific Surface Area (m^2/gm)	314	236	205	431	269	167
Montmorillonite (%)	50	36	45	70	42	8
Kaolinite (%)	34	38	18	17	40	29
Illite (%)	16	26	37	13	18	63

Free-free resonant column (FFRC) tests were performed as per proposed by ASTM D-4015. The seismic modulus at optimum moisture content for all six sites is shown in Table 4.4.

Table 4.4: Seismic Modulus Test Results

Property	Site Location					
	Fort Worth	Houston	Bryan	Paris	San Antonio	El Paso
Seismic Modulus (ksi)	14	19	21	21	20	9

4.4 Preparation and Conditioning of Specimens

The volume change that may occur with a potentially expansive soil depends on several factors, including the effects of compaction and moisture conditioning. Proper compaction of the subgrade at the appropriate moisture content is typically the most economical means of mitigating problems associated with expansive soils.

The current Texas Department of Transportation (TxDOT) compaction practice consists of compacting clayey specimens as per Tex-114-E - Laboratory Compaction Characteristics and Moisture-Density Relationship of Subgrade and Embankment Soils. In this procedure, appropriate amount of material is thoroughly mixed with water to ensure even distribution of water throughout. The specimens are then allowed to cure before compacting. The samples, 6 in. in height and 4 in. in diameter, are compacted in four 1.5 in. thick lifts at 25 blows per lift using a 5.5-lb hammer with a drop height of 12 in.. Specimens are then extruded and conditioned as appropriate.

As stated by Sabnis et al. (2008), several problems are observed with this procedure. Such problems include separation of the specimens at the interface of the layers during the drying process as well as capillary lamination created at the interface of the compaction lifts during the saturation process. The permeability of the specimens is so low that the middle of the specimens is sometimes dry after ten days of capillary saturation. During triaxial tests, it is not uncommon that the specimens fail at the interface of the lifts. Also, the height of the specimens (6 in.) is found to be unreliable for strength and stiffness tests.

For the purpose of minimizing these problems, Sabnis et al. (2008) recommended static compaction for preparing the specimens. In this method, specimens with dimensions of 4 in. by 8 in. are prepared in one single lift using a static compactor. All clay specimens are prepared at optimum moisture content and then subjected to moisture conditioning (either drying or wetting). For detailed compaction and moisture conditioning procedures please refer to Sabnis et al. (2008).

4.4.1 Drying Phase

The compacted specimens are extruded, covered with cellophane wrap and subjected to drying in a conventional oven at 104ºF. This temperature is significantly lower than the 140ºF normally used by

TxDOT. The temperature is reduced to ensure that the specimens would not suffer severe cracking during drying. After every 24 hours, the specimen is taken out of the oven and changes in the dimensions (length and diameter) and weights of the specimens are measured and recorded, and FFRC tests are performed on them until the decrease in weight in two consecutive days is about 0.1%. As a result of the temperature used, no major cracks were evident on the specimens. Typically, the variations in dimensions, modulus and moisture become reasonably constant after 10 to 15 days.

Typical shrinkage of the specimens is shown in Figure 4.1. The changes in diameter and length are more pronounced between 100 hrs and 300 hours, after which the specimen shrinks rather gradually. As shown in Figure 4.2, about three weeks (approximately 500 hours) are necessary to bring the specimens to constant moisture content. Under these conditions, the modulus increase rapidly during the first ten days, but the change in modulus is rather small past that time.

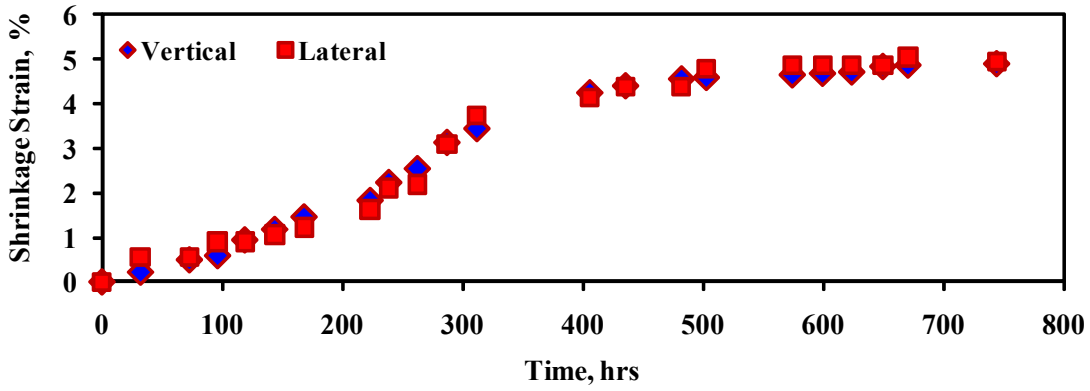

Figure 4.1: Change in Shrinkage Strain vs. Time during Drying

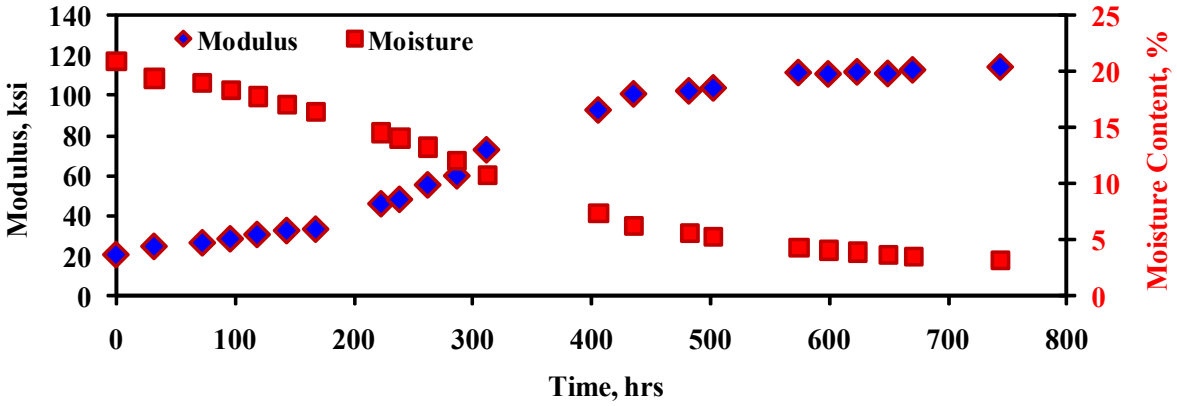

Figure 4.2: Change in Seismic Modulus and Moisture Content vs. Time during Drying

4.4.2 Saturation Phase

The specimens are extruded and covered with cellophane wrap. A filter paper and a porous stone are placed on top of the specimen. Additionally, a hollow plastic cylinder is securely placed on top of the specimen using a membrane. A hose clamp is used to ensure that water would not penetrate from the sides. The specimen is placed on top of a porous stone and subjected from top to bottom saturation by filling the plastic mold with water. The entire lengths of the specimens can be saturated in less than two days. Changes in the dimensions and weights of the specimens are measured, and FFRC tests are performed on them until the specimens become saturated throughout.

Figures 4.3 and 4.4 show typical results of the wetting phase. As per Figure 4.3, the diametric expansion of the specimen was recorded as about 1% whereas vertical expansion was approximately 2.5%. Typical change in modulus and moisture content with time is displayed in Figure 4.4. As initially moisture content increases, seismic modulus also increases after which it starts decreasing until it becomes almost negligible when the specimen gets saturated.

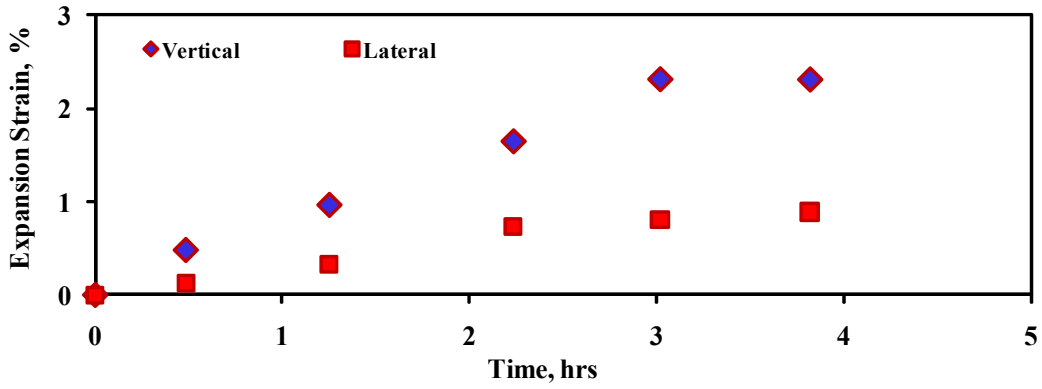

Figure 4.3: Change in Expansion Strain vs. Time during Saturation

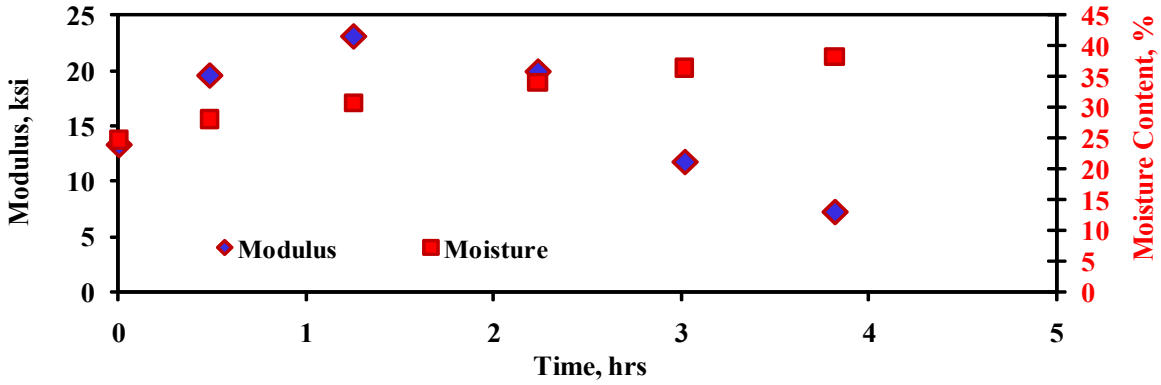

Figure 4.4: Change in Seismic Modulus and Moisture Content vs. Time during Saturation

4.5 Development of Relationships

A number of parameters were measured with different moisture conditioning processes. These parameters were used to develop trends, relationships and models for estimating the changes in strains and modulus with moisture. The main parameters used in establishing relationships are moisture content, shrinkage and expansion strains and seismic modulus. The relationships are presented for three different moisture conditioning processes represented in Figure 4.5. In the first process, called Dry-from-Optimum (DFO), specimens were compacted at their corresponding optimum moisture contents and then subjected to drying. In the second process, Saturated-from-Optimum (SFO), specimens prepared at their optimum moisture contents were subjected to saturation. The third process Dry-from-Saturated (DFS) consisted of moisture conditioning specimens prepared at their corresponding optimum moisture contents to saturation first and then drying the saturated specimens. Typical test results of the three moisture conditioning processes will be presented in the following sections using the test data of clay material from Fort Worth.

The relationship between these three processes is schematically represented in Figure 4.5. The origin represents the optimum moisture content (OMC) and zero strain. As the specimen is moisture conditioned, its moisture content increases with increase in expansion strain, which is represented as the SFO model. As the specimen is subjected to drying process its moisture content decreases and shrinkage strain increases, which is represented as the DFO model. Drying after moisture conditioning process is also shown as the DFS model.

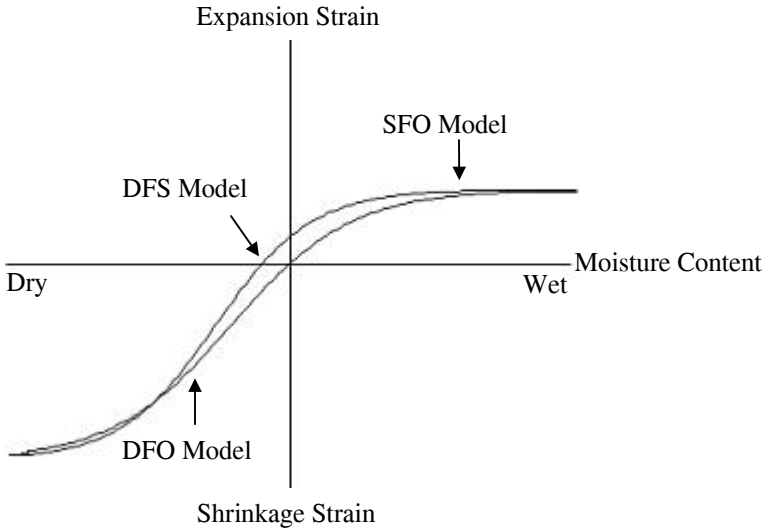

Figure 4.5: Conditioning Process Model

4.5.1 Dry from Optimum Process (DFO)

The shrinkage strains and corresponding moisture contents as shown in Figures 4.1 and 4.2 are related in Figure 4.6. The shrinkage strains and moisture content seem well correlated. Shrinkage strains increase rapidly until moisture content is decreased to 5% after which, it is almost constant.

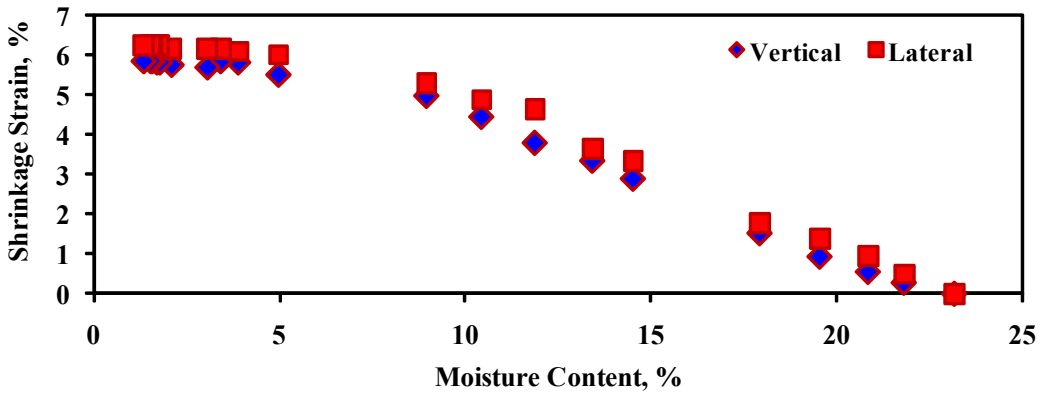

Figure 4.6: Change in Shrinkage Strain vs. Moisture Content (Fort Worth)

Typical variations in seismic modulus with moisture content for one specimen are shown in Figure 4.7. The modulus increased rapidly until moisture content is decreased to 5% after which it leveled off to a constant value of about 220 ksi.

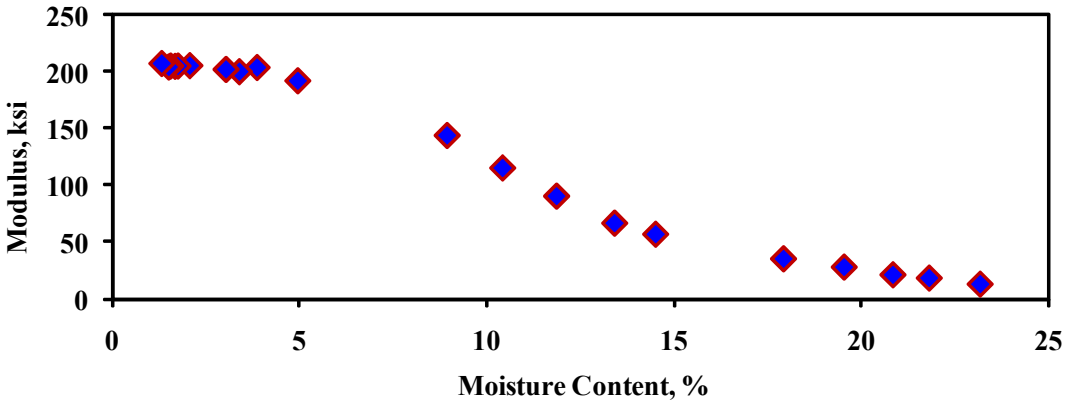

Figure 4.7: Change in Seismic Modulus vs. Moisture Content (Fort Worth)

4.5.2 Saturated from Optimum Process (SFO)

Similarly, the relationships of expansion strains and moisture content are shown in Figure 4.8. With increase in the moisture content, the lateral and vertical expansion strains also increased substantially to 1% and 2.5%, respectively.

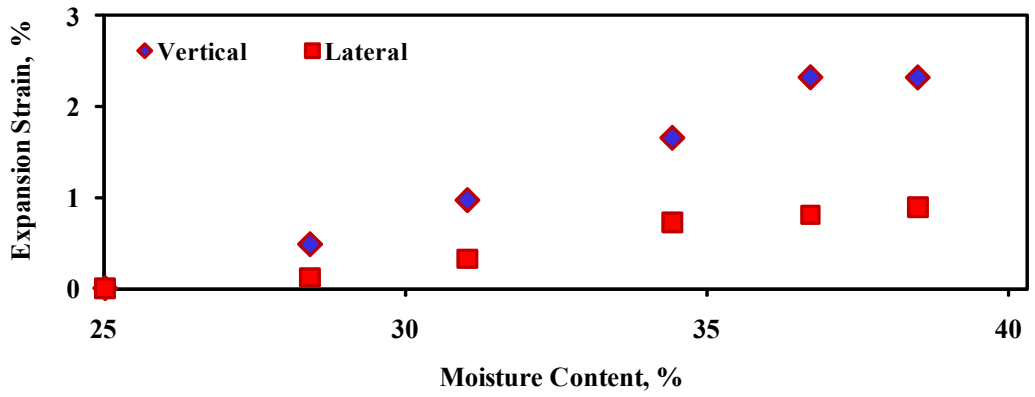

Figure 4.8: Typical Variations in Expansion Strains with Moisture Content (Fort Worth)

Typical variations in seismic modulus with moisture content for one specimen are shown in Figure 4.9. The modulus initially increases until the moisture content increases to about 30% after which the modulus starts decreasing until it becomes less than 10 ksi at a moisture content of about 38%.

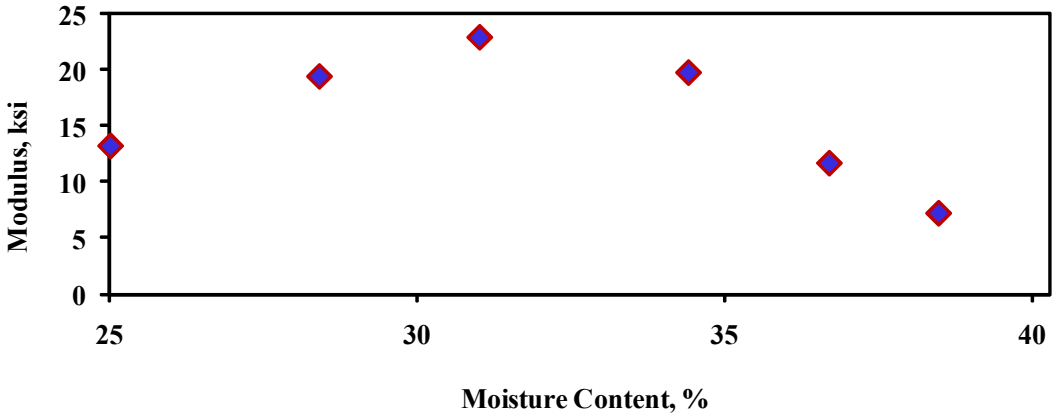

Figure 4.9: Typical Variations in Seismic Modulus with Moisture Content (Fort Worth)

4.5.3 Dry from Saturation Process (DFS)

The relationships of shrinkage strains and moisture content are shown in Figure 4.10. The lateral and vertical shrinkage strains initially decrease rapidly and then become almost constant as the specimen gets completely dried.

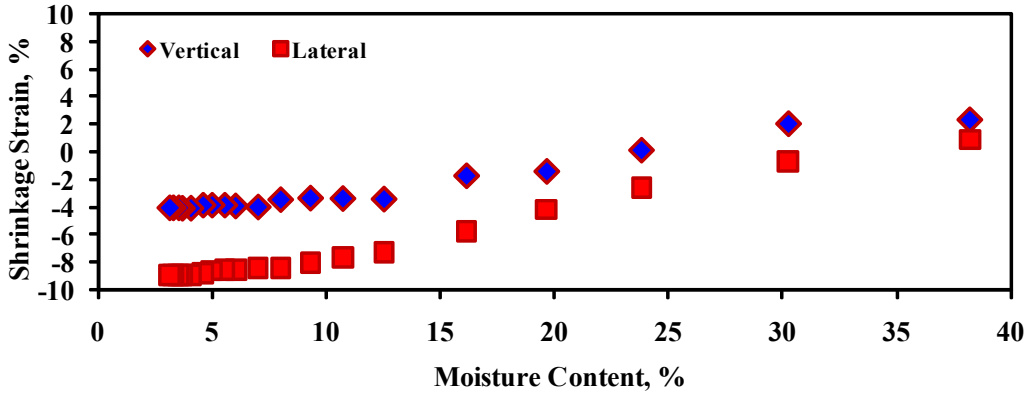

Figure 4.10: Typical Variations in Shrinkage Strains with Moisture Content (Fort Worth)

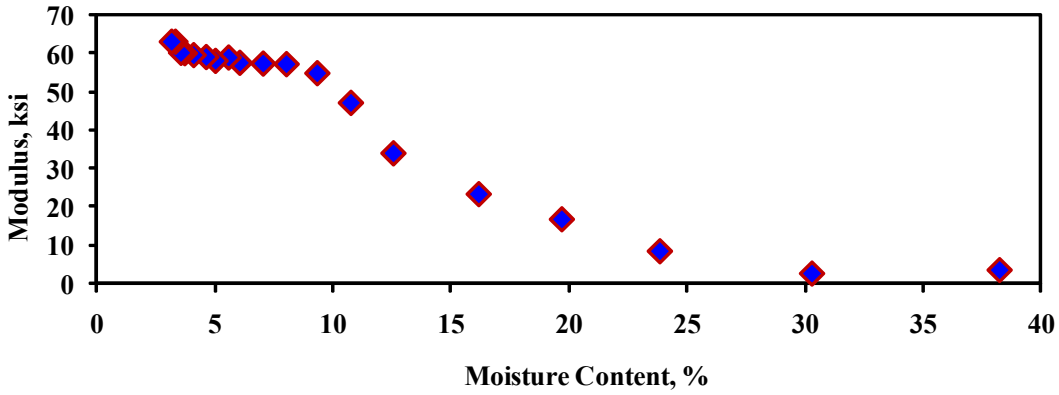

Figure 4.11: Typical Variations in Seismic Modulus with Moisture Content (Fort Worth)

Typical variation in seismic modulus with moisture content for one specimen is shown in Figure 4.11. The modulus increased rapidly until moisture content is decreased to 10% after which it leveled off to a constant value of about 60 ksi.

4.6 Moisture Conditioning Process

The variations in modulus and lateral/vertical strains were evaluated under two different moisture conditioning processes. In the first process, called combined Dry-from-Optimum and Saturated-from-Optimum (combined DFO and SFO), as the name implies, DFO specimens were

combined with SFO specimens. This combination was implemented for simplicity and ease of evaluation. Sabnis (2008) proposed two separate equations for DFO and SFO processes. With further analysis, one equation was obtained to better describe both moisture conditioning processes. The second process, called Dry-from-Saturation (DFS), consisted of moisture conditioning specimens prepared at their corresponding optimum moisture contents to saturation first and then drying the saturated specimens.

4.7 Normalization Process

While developing the mathematical models, the moisture contents, strains and moduli were first normalized, in order to generalize the relationships for the different types of clay materials.

The moisture contents were normalized by dividing an individual moisture content by the OMC (Equation 4.1). Moduli were normalized by dividing the individual modulus by the modulus at OMC (Equation 4.2). For the lateral and vertical strains, the minimum strain values were subtracted from the individual strains and then divided by the difference between the minimum and maximum strains (Equation 4.3). Table 4.5 summarizes the minimum and maximum strain values for both processes.

$$NMC = \frac{Individual\ Moisture\ Content}{OMC} \tag{4.1}$$

$$E_n = \frac{Individual\ Modulus}{Modulus\ at\ OMC} \tag{4.2}$$

$$\varepsilon_n = \frac{\varepsilon - \varepsilon_{\min}}{\varepsilon_{\max} - \varepsilon_{\min}} \tag{4.3}$$

Table 4.5: Maximum and Minimum Strain Values

Site Location	Combined DFO and SFO				DFS			
	Lateral Strain		Vertical Strain		Lateral Strain		Vertical Strain	
	εmin	εmax	εmin	εmax	εmin	εmax	εmin	εmax
Fort Worth	-6.45	1.05	-6.21	2.75	-8.90	1.05	-4.08	2.75
Bryan	-4.65	1.66	-4.95	4.13	-7.49	1.66	-3.83	4.13
Paris	-6.80	1.55	-6.71	4.30	-9.20	1.55	-5.49	4.30
San Antonio	-5.45	1.70	-5.58	4.66	-8.45	1.70	-2.29	4.66
El Paso	-2.10	0.41	-1.49	0.71	-4.46	0.41	-0.60	0.71

The normalized lateral and vertical strains from the combined DFO and SFO processes are related to the normalized moisture content in Figure 4.12. Figure 4.13 shows the variation in normalized lateral and vertical strains with normalized moisture content for the DFS process. The normalized lateral and vertical strains and normalized moisture content seem well correlated.

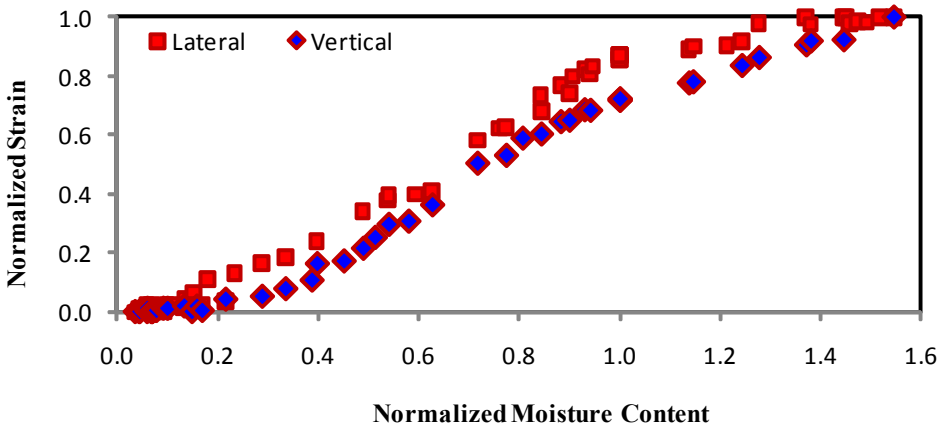

Figure 4.12: Typical Variations in Normalized Lateral and Vertical Strains with Normalized Moisture Content (Combined DFO and SFO Process)

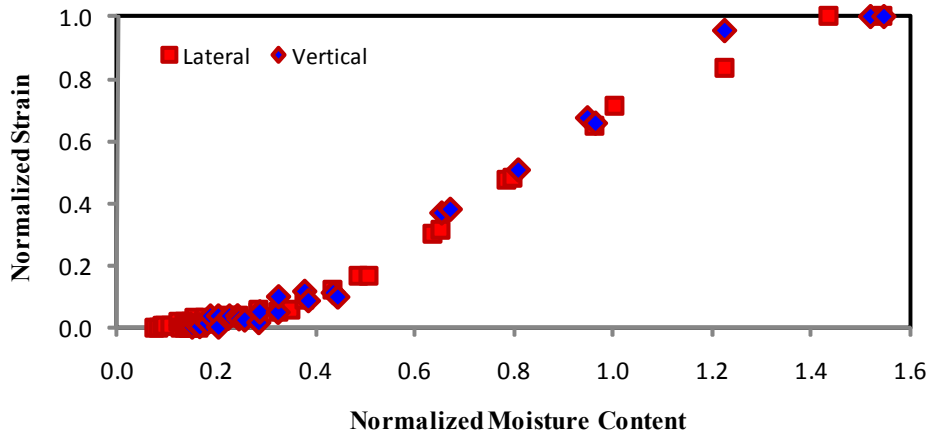

Figure 4.13: Typical Variations in Normalized Lateral and Vertical Strains with Normalized Moisture Content (DFS Process)

The variation in normalized modulus with normalized moisture content for the combined DFO and SFO process is shown in Figure 4.14. The normalized modulus increases until the NMC decreases to 0.2; after which it is almost a constant. In this case, the maximum normalized modulus at a "Combined DFO and SFO condition" was approximately 14, which indicates that upon the drying process modulus increased 14 times as compared to its value at the OMC.

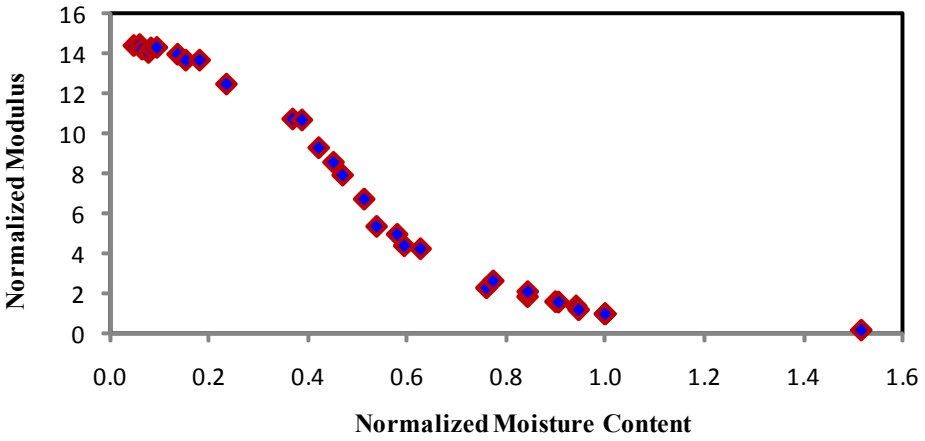

Figure 4.14: Typical Variation in Normalized Modulus with Normalized Moisture Content (Combined DFO and SFO Process)

The variation in normalized modulus with normalized moisture content for the DFS process is shown in Figure 4.15. The normalized modulus initially increases until the NMC decreases to 0.2, after which it is almost a constant. However, the normalized modulus is significantly higher than the previous conditioning process.

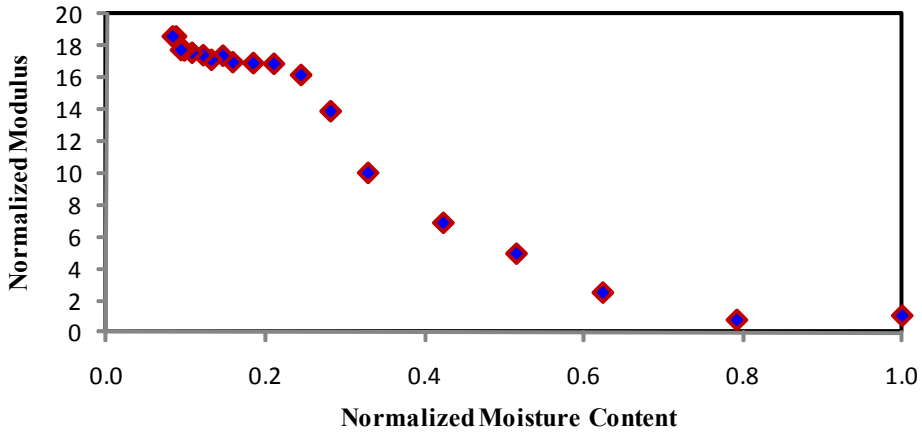

Figure 4.15: Typical Variation in Normalized Modulus with Normalized Moisture Content (DFS Process)

4.8 Prediction Model

A number of mathematical relationships can describe the correlation between the normalized lateral and vertical strains and the normalized modulus with NMC. To select the mathematical models, an extensive curve fitting analysis was performed with the use of an off-the-shelf software package

called Table Curve 2D v5 Automated Curve Fitting and Equation Discovery to compare and evaluate many different curve fit equations. Given the number and complexity of curve fit equations, certain parameters were focused on to minimize the number of constants and equations to be able to simplify a model that will be adequate to the laboratory tests and measured data.

After evaluating each possible equation, a three parameter sigmoid equation was found to closely correlate to the measured data for all cases. The sigmoid equation is in the form of:

$$y = \frac{A}{1 + e^{-(\frac{NMC - B}{C})}} \tag{4.4}$$

where y is either the normalized strain, ε_n or normalized modulus, E_n,; A, B, C = parameters obtained from curve fitting; and NMC = normalized moisture content.

The fit parameters for the combined DFO and SFO strain process are summarized in Table 4.6. A sensitivity analysis indicates that the results are not as sensitive to parameters A and B as to parameter C. Due to the fact that coefficient A averaged to a value of 1 and coefficient B averaged to values of 0.75 and 0.90 for lateral and vertical strain, respectively, a one parameter sigmoid equation was obtained for this process, as shown in Table 4.7. Similarly, in the DFS strain process, parameter C was set to a constant of 0.17 and 0.20 for lateral and vertical strain, respectively, leading to a one parameter sigmoid equation (see Table 4.8).

Table 4.6: Best Fit Parameters - Normalized Shrinkage Strains vs. Normalized Moisture Content (Combined DFO and SFO Process)

Site Location	Lateral Strain				Vertical Strain			
	A	B	C	R^2	A	B	C	R^2
Fort Worth	0.98	0.66	0.18	0.99	0.92	0.72	0.19	0.99
Bryan	1.02	0.84	0.17	1.00	0.82	0.81	0.21	0.98
Paris	0.94	0.72	0.15	0.99	0.98	0.88	0.22	0.98
San Antonio	0.97	0.70	0.17	0.99	0.98	0.91	0.23	0.99
El Paso	1.01	0.75	0.16	0.99	1.07	0.94	0.16	1.00

Table 4.7: Modified Best Fit Parameters - Normalized Shrinkage Strains vs. Normalized Moisture Content (Combined DFO and SFO Process)

Site Location	Lateral Strain				Vertical Strain			
	A	B	C	R^2	A	B	C	R^2
Fort Worth	1.0	0.75	0.19	0.97	1.0	0.9	0.25	0.94
Bryan	1.0	0.75	0.18	0.98	1.0	0.9	0.26	0.97
Paris	1.0	0.75	0.18	0.99	1.0	0.9	0.23	0.98
San Antonio	1.0	0.75	0.18	0.99	1.0	0.9	0.24	0.99
El Paso	1.0	0.75	0.16	0.99	1.0	0.9	0.15	0.99

Table 4.8: Best Fit Parameters - Normalized Shrinkage Strains vs. Normalized Moisture Content (DFS Process)

Site Location	Lateral Strain				Vertical Strain			
	A	B	C	R^2	A	B	C	R^2
Fort Worth	1.0	0.81	0.17	0.99	1.0	0.81	0.20	0.99
Bryan	1.0	0.72	0.17	0.98	1.0	0.75	0.20	0.99
Paris	1.0	0.69	0.17	0.98	1.0	0.69	0.20	0.99
San Antonio	1.0	0.81	0.17	0.98	1.0	0.77	0.20	0.99
El Paso	1.0	0.93	0.17	0.99	1.0	0.59	0.20	0.95

A two parameter sigmoid equation was used for estimating moduli for both moisture conditioning regimes, by setting coefficient C to average constant values of -0.17 and -0.12 for the combined DFO and SFO and DFS process, respectively, as shown in Table 4.9.

Table 4.9: Best Fit Parameters - Normalized Modulus vs. Normalized Moisture Content

Site Location	Combined DFO and SFO				DFS			
	A	B	C	R^2	A	B	C	R^2
Fort Worth	-16.44	0.46	-0.17	0.99	-20.12	0.36	-0.12	0.99
Bryan	-10.47	0.46	-0.17	0.97	-112.04	0.33	-0.12	0.99
Paris	-13.66	0.49	-0.17	0.98	-13.08	0.20	-0.12	0.96
San Antonio	-6.06	0.63	-0.17	0.97	-50.38	0.12	-0.12	0.97
El Paso	-59.57	0.17	-0.17	0.98	-332.58	0.03	-0.12	0.99

4.9 Presentation of Results

Figure 4.16 shows the normalized lateral and vertical strains and NMC best fit curves obtained using Equation 4.4. The best fit curves follow the measured data quite well. The values of parameter C

for the lateral and vertical strains (combined DFO and SFO process) are summarized in Table 4.7. The lateral strains correlated well with the NMC since the R^2 values were close to 1.

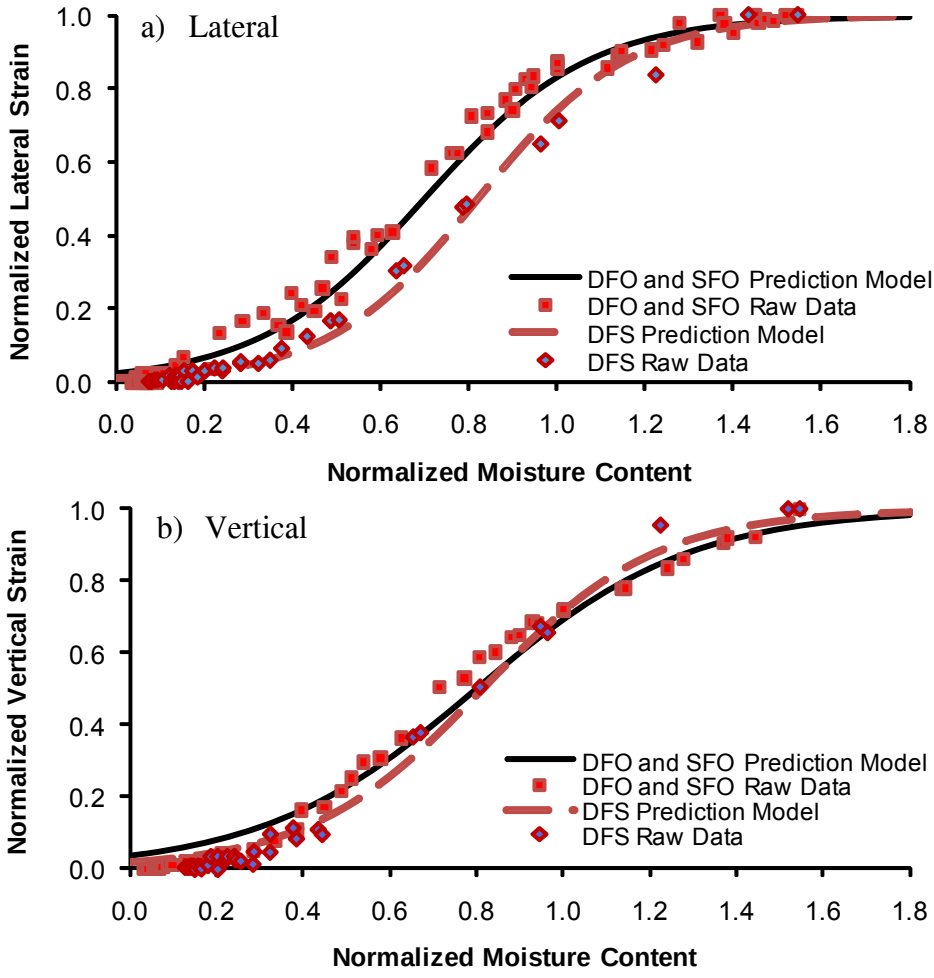

Figure 4.16: Strain Prediction Model (Fort Worth)

The normalized modulus and NMC are related as shown in Figure 4.17. The values of A and B for both the combined DFO and SFO and DFS processes are summarized in Table 4.9. The normalized modulus was well correlated to NMC with R^2 values ranging from 0.96 to more than 0.99.

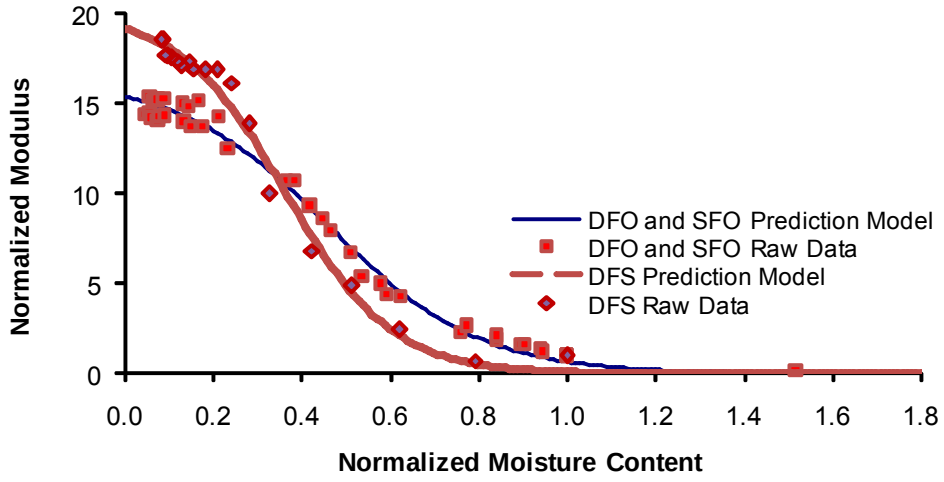

Figure 4.17: Modulus Prediction Model (Fort Worth)

The fundamental objective of obtaining these trends and relationships is to be able to use the models to obtain fit parameters and ultimately predict strains and modulus at different moisture contents based on index and chemical-mineralogical properties of soils. Once the development of these prediction models was analyzed and evaluated, the next step was to relate these results to more readily-available parameters, such as common index properties. This correlation analysis is presented in the following chapter. Chapter 6 is dedicated to relating the results to different chemical-mineralogical properties of soils.

CHAPTER 5: IMPACT OF INDEX PROPERTIES

5.1 Introduction

After developing the mathematical models, the next step was to relate them to common index properties, including plasticity index, liquid limit, plastic limit, optimum moisture content, dry unit weight, and seismic modulus. The process was ultimately expanded to be able to use the developed models to predict strain and modulus at different moisture content based on index properties. The trends and relationships obtained are discussed in this chapter.

Figure 5.1 summarizes the steps followed for establishing relationships for estimating strains and modulus from index properties of soils. The first step consisted of performing the appropriate laboratory tests and obtaining the main parameters used in establishing relationships. The next step involved the process of normalization in order to generalize the relationships for different types of clay materials. The process of normalization of the lateral and vertical strains consists of determining the minimum and maximum strains. The selection of a mathematical model capable of describing the correlation between the normalized lateral and vertical strains and the normalized modulus with normalized moisture content was the next step. The selection of the best fit model was performed by the analysis, comparison and evaluation of many different curve fit equations. The next step involved the estimation of fit parameters and their correlation with index parameters of soils, as explained in the following section. The fit parameters and the minimum and maximum strains can then be used as input to Equations 4.3 and 4.4 for predicting strains and/or modulus by knowing the moisture content.

5.2 Estimation of Fit Parameters

The development process started with a trend analysis among the index properties and the fit parameters of the equations presented in the previous chapter. Equation 4.4 was proposed as the best fit model to estimate the lateral and vertical strains as well as the modulus at a particular moisture contents for both the combined DFO and SFO process and the DFS process. The results of the trend analysis between the fit parameters and the index properties of all clay materials except Houston are shown in Tables 5.1 through 5.4. The results from the Houston clay were excluded for validation purposes since it is not appropriate to validate a model with data used in the development of the model.

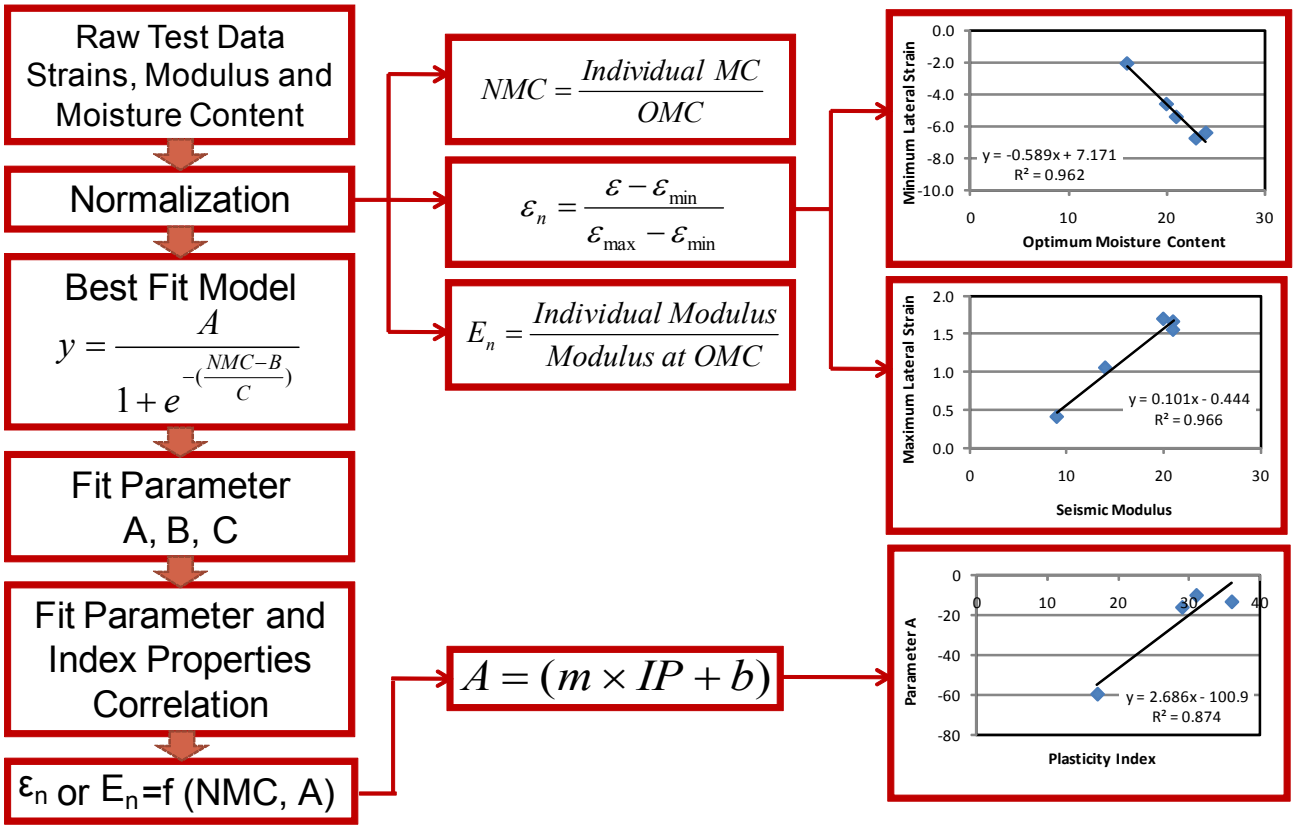

Figure 5.1: Flowchart of Strain or Modulus Prediction Based on Index Properties

A linear regression was made between each of the fit parameters A through C and the index parameters of the soils. An example of estimating the fit parameter C for lateral strain from the index parameters is shown in Figure 5.2. The coefficients of determination (R^2 values) were used as an indication of quality of fit. In this study, an index parameter was considered correlated with a fit parameter when the R^2 value was between 0.75 and 1.0. When the R^2 was between 0.6 and 0.75, the index parameter was considered marginally correlated.

5.2.1 Combined DFO and SFO Process

For the lateral strain, fit parameter C is correlated to the liquid limit (LL), plastic limit (PL), optimum moisture content (OMC), dry unit weight (DUW), and seismic modulus (SM), whereas the plasticity index (PI) is poorly correlated to Parameter C (see Table 5.1). As such, only the LL, PL, OMC, DUW and SM were further considered in the development of the models. For the vertical strain, fit parameter C is correlated to PI, LL, PL, OMC, and SM, whereas the DUW is poorly correlated. As such, all index properties except DUW were considered in the development of the models.

Regarding the modulus, fit parameter A is well correlated to PI, LL, PL, DUW and SM and marginally correlated with the OMC. As such, all index properties except OMC were considered in the development of the models. On the other hand, fit parameter B correlates only to PI, PL and DUW as shown in Table 5.2.

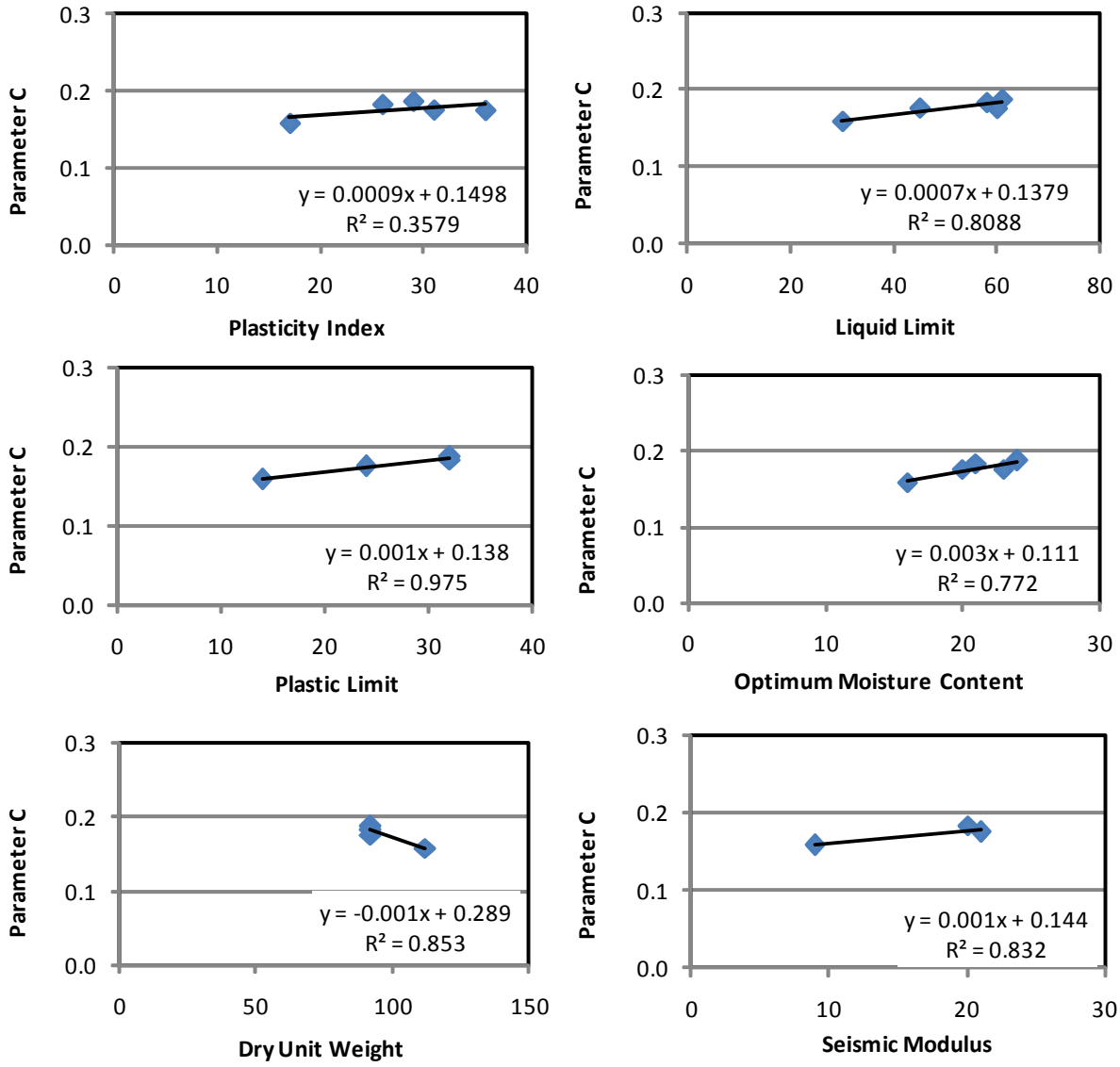

Figure 5.2: Example of Correlations between Index Properties of Soils and Parameter C (Lateral Strain, Combined DFO and SFO Process)

Table 5.1: Correlation Analysis between Parameter C and Index Properties
(Combined DFO and SFO Process)

Index Property	Lateral Strain			Vertical Strain		
	Slope	Intercept	R^2	Slope	Intercept	R^2
Plasticity Index (PI)	9.33.E-04	0.15	0.36	7.97.E-03	0.02	0.97
Liquid Limit (LL)	7.44.E-04	0.14	0.81	3.00.E-03	0.06	0.99
Plastic Limit (PL)	1.47.E-03	0.14	0.98	4.91.E-03	0.09	0.87
Optimum Moisture Content (OMC)	3.10.E-03	0.11	0.77	0.01	-0.04	0.90
Dry Unit Weight (DUW)	-1.17.E-03	0.29	0.85	-2.42.E-03	0.47	0.31
Seismic Modulus (SM)	1.63.E-03	0.14	0.83	0.01	0.08	0.95

Table 5.2: Correlation Analysis between Modulus and Index Properties
(Combined DFO and SFO Process)

Index Property	Parameter A			Parameter B		
	Slope	Intercept	R^2	Slope	Intercept	R^2
Plasticity Index (PI)	2.69	-100.92	0.87	0.02	-0.11	0.92
Liquid Limit (LL)	1.57	-105.74	0.93	0.01	-0.01	0.71
Plastic Limit (PL)	2.55	-89.05	0.82	0.02	-0.08	0.79
Optimum Moisture Content (OMC)	5.42	-134.04	0.60	0.04	-0.36	0.51
Dry Unit Weight (DUW)	-2.38	206.51	0.97	-0.02	2.18	0.85
Seismic Modulus (SM)	3.61	-82.55	0.78	0.03	-5.33.E-03	0.68

5.2.2 DFS Process

For the lateral strain, fit parameter B is well correlated to PI, OMC, and SM and marginally correlated to the LL and DUW. PL is considered poorly correlated (see Table 5.3). As such, only the PI, OMC and SM were further considered in the development of the models. Also shown in Table 5.3 is the correlation analysis for the vertical strain. This table shows that fit parameter B is correlated to PI, LL, PL, OMC, and SM, whereas the DUW is considered marginally correlated. As such, all index properties except DUW were considered in the development of the models.

Table 5.3: Correlation Analysis between Parameter B and Index Properties (DFS Process)

Index Property	Lateral Strain			Vertical Strain		
	Slope	Intercept	R^2	Slope	Intercept	R^2
Plasticity Index (PI)	-0.01	1.15	0.94	0.01	0.36	0.79
Liquid Limit (LL)	-0.01	1.09	0.65	0.01	0.41	0.91
Plastic Limit (PL)	-9.53.E-03	0.81	0.01	0.01	0.42	0.97
Optimum Moisture Content (OMC)	-0.03	1.43	0.77	0.03	0.15	0.92
Dry Unit Weight (DUW)	0.01	0.05	0.64	-0.01	1.54	0.73
Seismic Modulus (SM)	-0.02	1.08	0.98	0.01	0.48	0.76

In regards to the modulus, fit parameter A is well correlated to PI, LL, OMC, DUW and SM, and marginally correlated to PL (see Table 5.4). As such, all index properties except PL were considered in the development of the models. On the other hand, fit parameter B correlates only to PI and OMC whereas SM is considered marginally correlated and the rest of the index properties are poorly correlated, as shown in Table 5.4.

5.3 Estimation of Maximum and Minimum Strains

As indicated in Chapter 4, the process of normalization of the lateral and vertical strains consisted of knowing the minimum and maximum strains as reported in Table 4.5. The same linear

regression process as the previous section was used to estimate these parameters from the index parameters of the soils. The results of the trend analysis between the minimum and maximum strains and the index properties of all clay materials except Houston are shown in Tables 5.5 through 5.7. Once again, the results from the Houston clay were excluded for future validation purposes. An example of estimating the minimum and maximum strains for lateral strain from the index parameters is shown in Figures 5.3 and 5.4.

5.3.1 Combined DFO and SFO Process

For the lateral and vertical strains, the minimum strain values are correlated to the PI, LL, OMC, DUW, and SM, whereas the PL is marginally correlated to minimum strain (see Table 5.5). The maximum strains, is well correlated to PI, OMC, DUW and SM, whereas the LL is marginally correlated and the PL is poorly correlated. For the vertical strains, the maximum strain is also well correlated to LL.

Table 5.4: Correlation Analysis between Modulus and Index Properties (DFS Process)

Index Property	Parameter A			Parameter B		
	Slope	Intercept	R^2	Slope	Intercept	R^2
Plasticity Index (PI)	17.03	-600.61	0.85	0.02	-0.38	0.80
Liquid Limit (LL)	9.73	-600.07	0.95	0.01	-0.06	0.27
Plastic Limit (PL)	15.46	-498.30	0.74	3.32.E-03	0.13	0.05
Optimum Moisture Content (OMC)	40.79	-954.14	0.92	0.03	-0.55	0.78
Dry Unit Weight (DUW)	-11.70	1054.66	0.77	-4.01.E-03	0.61	0.08
Seismic Modulus (SM)	23.26	-539.90	0.91	0.02	-0.12	0.60

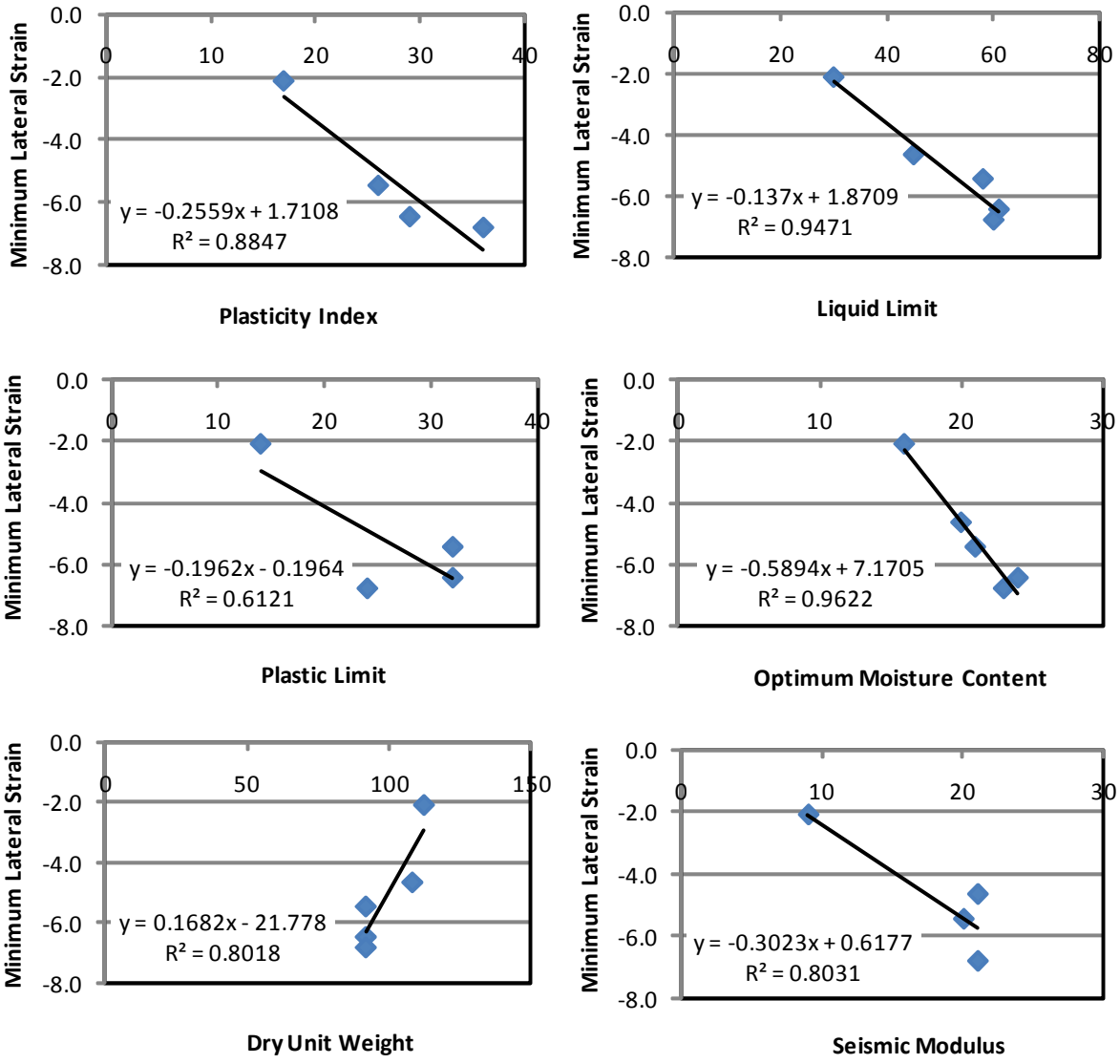

Figure 5.3: Summary of Correlations between Index Properties of Soils and Minimum Lateral Strain (Combined DFO and SFO Process)

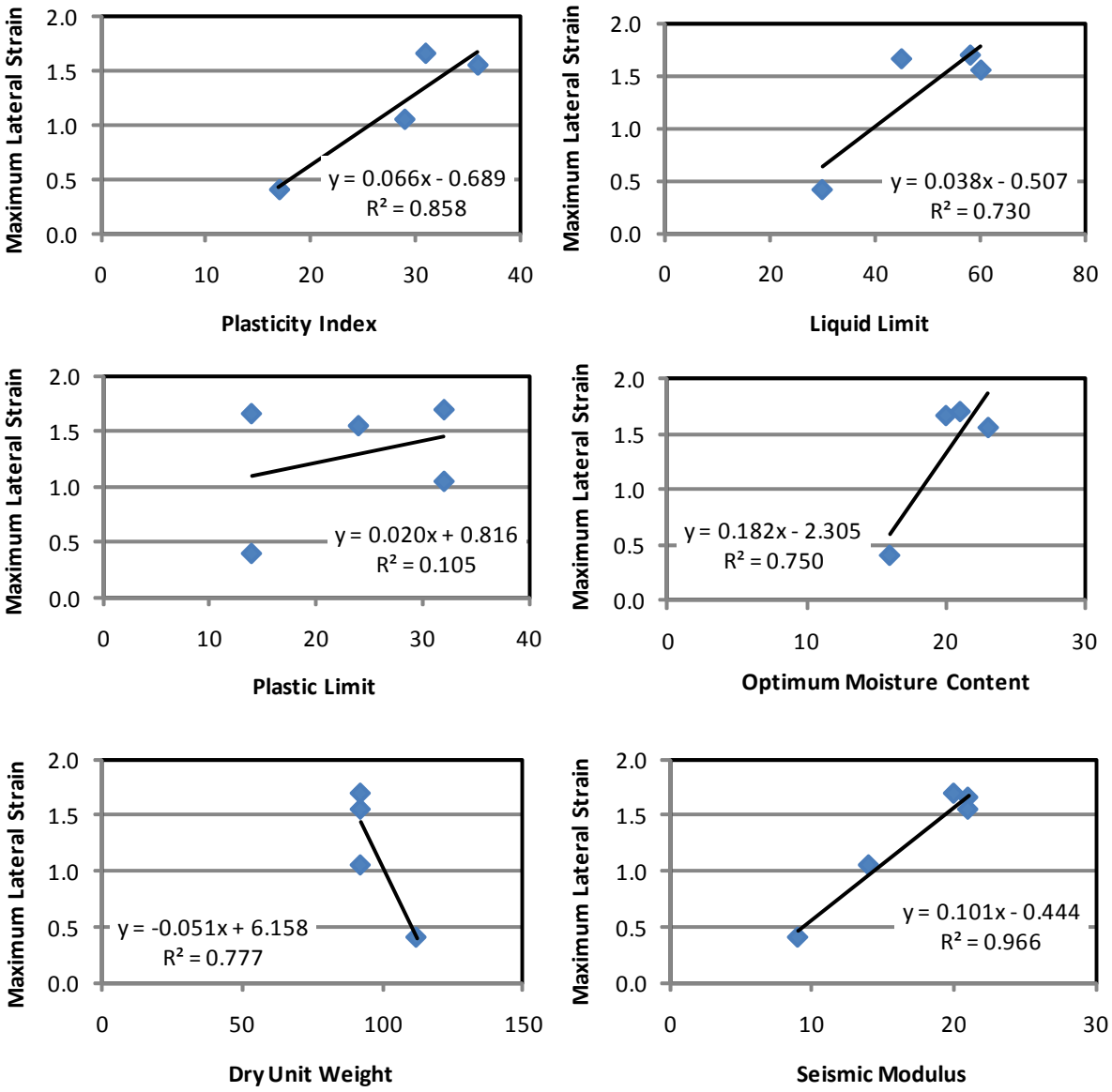

Figure 5.4: Summary of Correlations between Index Properties of Soils and Maximum Lateral Strain (Combined DFO and SFO Process and DFS Process)

Table 5.5: Correlation Analysis between Minimum Strain and Index Properties (Combined DFO and SFO Process)

Index Property	Lateral Strain			Vertical Strain		
	Slope	Intercept	R^2	Slope	Intercept	R^2
Plasticity Index (PI)	-0.26	1.71	0.88	-0.26	2.31	0.80
Liquid Limit (LL)	-0.14	1.87	0.95	-0.15	2.60	0.92
Plastic Limit (PL)	-0.20	-0.20	0.61	-0.23	0.76	0.65
Optimum Moisture Content (OMC)	-0.59	7.17	0.96	-0.63	8.22	0.92
Dry Unit Weight (DUW)	0.17	-21.78	0.80	0.23	-27.67	0.96
Seismic Modulus (SM)	-0.30	0.62	0.80	-0.36	1.78	0.90

Table 5.6: Correlation Analysis between Maximum Strain and Index Properties (Combined DFO and SFO Process and DFS Process)

Index Property	Lateral Strain			Vertical Strain		
	Slope	Intercept	R^2	Slope	Intercept	R^2
Plasticity Index (PI)	0.07	-0.69	0.86	0.20	-2.65	0.93
Liquid Limit (LL)	0.04	-0.51	0.73	0.12	-2.38	0.83
Plastic Limit (PL)	0.02	0.82	0.11	0.07	1.59	0.17
Optimum Moisture Content (OMC)	0.18	-2.31	0.75	0.57	-7.88	0.82
Dry Unit Weight (DUW)	-0.05	6.16	0.78	-0.16	18.60	0.79
Seismic Modulus (SM)	0.10	-0.44	0.97	0.30	-1.73	0.95

5.3.2 DFS Process

For the lateral strain, the minimum strain is well correlated to PI, LL, OMC, DUW and SM; whereas the PL is marginally correlated (see Table 5.7). Also shown in Table 5.7 is the correlation

analysis for the vertical strain. This table shows that minimum strain is well correlated only to PI and LL, whereas the OMC, DUW and SM are considered marginally correlated and Pl is poorly correlated. The maximum strain correlation is the same as the one shown in Table 5.6 because they represent the same point.

Table 5.7: Correlation Analysis between Minimum Strain and Index Properties (DFS Process)

Index Property	Lateral Strain			Vertical Strain		
	Slope	Intercept	R^2	Slope	Intercept	R^2
Plasticity Index (PI)	-0.25	-0.49	0.85	-0.26	3.96	0.96
Liquid Limit (LL)	-0.14	-0.51	0.96	-0.13	2.80	0.83
Plastic Limit (PL)	-0.22	-2.20	0.70	-0.06	-1.85	0.08
Optimum Moisture Content (OMC)	-0.59	4.63	0.92	-0.51	7.27	0.71
Dry Unit Weight (DUW)	0.17	-24.74	0.79	0.16	-19.52	0.65
Seismic Modulus (SM)	-0.33	-1.49	0.88	0.30	1.37	0.72

.

CHAPTER 6: IMPACT OF SOIL CHEMISTRY

6.1 Introduction

In order to further refine the estimation of the changes in modulus and strains, models were developed to relate them to common chemical and mineralogical properties of soils, including organic content, soluble sulfates, cation exchange capacity, specific surface area and clay minerals. Each step in this procedure is explained next.

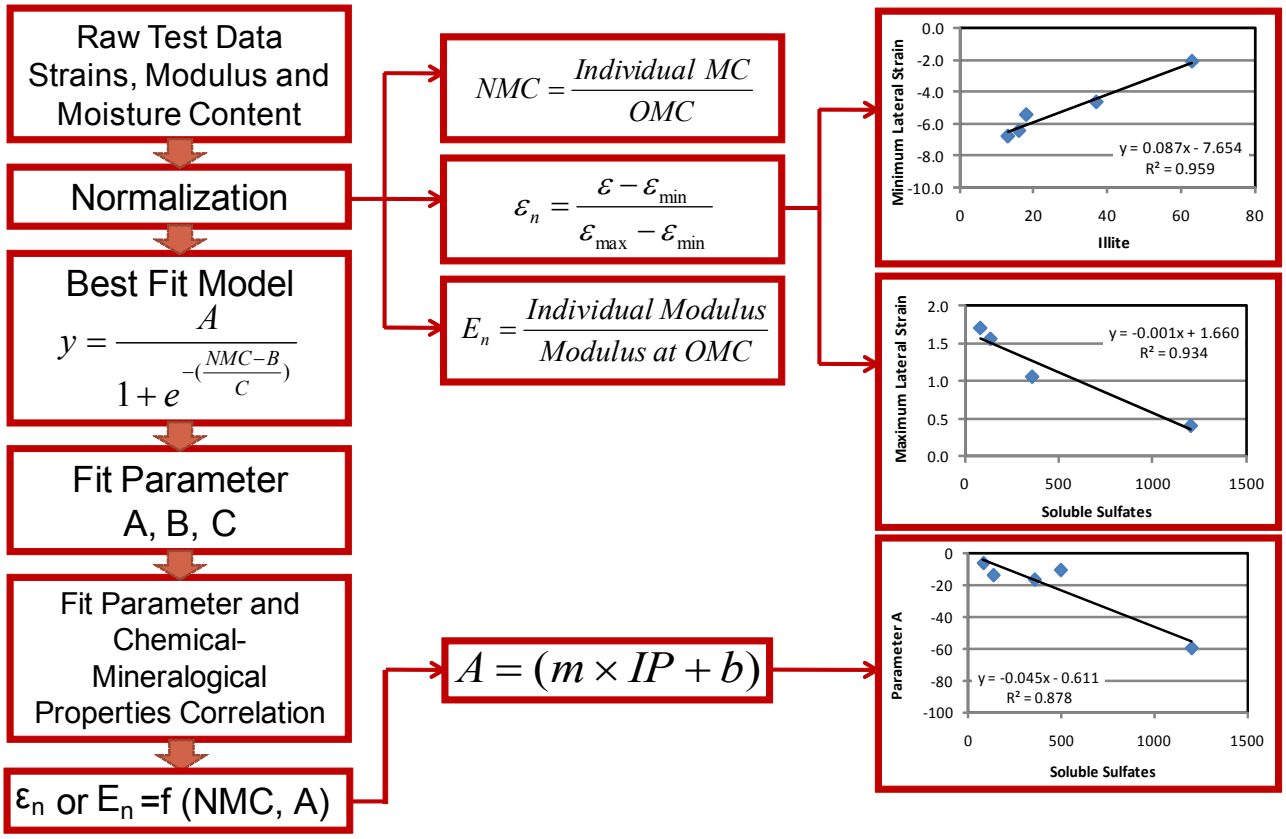

Figure 6.1: Flowchart of Strain or Modulus Prediction Based on Chemical-Mineralogical Properties

Figure 6.1 summarizes the steps followed for establishing relationships for estimating strains and modulus from chemical-mineralogical properties of soils. The first step involved the execution of the appropriate laboratory tests in order to obtain the main parameters used in establishing relationships. The next step involved the normalization process in order to allow the data from the different types of clay materials to be compared by bringing them to a common scale. The process of normalization of the

lateral and vertical strains consists of determining the minimum and maximum strains. Next is the selection of the appropriate mathematical models capable of describing the correlation between the normalized lateral and vertical strains and the normalized modulus with normalized moisture content and adequate to the laboratory tests and measured data. The next step involved the estimation of fit parameters and their correlation with chemical-mineralogical parameters of soils, as explained below. The fit parameters and the minimum and maximum strains can then be used as input to Equations 4.3 and 4.4 for predicting strains and/or modulus by knowing the moisture content.

6.2 Estimation of Fit Parameters

This procedure again started with a trend analysis among the chemical-mineralogical properties and the fit parameters of the equations presented in Chapter 4. The results of the trend analysis between the fit parameters and the chemical- mineralogical properties of all clay materials except Houston are shown in Tables 6.1 through 6.4. One more time, the results from the Houston clay were excluded for validation purposes.

A linear regression was made between each of the fit parameters A through C and the chemical-mineralogical parameters of the soils. An example of estimating the fit parameter C for lateral strain from the chemical-mineralogical parameters is shown in Figure 6.2. Again, the R^2 values were used as an indication of quality of fit with values ranging from 0.75 to 1.0 to indicate good correlation with a fit parameter and values ranging from 0.6 to 0.75 to indicate marginal correlation.

6.2.1 Combined DFO and SFO Process

For the lateral strain, fit parameter C is correlated to the organic content (OC), cation exchange capacity (CEC), specific surface area (SSA), montmorillonite (M), kaolinite (K) and illite (I), and marginally correlated with soluble sulfates (SS) (see Table 6.1). For the vertical strain, fit parameter C is correlated to SS, CEC, and I, whereas the OC and M are considered marginally correlated and the SSA and K are poorly correlated. Regarding the modulus, both fit parameters A and B are well correlated to only SS, M, and I, whereas the OC, CEC, SSA and K are poorly correlated (Table 6.2).

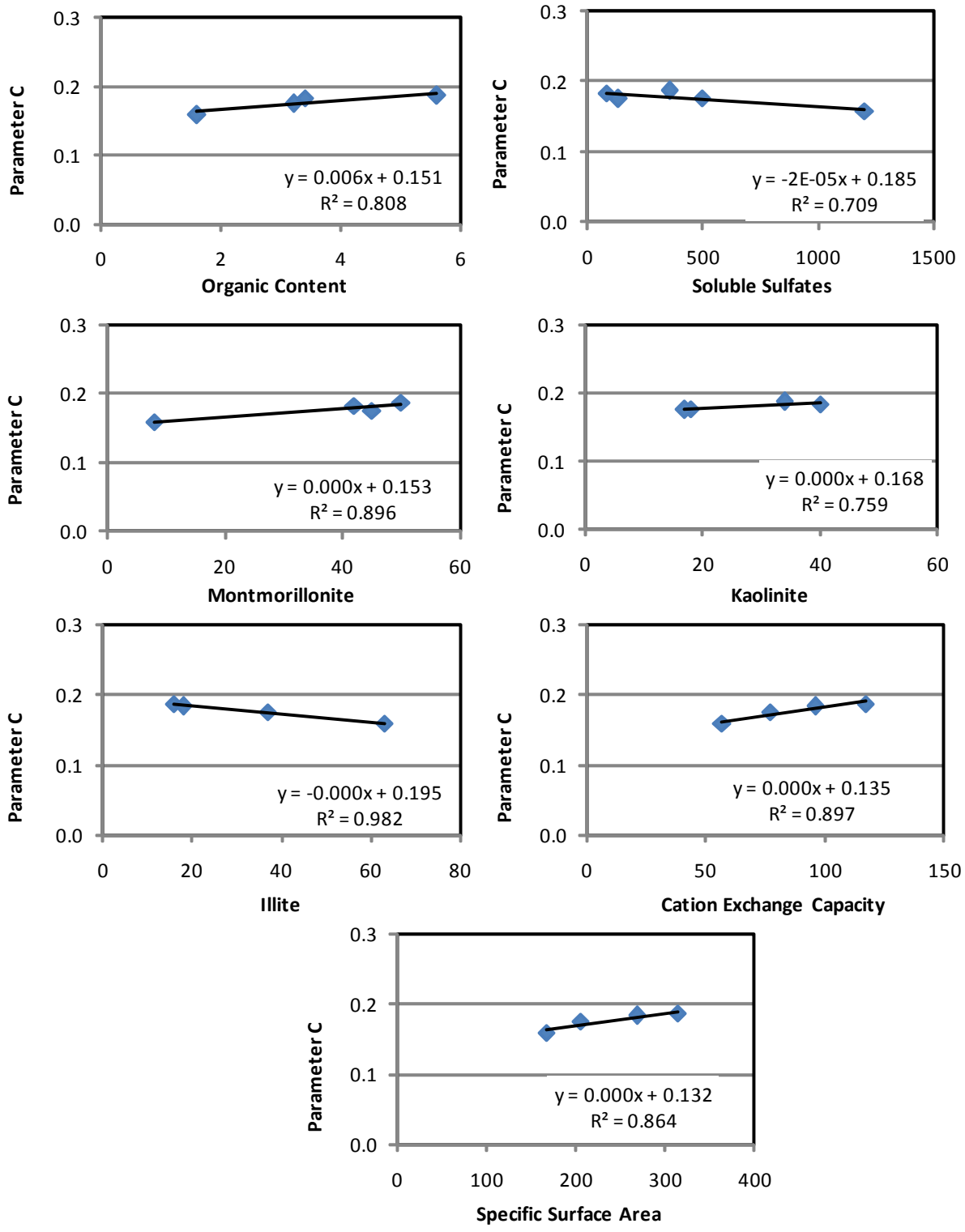

Figure 6.2: Example of Correlations between Chemical-Mineralogical Properties of Soils and Parameter C (Lateral Strain, Combined DFO and SFO Process)

Table 6.1: Correlation Analysis between Parameter C and Chemical-Mineralogical Properties (Combined DFO and SFO Process)

Geochemical Property	Lateral Strain			Vertical Strain		
	Slope	Intercept	R^2	Slope	Intercept	R^2
Organic Content (OC)	0.01	0.15	0.81	0.02	0.14	0.68
Soluble Sulfates (SS)	-2.06.E-05	0.19	0.71	-8.16.E-05	0.25	0.89
Cation Exchange Capacity (CEC)	4.68.E-04	0.14	0.90	1.19.E-03	0.10	0.75
Specific Surface Area (SSA)	1.80.E-04	0.13	0.86	1.82.E-04	0.17	0.19
Montmorillonite (M)	6.29.E-04	0.15	0.90	1.49.E-03	0.15	0.73
Kaolinite (K)	4.32.E-04	0.17	0.76	-5.80.E-04	0.24	0.02
Illite (I)	-5.77.E-04	0.20	0.98	-1.86.E-03	0.27	0.97

Table 6.2: Correlation Analysis between Modulus and Chemical-Mineralogical Properties (Combined DFO and SFO Process)

Geochemical Property	Parameter A			Parameter B		
	Slope	Intercept	R^2	Slope	Intercept	R^2
Organic Content (OC)	9.69	-57.35	0.43	0.06	0.21	0.30
Soluble Sulfates (SS)	-0.05	-0.61	0.88	-3.59.E-04	0.61	0.92
Cation Exchange Capacity (CEC)	0.45	-64.7	0.40	3.34.E-03	0.12	0.36
Specific Surface Area (SSA)	0.11	-51.71	0.27	8.19.E-04	0.22	0.25
Montmorillonite (M)	1.21	-67.10	0.88	0.01	0.16	0.88
Kaolinite (K)	-0.05	-19.97	4.48.E-04	3.46.E-03	0.35	0.04
Illite (I)	-0.99	3.19	0.94	-0.01	0.69	0.81

6.2.2 DFS Process

For the lateral strain, fit parameter B is well correlated to SS, CEC, SSA, M and K; whereas the I is considered marginally correlated and OC is considered poorly correlated, as shown in Table 6.3.

Table 6.3: Correlation Analysis between Parameter B and Chemical-Mineralogical Properties (DFS Process)

Geochemical Property	Lateral Strain			Vertical Strain		
	Slope	Intercept	R^2	Slope	Intercept	R^2
Organic Content (OC)	-0.02	0.89	0.14	0.06	0.52	0.83
Soluble Sulfates (SS)	2.07.E-04	0.67	0.78	-1.92.E-04	0.83	0.84
Cation Exchange Capacity (CEC)	-2.81.E-03	1.09	0.88	3.51.E-03	0.43	0.82
Specific Surface Area (SSA)	-8.85.E-04	1.07	0.97	1.33.E-03	0.41	0.77
Montmorillonite (M)	-3.71.E-03	0.97	0.95	0.01	0.54	0.97
Kaolinite (K)	0.01	0.61	0.93	2.82.E-03	0.64	0.10
Illite (I)	3.49.E-03	0.71	0.71	-4.39.E-03	0.88	0.93

Table 6.4: Correlation Analysis between Modulus and Chemical-Mineralogical Properties (DFS Process)

Geochemical Property	Parameter A			Parameter B		
	Slope	Intercept	R^2	Slope	Intercept	R^2
Organic Content (OC)	71.25	-349.84	0.58	0.08	-0.10	0.92
Soluble Sulfates (SS)	-0.28	22.60	0.91	5.26.E-04	0.11	0.82
Cation Exchange Capacity (CEC)	4.33	-540.55	0.86	2.01.E-03	0.02	0.19
Specific Surface Area (SSA)	1.91	-585.43	0.79	3.63.E-04	0.11	0.07
Montmorillonite (M)	5.46	-340.61	0.85	0.01	-0.04	0.70
Kaolinite (K)	-0.01	-105.30	8.55.E-07	-3.51.E-03	0.31	0.06
Illite (I)	-6.21	77.03	0.97	-3.35.E-03	0.31	0.26

Fit parameter B for the vertical strain is correlated to all chemical-mineralogical parameters, except K, which is considered poorly correlated (see Table 6.3). For the modulus, fit parameter A is well correlated to SS, CEC, SSA, M and I, and fit parameter B correlates well only to OC and SS as shown in Table 6.4.

6.3 Estimation of Minimum and Maximum Strains

Again, a linear regression process was used to estimate the minimum and maximum strains parameters from the chemical-mineralogical parameters of the soils. The relationships between the minimum and maximum strains and their corresponding chemical-mineralogical properties for all clays except Houston are plotted in Figures 6.3 through 6.4. One more time, the coefficients of determination values were used as an indication of quality of fit of the minimum and maximum strains. The results of the trend analysis between the minimum and maximum strains and the chemical-mineralogical properties of all clay materials except Houston are shown in Tables 6.5 through 6.7 presented below.

6.3.1 Combined DFO and SFO Process

For the lateral and vertical strain, the minimum strain values are correlated to the SS, CEC, SSA, M and I, whereas the OC and the K are poorly correlated to minimum strain (see Table 6.5). As such, only the SS, CEC, SSA, M and I were further considered in the development of the models.

Regarding the maximum strain, it is the same for both the combined DFO and SFO process and the DFS process since they represent the same point. For the lateral strain, it is well correlated only to SS and I, whereas the rest of the chemical-mineralogical properties are poorly correlated. As such, only the SS and I were considered in the development of the models. For the vertical strain, the maximum strain values correlate to SS, M, and I whereas the rest of the chemical-mineralogical properties are poorly correlated, as shown in Table 6.6.

6.3.2 DFS Process

For the lateral and vertical strains, minimum strain is well correlated to SS, CEC, SSA, M and I; whereas the OC and K are poorly correlated as shown in Table 6.7. The maximum strain is the same as the combined DFO and SFO process, as presented in Table 6.6, because they represent the same point.

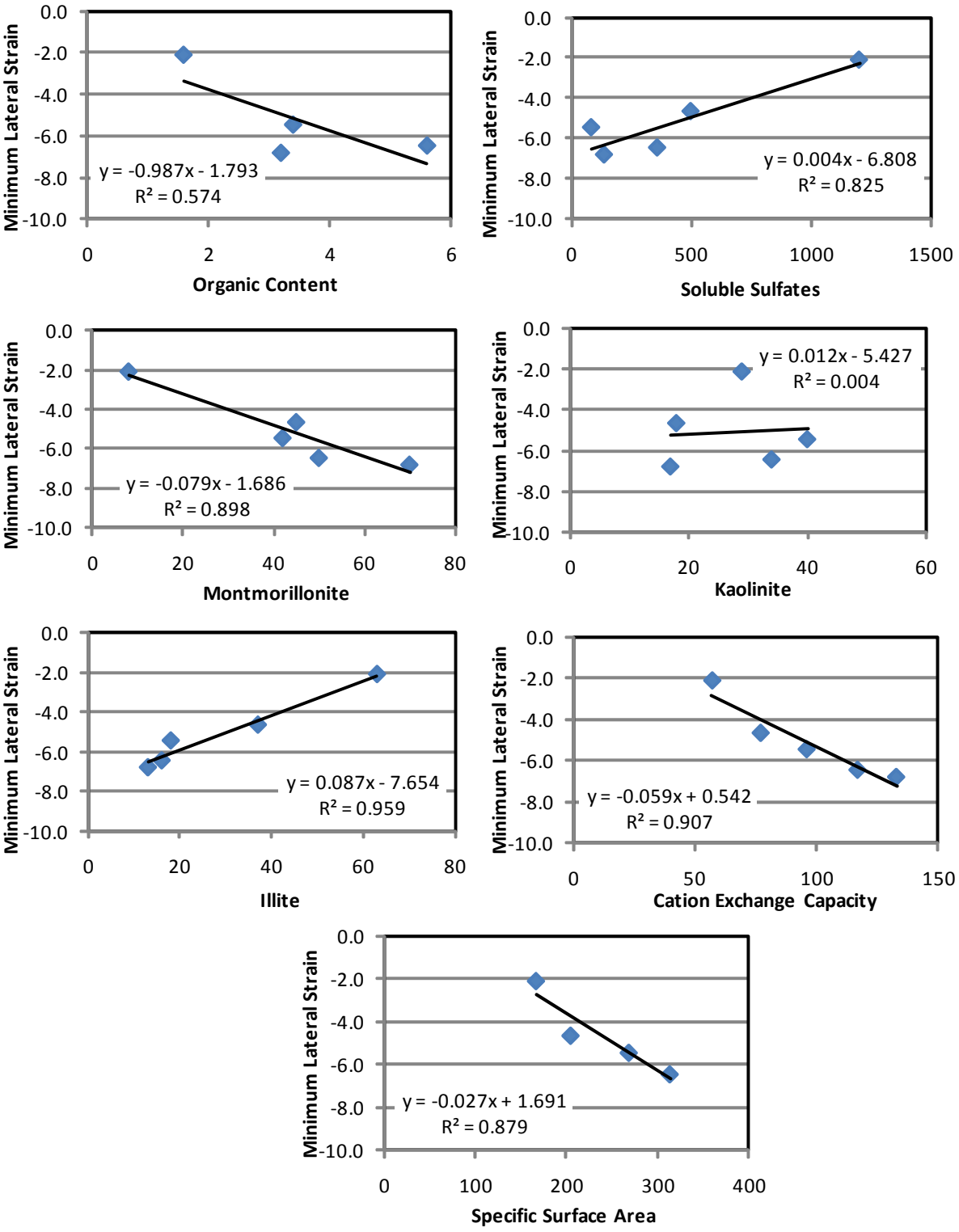

Figure 6.3: Summary of Correlations between Chemical-Mineralogical Properties of Soils and Minimum Lateral Strain (Combined DFO and SFO Process)

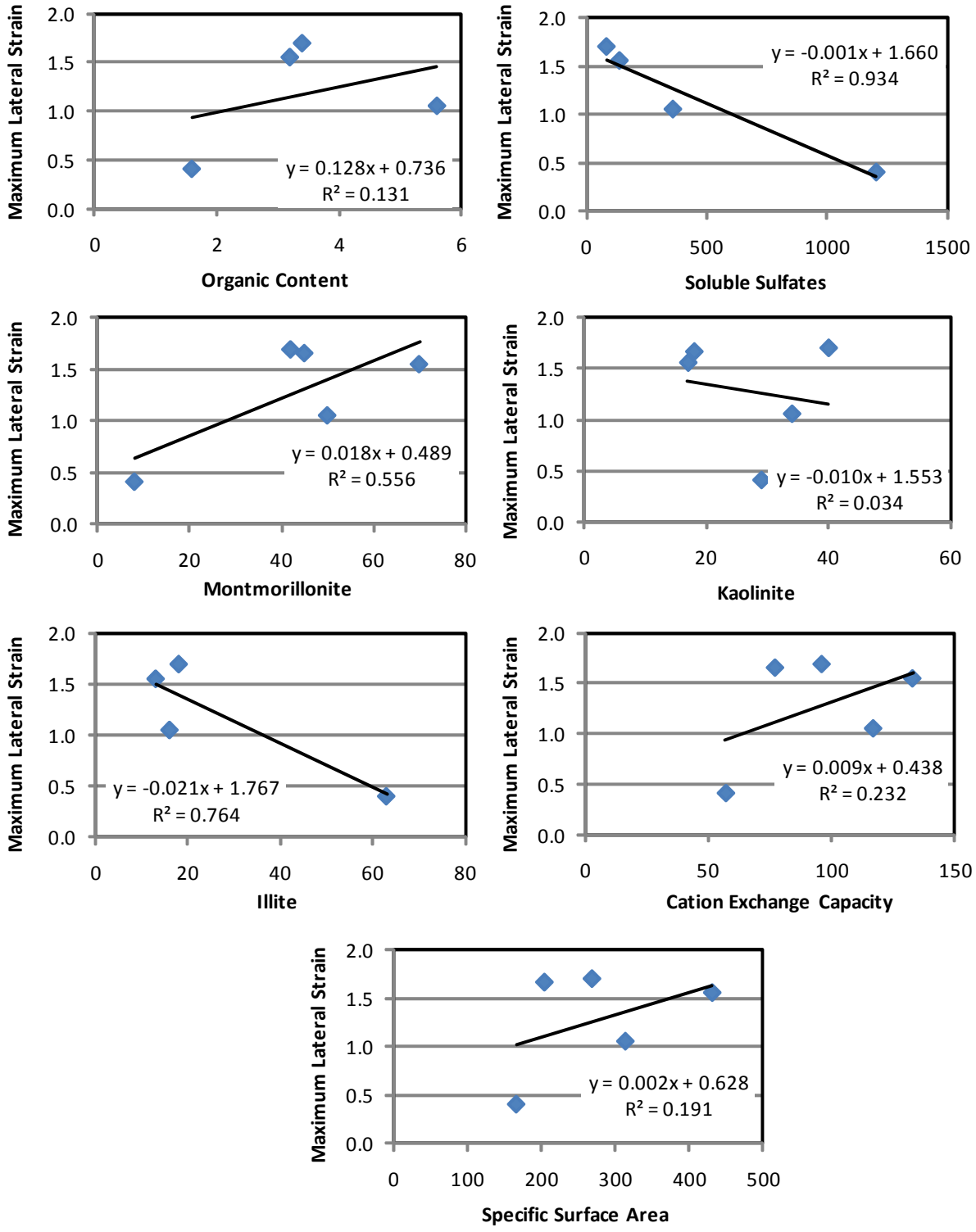

Figure 6.4: Summary of Correlations between Chemical-Mineralogical Properties and Maximum Lateral Strain (Combined DFO and SFO Process and DFS Process)

Table 6.5: Correlation Analysis between Minimum Strain and Chemical-Mineralogical Properties (Combined DFO and SFO Process)

Geochemical Property	Lateral Strain			Vertical Strain		
	Slope	Intercept	R^2	Slope	Intercept	R^2
Organic Content (OC)	-0.99	-1.79	0.57	-1.07	-1.32	0.54
Soluble Sulfates (SS)	3.78.E-03	-6.81	0.83	4.32.E-03	-6.95	0.89
Cation Exchange Capacity (CEC)	-0.06	0.54	0.91	-0.06	0.90	0.82
Specific Surface Area (SSA)	-0.03	1.69	0.88	-0.01	-3.50	0.94
Montmorillonite (M)	-0.08	-1.69	0.90	-0.09	-1.20	0.91
Kaolinite (K)	0.01	-5.43	4.31.E-03	0.02	-5.51	0.01
Illite (I)	0.09	-7.65	0.96	0.10	-7.80	0.95

Table 6.6: Correlation Analysis between Maximum Strain and Chemical-Mineralogical Properties (Combined DFO and SFO Process and DFS Process)

Geochemical Property	Lateral Strain			Vertical Strain		
	Slope	Intercept	R^2	Slope	Intercept	R^2
Organic Content (OC)	0.13	0.74	0.13	0.40	1.71	0.14
Soluble Sulfates (SS)	-1.08.E-03	1.66	0.93	-3.44.E-03	5.10	0.93
Cation Exchange Capacity (CEC)	0.01	0.44	0.23	0.03	0.43	0.31
Specific Surface Area (SSA)	2.33.E-03	0.63	0.19	0.01	1.03	0.27
Montmorillonite (M)	0.02	0.49	0.56	0.06	0.47	0.81
Kaolinite (K)	-0.01	1.55	0.03	-0.02	3.92	0.02
Illite (I)	-0.02	1.77	0.76	-0.07	5.90	0.84

Table 6.7: Correlation Analysis between Minimum Strain and Chemical-Mineralogical Properties (DFS Process)

Geochemical Property	Lateral Strain			Vertical Strain		
	Slope	Intercept	R^2	Slope	Intercept	R^2
Organic Content (OC)	-1.01	-4.28	0.56	-0.76	-0.49	0.35
Soluble Sulfates (SS)	4.08.E-03	-9.56	0.91	4.47.E-03	-5.95	0.99
Cation Exchange Capacity (CEC)	-0.06	-2.22	0.82	-0.06	3.30	0.97
Specific Surface Area (SSA)	-0.01	-6.34	0.83	-0.02	2.52	0.96
Montmorillonite (M)	-0.08	-4.25	0.87	-0.08	0.19	0.92
Kaolinite (K)	3.71.E-03	-7.81	3.72.E-04	0.10	-5.99	0.28
Illite (I)	0.09	-10.36	0.98	0.08	-6.22	0.89

CHAPTER 7: CASE STUDY – VALIDATION OF MODELS

7.1 Prediction Process

Equation 4.4 is proposed as the general equation to estimate the lateral and vertical strains as well as the modulus at a particular moisture content for both the combined DFO and SFO and the DFS processes. Figure 7.1 summarizes the steps used in predicting strains and modulus from index and/or chemical-mineralogical properties of soils.

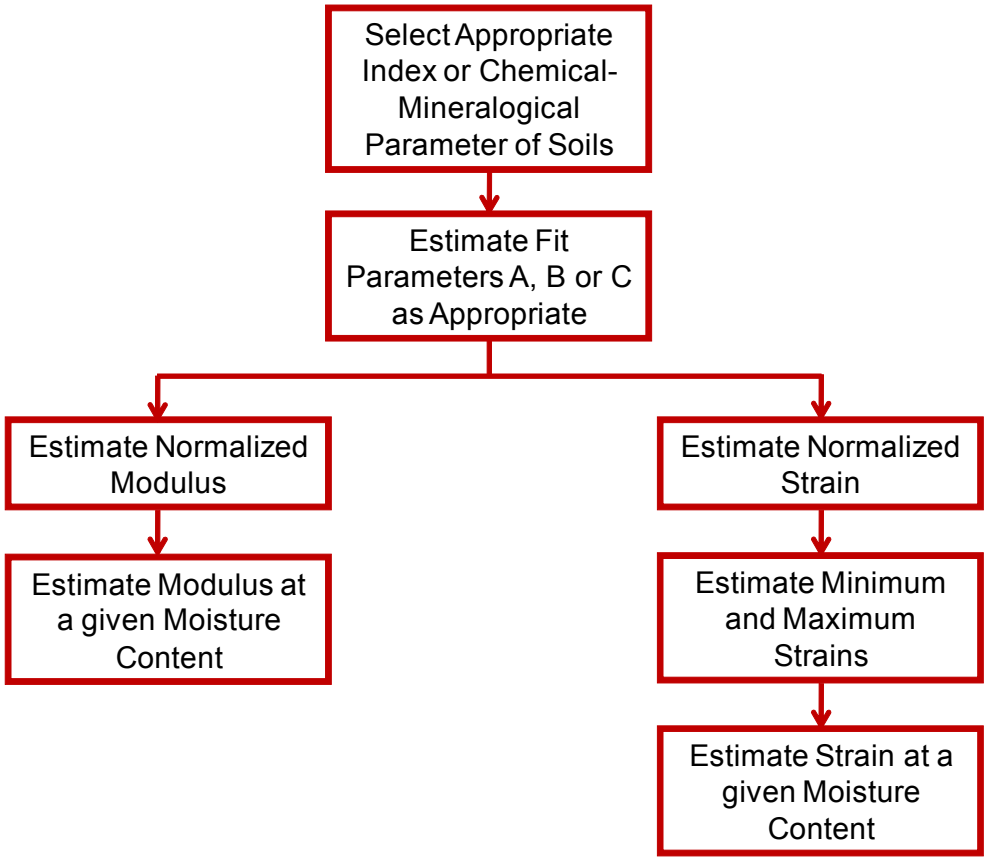

Figure 7.1: Flowchart of Strain and Modulus Prediction Relationship Based on Index and/or Chemical-Mineralogical Properties of Soils.

The first step involves the prediction of the appropriate fit parameters from the most appropriate index properties from Tables 5.1 through 5.4 or from the chemical-mineralogical properties from Tables 6.1 through 6.4. The next step involves the estimation of the minimum and maximum strains from the index parameters proposed in Tables 5.5 through 5.7 or from the chemical-mineralogical parameters

presented in Tables 6.5 through 6.7. The minimum and maximum strains and the fit parameters can then be used as input to Equations 4.3 and 4.4 for predicting strains and/or modulus by knowing the moisture content. In this manner, the variations in stiffness and volume change of the different clay materials can be readily predicted just by knowing the index and/or chemical-mineralogical properties of the soils.

To illustrate this process, the relationships between Parameter C and their corresponding index properties in Figure 5.1 will be studied. From this figure, the plastic limit, the highest R^2 value, is used as the input index parameter. The slope and intercept for this parameter as shown in Figure 5.1 can be used to estimate parameter C for the lateral strain. This example can be replicated for all other index properties considered in Table 5.1 or chemical-mineralogical properties considered in Table 6.1 by using the corresponding slope and intercept. By knowing the parameter C, the normalized strain can be estimated. The slope, intercept and R^2 for each set of index properties are included in Appendix D for lateral and vertical strains and Appendix E for modulus, while Appendix F and Appendix G includes the slope, intercept and R^2 for lateral and vertical strains and modulus, respectively, for each set of chemical-mineralogical properties.

The next step is to estimate the minimum and maximum strains in order to find the actual strain. From Figures 5.2 and 5.3, the PI is used as input in the graphs that present the relationship between the variations of minimum and maximum strains with PI. A summary of the variations of minimum and maximum strains with index properties for both moisture conditioning processes is included in Appendix H, while the chemical-mineralogical relationships are included in Appendix I.

In this particular case, the R^2 is 0.88 and 0.86 for the minimum and maximum strains, respectively; therefore, the best fit line describes the relationship quite well. This example can also be replicated for all other index or chemical-mineralogical properties considered.

The highest R^2 value was used in the previous example for the prediction of a fit parameter. The use of the highest R^2 would possibly be the best approach to follow in such prediction, however, since PI, LL, DUW and OMC are commonly known, Sabnis et al. (2008) developed the following model to combine the information from all these parameters.

$$A^* = \frac{A_{PI} \times W_{A-PI} + A_{LL} \times W_{A-LL} + A_{DUW} \times W_{A-DUW} + A_{OMC} \times W_{A-OMC}}{W_{A-PI} + W_{A-LL} + W_{A-DUW} + W_{A-OMC}} \tag{7.1}$$

where A^* = Weighted Average Parameter A, A_{PI} = Parameter A from PI relationship, A_{LL} = Parameter A from LL relationship, A_{OMC} = Parameter A from OMC relationship and A_{DUW} = Parameter A from DUW, $W_{A\text{-}PI}$ = Weight factor for PI parameter, $W_{A\text{-}LL}$ = Weight factor for LL parameter, $W_{A\text{-}OMC}$ = Weight factor for OMC parameter and $W_{A\text{-}DUW}$ = Weight factor for DUW parameter. Please note that the term parameter A is used as a general representation of the fit parameters in all the equations presented in Tables 4.7 through 4.9 for simplification. Equation 5.1 can be simplified as follows:

$$A^* = \frac{\sum A_i W_i}{\sum W_i} \tag{7.2}$$

In order to make this model versatile so that it can be used with any missing data, the R^2 value from each of the relationships is used as a weighting multiplication factor:

$$W_i = \frac{G_i}{\sum G_i} \tag{7.3}$$

Where G_i is the contribution factor, which is calculated based on $(R^2)i$ values as follows:

For R^2 values equal to or greater than 0.8, a factor of 4 is multiplied to get G_i. Similarly, the R^2 values between 0.6 and 0.8 are multiplied by a factor of 2 to get G_i. For the R^2 value less than 0.6, a multiplication factor of unity is used.

The same philosophy is applicable for the chemical-mineralogical parameters of soils. The highest R^2 value can be used for the prediction of a fit parameter and/or minimum and maximum strain values. However, if all or some of the chemical-mineralogical properties are known, the model described above may also be implemented to combine the information from all these parameters.

As stated by Sabnis et al. (2008), this process is quite flexible since any or all of the soil index parameters can be used to estimate the strains and modulus. If one or more of the index and/or chemical-mineralogical properties are not available, their corresponding term in Equation 5.1 can be simply omitted. For detailed information on this process, please refer to Sabnis et al. (2008).

7.2 Validation using Index Properties

The clay material from Houston, which was not used to develop the model, was used to validate the lateral and vertical strains and modulus for the combined DFO and SFO model. Index properties of the Houston clay are shown in Table 4.1.

As explained in the previous section, the first step in the validation process involves the prediction of the appropriate fit parameter from any index property from Tables 5.1 through 5.4 by knowing the slope and intercept of the linear trend line. In this case, the combined DFO and SFO model is used as an example for predicting the lateral and vertical strains and modulus. To continue using the example from Figure 5.1, the index property with the highest R^2 value, in this case the plastic limit (R^2=0.98), is used as the input in the graph that presents the relationship between the variations of parameter C with plastic limit for the lateral strain. Similarly, the highest R^2 value of 0.99 was used to estimate parameter C for the vertical strain by using the liquid limit as the input index parameter. From the graphs, the following equations are obtained in order to predict parameter C for lateral and vertical strains:

$$Parameter\ C, Lateral\ Strain = 0.001 \times PL + 0.138 \tag{7.4}$$

$$Parameter\ C, Vertical\ Strain = 0.003 \times LL + 0.059 \tag{7.5}$$

For a plastic limit of 19 and a liquid limit of 54 as obtained from the Houston clay, Parameter C is 0.16 and 0.22 for lateral and vertical strains, respectively. By knowing the Parameter C, the normalized strain can be estimated by using Equation 4.4.

The next step is to estimate the minimum and maximum strains from the index parameters proposed in Tables 5.5 through 5.7 in order to find the actual strain. This time, the liquid limit and seismic modulus properties of the Houston clay were randomly selected as input parameters to estimate minimum and maximum strains, respectively for the lateral strain. From Figures 5.2 and 5.3:

$$Minimum\ Lateral\ Strain, \varepsilon_{\min} = -0.137 \times LL + 1.87 \tag{7.6}$$

$$Maximum\ Lateral\ Strain, \varepsilon_{\max} = 0.101 \times PL - 0.443 \tag{7.7}$$

The minimum and maximum strains for the vertical strain were estimated by randomly selecting the liquid limit and plasticity index as the input index parameters:

$$Minimum\ Vertical\ Strain, \varepsilon_{\min} = -0.149 \times LL + 2.597 \quad (7.8)$$

$$Maximum\ Vertical\ Strain, \varepsilon_{\max} = 0.199 \times PI - 2.654 \quad (7.9)$$

For a liquid limit of 54, plastic limit of 19 and plasticity index of 35, as obtained from the Houston clay, the minimum and maximum strains are -5.53 and 1.48 for the lateral strain and -5.45 and 4.31 for the vertical strain, respectively.

The obtained values can now be used as input to Equation 4.3 for predicting the combined DFO and SFO lateral and vertical strains, by knowing the moisture content. The variations in measured and estimated lateral and vertical strains with normalized moisture content are compared in Figure 7.2. The trend between the measured strains is similar to the strains for the prediction model. The estimated and measured strains compare favorably.

The same procedure was followed to predict the modulus. The seismic modulus and plasticity index properties of the Houston clay were used as input parameters to estimate parameters A and B, respectively:

$$Parameter\ A = 4.177 \times PL - 96.574 \quad (7.10)$$

$$Parameter\ B = 0.018 \times PI - 0.113 \quad (7.11)$$

The values of parameters A and B (-17.21 and 0.52, respectively) were used as input to Equation 4.4 for predicting the normalized modulus for the combined DFO and SFO process at varying moisture contents. The raw data collected for the Houston clay was compared against the predicted model, as shown in Figure 7.3. The estimated and measured moduli compare favorably since the trend between measured modulus is similar to the modulus of the prediction model.

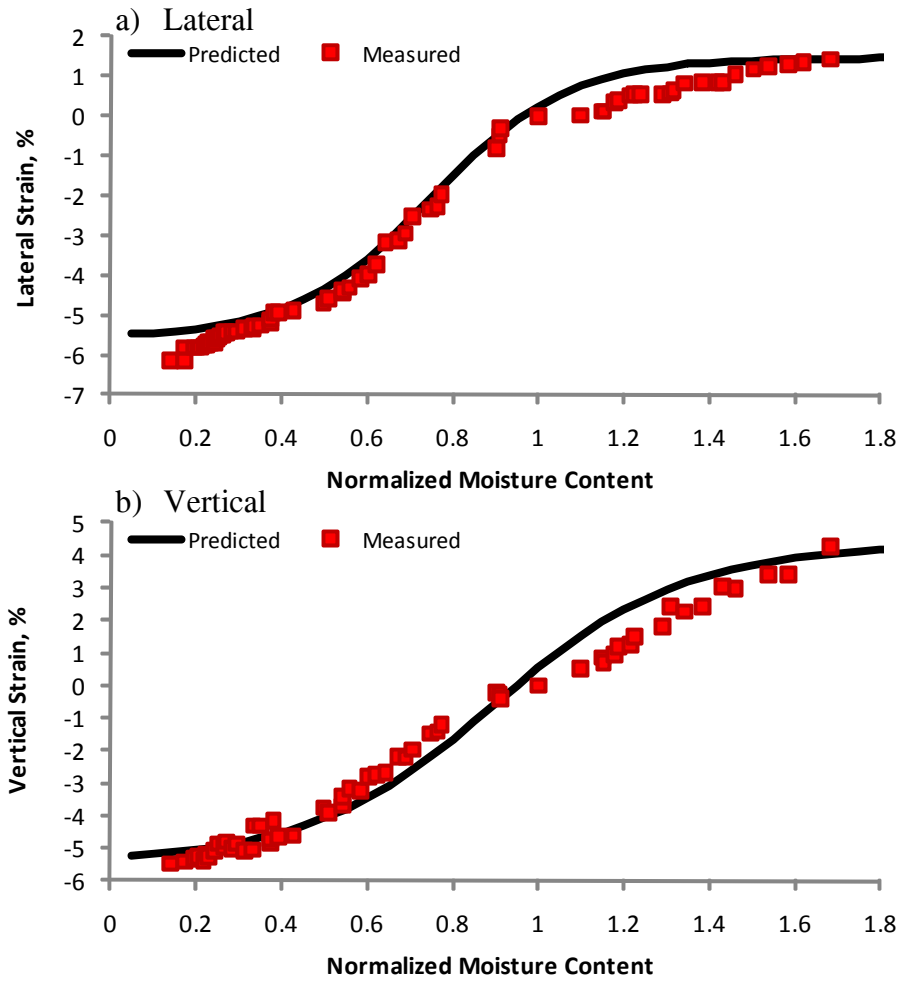

Figure 7.2: Comparison of Measured and Predicted Lateral and Vertical Strains and Normalized Moisture Content for the Houston Clay Material using Index Properties

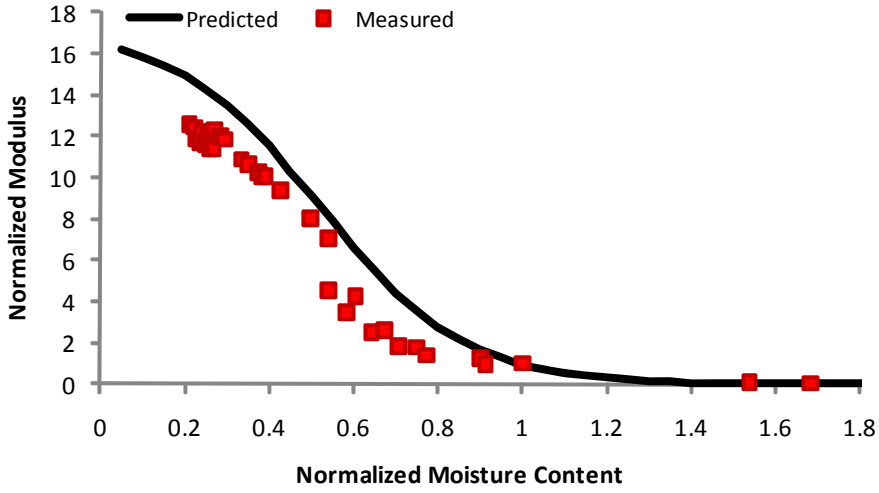

Figure 7.3: Comparison of Measured and Predicted Normalized Modulus and Normalized Moisture Content for the Houston Clay Material using Index Properties

7.3 Validation using Chemical-Mineralogical Properties

One more time, the clay material from Houston, which was not used to develop the model, was also used to validate the lateral strain and modulus models but now from its chemical-mineralogical properties, which are displayed in Table 4.3.

The first step in the validation process involves the prediction of a fit parameter from any chemical-mineralogical property by knowing the slope and intercept of the linear trend line. This case also presents the combined DFO and SFO model as an example for predicting the lateral and vertical strains as well as the modulus.

Consider the following example from Figure 6.1. The organic content property (R^2=0.81) is randomly used as the input in the graph that presents the relationship between the variations of parameter C for the lateral strain with organic content. Similarly, the random R^2 value of 0.89 was used to estimate parameter C for the vertical strain by using the soluble sulfates as the input chemical-mineralogical parameter. From the graphs, the following equations are obtained in order to predict parameter C for lateral and vertical strains:

$$Parameter\ C, Lateral\ Strain = 0.006 \times OC + 0.151 \tag{7.12}$$

$$Parameter\ C, Vertical\ Strain = -8E-05 \times SS + 0.252 \tag{7.13}$$

For an organic content value of 3.2 and a soluble sulfate content value of 247, as obtained from the Houston clay material, parameter C equals 0.17 and 0.23 for lateral and vertical strains, respectively.

The next step is to estimate the minimum and maximum strains from the chemical-mineralogical parameters proposed in Tables 6.5 through 6.7 in order to find the actual strain. This time, the soluble sulfates property of the Houston clay was used as the input parameter. From Figures 6.2 and 6.3:

$$Minimum\ Lateral\ Strain, \varepsilon_{\min} = 0.003 \times SS - 6.808 \tag{7.14}$$

$$Maximum\ Lateral\ Strain, \varepsilon_{\max} = -0.001 \times SS + 1.659 \tag{7.15}$$

The prediction of vertical minimum and maximum strains was estimated by selecting the chemical-mineralogical parameters with the highest R^2 value, in this case illite and soluble sulfates, for minimum and maximum strains, respectively, as the input parameters as indicated in the following equations:

$$Minimum\ Vertical\ Strain, \varepsilon_{min} = 0.095 \times I - 7.803 \quad (7.16)$$

$$Maximum\ Vertical\ Strain, \varepsilon_{max} = -0.003 \times SS + 5.098 \quad (7.17)$$

For an illite value of 26, and a soluble sulfate content value of 247, as obtained from the Houston clay material, minimum and maximum strain values are -6.07 and 1.41 for the lateral strain and -5.33 and 4.36 for the vertical strain, respectively.

Figure 7.4 shows the predicted and measured model for the Houston material in terms of lateral and vertical strains versus normalized moisture content. This figure shows that the measured data closely correlated to the predicted model.

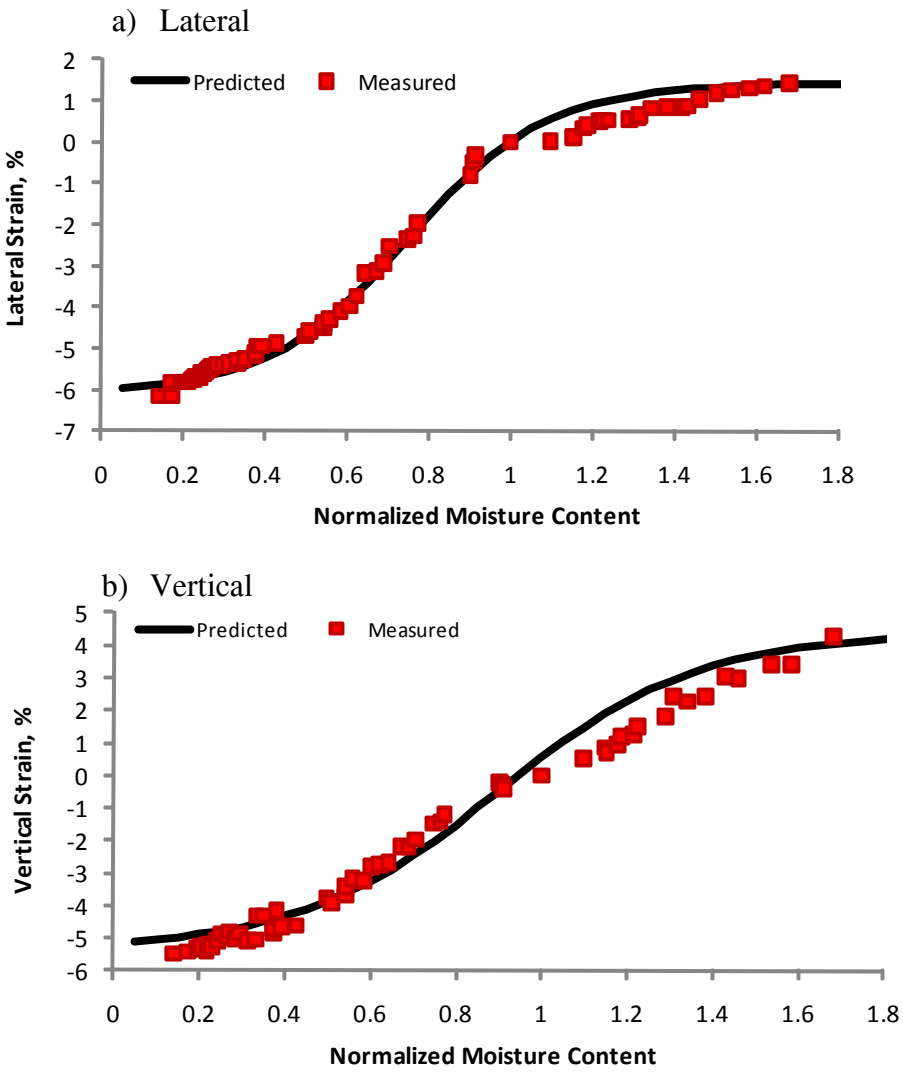

Figure 7.4 Measured and Predicted Lateral and Vertical Strains and Normalized Moisture Content for the Houston Clay using Chemical-Mineralogical Properties

The same practice is used for the prediction of the modulus. The soluble sulfates property of the Houston clay was used as input parameters to estimate parameters A and B, respectively:

$$Parameter\ A = -0.0453 \times SS - 0.6106 \tag{7.18}$$

$$Parameter\ B = -0.0004 \times SS + 0.6064 \tag{7.19}$$

Parameters A and B equal to -11.80 and 0.52, respectively. These values were used as input to Equation 4.4 for predicting the modulus for the combined DFO and SFO process at varying moisture contents. A prediction model for the Houston material was developed in terms of normalized moisture content versus normalized modulus. For validation purposes, the data collected from the lab was compared against the predicted model, as shown in Figure 7.5. Once again, the estimated and measured normalized data for the modulus compare favorably since it follows a similar trend.

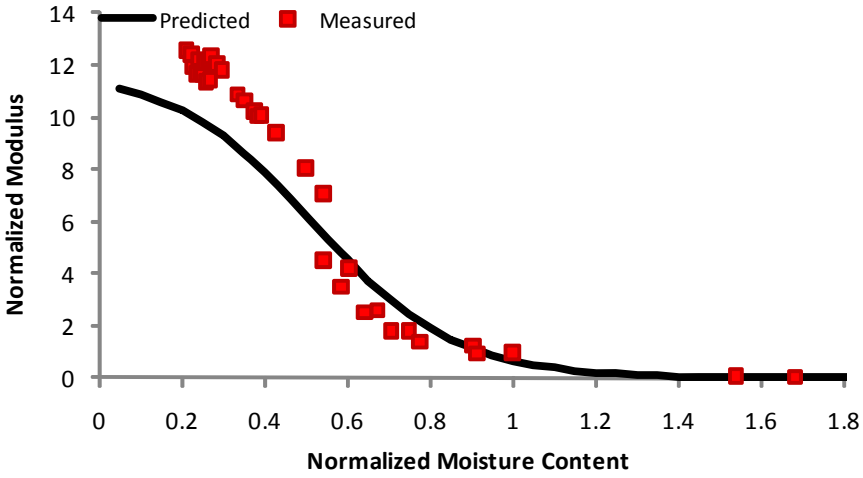

Figure 7.5: Comparison of Measured and Predicted Normalized Modulus and Normalized Moisture Content for the Houston Clay Material using Chemical-Mineralogical Properties

This validation analysis demonstrated that the models for estimating the strain or modulus are simple, accurate and versatile. In this manner, the variations in stiffness and volume change of the different clay materials can be readily predicted just by knowing the index and/or chemical mineralogical properties of the soils and utilize them in the numerical modeling of longitudinal cracking.

CHAPTER 8: SUMMARY AND CONCLUSIONS

The primary aim of the present work was to develop mathematical models that allow analyzing the behavior of expansive clays under different moisture conditioning processes. In order to develop such models, clay materials from six different sites in Texas, namely Fort Worth, Houston, El Paso, San Antonio, Paris and Bryan Districts, were analyzed and evaluated.

All clay specimens were prepared at optimum moisture content and were subjected to different moisture conditioning (drying or wetting) processes. The variations in modulus and lateral/vertical strains were then evaluated under two different moisture conditions, namely combined Dry-from-Optimum and Saturated-from-Optimum (combined DFO and SFO), and Dry-from-Saturation (DFS).

Correlation analyses were performed between curve-fit equation parameters, index properties and chemical-mineralogical properties of clays. Curve-fit parameters were also correlated to minimum and maximum strains. Multiple mathematical relationships were studied to predict shrinkage strains and modulus of clay materials at particular moisture content by using index and chemical-mineralogical properties of the clay. A three parameter sigmoidal equation was found to be the best fit model. Both statistical method and real data were utilized to validate the success of the model. All mathematical relationships showed reasonably good prediction capabilities within PI range from 15 to 40. Table 8.1 summarizes the mathematical models found for lateral and vertical strains and modulus for the Combined DFO and SFO and DFS moisture conditioning processes. Also shown are the best index and chemical/mineralogical predictors for each model. Table 8.2 illustrates the best index and chemical mineralogical parameters to estimate minimum and maximum strains.

Table 8.1: Best Fit Parameters Predictors

Moisture Condition	Estimated Parameter	Curve Fit Equation	Top Fit Predictors	
			Index[a]	Chemical-Mineralogical[b]
Combined DFO and SFO	Normalized Lateral Strain	$\varepsilon_n = \frac{1}{1+e^{-(\frac{NMC-0.75}{C})}}$	PL (0.98) C=1.47E-03(PL)+0.14 DUW (0.85) C=-1.17E-03(DUW)+0.29 SM (0.83) C=1.63E-03(SM)+0.14	I (0.98) C=-5.77E-04(I)+0.20 CEC (0.90) C=4.68E-04(CEC)+0.14 M (0.90) C=6.29E-04(M)+0.15
	Normalized Vertical Strain	$\varepsilon_n = \frac{1}{1+e^{-(\frac{NMC-0.90}{C})}}$	LL (0.99) C=3.00E-03(LL)+0.06 PI (0.97) C=7.97E-03(PI)+0.02 SM (0.95) C=0.01(SM)+0.08	I (0.97) C=-1.86E-03(I)+0.27 SS (0.89) C=-8.16E-05(SS)+0.25 CEC (0.75) C=1.19E-03(CEC)+0.10
	Normalized Modulus	$E_n = \frac{-A}{1+e^{-(\frac{NMC-B}{-0.17})}}$	DUW (0.97) A=-2.38(DUW)+206.51 LL (0.93) A=1.57(LL)-105.74 PI (0.87) A=2.69(PI)-100.92	I (0.94) A=-0.99(I)+3.19 SS (0.88) A=-0.05(SS)-0.61 M (0.88) A=1.21(M)-67.10
			PI (0.92) B=0.02(PI)-0.11 DUW (0.85) B=-0.02(DUW)+2.18 PL (0.79) B=0.02(PL)-0.08	SS (0.92) B=-3.59E-04(SS)+0.61 M (0.88) B=0.01(M)+0.16 I (0.81) B=-0.01(I)+0.69
DFS	Normalized Lateral Strain	$\varepsilon_n = \frac{1}{1+e^{-(\frac{NMC-B}{0.17})}}$	SM (0.98) B=-0.02(SM)+1.08 PI (0.94) B=-0.01(PI)+1.15 OMC (0.77) B=-0.03(OMC)+1.43	SSA (0.97) B=-8.85E-04(SSA)+1.07 M (0.95) B=-3.71E-03(M)+0.97 K (0.93) B=0.01(K)+0.61
	Normalized Vertical Strain	$\varepsilon_n = \frac{1}{1+e^{-(\frac{NMC-B}{0.20})}}$	PL (0.97) B=0.01(PL)+0.42 OMC (0.92) B=0.03(OMC)+0.15 LL (0.91) B=0.01(LL)+0.41	M (0.97) B=0.01(M)+0.54 I (0.93) B=-4.39E-03(I)+0.88 SS (0.84) B=-1.92E-04(SS)+0.83
	Normalized Modulus	$E_n = \frac{-A}{1+e^{-(\frac{NMC-B}{-0.12})}}$	LL (0.95) A=9.73(LL)-600.07 OMC (0.92) A=40.79(OMC)-954.14 SM (0.91) A=23.26(SM)-539.90	I (0.97) A=-6.21(I)+77.03 SS (0.91) A=-0.28(SS)+22.60 CEC (0.86) A=4.33(CEC)-540.55
			PI (0.80) B=0.02(PI)-0.38 OMC (0.78) B=0.03(OMC)-0.55	OC (0.92) B=0.08(OC)-0.10 SS (0.82) B=5.26E-04(SS)+0.11

[a] PI, LL, PL, OMC, DUW and SM, plasticity index, liquid limit, plastic limit, optimum moisture content, dry unit weight and seismic modulus, respectively.

[b] OC, SS, M, K, I, CEC and SSA, organic content, soluble sulfates, montmorillonite, kaolinite, illite, cation exchange capacity, and specific surface area, respectively.

Table 8.2: Best Minimum and Maximum Strain Predictors

Top Index[a] Predictors			
Moisture Condition	**Estimated Parameter**	**Minimum Strain**	**Maximum Strain**
Combined DFO and SFO	Normalized Lateral Strain	OMC (0.96) ε_{min}=-0.59(OMC)+7.17 LL (0.95) ε_{min}=-0.14(LL)+1.87 PI (0.88) ε_{min}=-0.26(PI)+1.71	SM (0.97) ε_{max}=0.10(SM)-0.44 PI (0.86) ε_{max}=0.07(PI)-0.69 DUW (0.78) ε_{max}=-0.05(DUW)+6.16
	Normalized Vertical Strain	DUW (0.96) ε_{min}=0.23(DUW)-27.67 LL (0.92) ε_{min}=-0.15(LL)+2.60 OMC (0.92) ε_{min}=-0.63(OMC)+8.22	SM (0.95) ε_{max}=0.30(SM)-1.73 PI (0.93) ε_{max}=0.20(PI)-2.65 LL (0.83) ε_{max}=0.12(LL)-2.38
DFS	Normalized Lateral Strain	LL (0.96) ε_{min}=-0.14(LL)-0.51 OMC (0.92) ε_{min}=-0.59(OMC)+4.63 SM (0.88) ε_{min}=-0.33(SM)-1.49	SM (0.97) ε_{max}=0.10(SM)-0.44 PI (0.86) ε_{max}=0.07(PI)-0.69 DUW (0.78) ε_{max}=-0.05(DUW)+6.16
	Normalized Vertical Strain	PI (0.96) ε_{min}=-0.26(PI)+3.96 LL (0.83) ε_{min}=-0.13(LL)+2.80	SM (0.95) ε_{max}=0.30(SM)-1.73 PI (0.93) ε_{max}=0.20(PI)-2.65 LL (0.83) ε_{max}=0.12(LL)-2.38
Top Chemical-Mineralogical[b] Predictors			
Combined DFO and SFO	Normalized Lateral Strain	I (0.96) ε_{min}=0.09(I)-7.65 CEC (0.91) ε_{min}=-0.06(CEC)+0.54 M (0.90) ε_{min}=-0.08(M)-1.69	SS (0.93) ε_{max}=-1.08E-03(SS)+1.66 I (0.76) ε_{max}=-0.02(I)+1.77
	Normalized Vertical Strain	I (0.95) ε_{min}=0.10(I)-7.80 SSA (0.94) ε_{min}=-0.01(SSA)-3.50 M (0.91) ε_{min}=-0.09(M)-1.20	SS (0.93) ε_{max}=-3.44E-03(SS)+5.10 I (0.84) ε_{max}=-0.07(I)+5.90 M (0.81) ε_{max}=0.06(M)+0.47
DFS	Normalized Lateral Strain	I (0.98) ε_{min}=0.09(I)-10.36 SS (0.91) ε_{min}=4.08E-03(SS)-9.56 M (0.97) ε_{min}=-0.08(M)-4.25	SS (0.93) ε_{max}=-1.08E-03(SS)+1.66 I (0.76) ε_{max}=-0.02(I)+1.77
	Normalized Vertical Strain	SS (0.99) ε_{min}=4.47E-03(SS)-5.95 CEC (0.97) ε_{min}=-0.06(CEC)+3.30 SSA (0.96) ε_{min}=-0.02(SSA)+2.52	SS (0.93) ε_{max}=-3.44E-03(SS)+5.10 I (0.84) ε_{max}=-0.07(I)+5.90 M (0.81) ε_{max}=0.06(M)+0.47

[a] PI, LL, PL, OMC, DUW and SM, plasticity index, liquid limit, plastic limit, optimum moisture content, dry unit weight and seismic modulus, respectively.
[b] OC, SS, M, K, I, CEC and SSA, organic content, soluble sulfates, montmorillonite, kaolinite, illite, cation exchange capacity, and specific surface area, respectively.

REFERENCES

AASHTO (1993) “AASHTO Guide for Design of Pavement” Federal Highway Administration

Adams, A. G., Dukes, O. M., Tabet, W., Cerato, A. B. and Miller, G. A (2008) “Sulfate Induced Heave in Oklahoma Soils due to Lime Stabilization” GeoCongress 2008: Characterization, Monitoring, and Modeling of GeoSystems, pp.444-450.

Altmeyer, W. T. (1955) Discussion of Engineering Properties of Expansive Clays. Proc. Am. Soc. Civil Eng. 81 (Separate No. 658): 17-19.

Bulut, R., Lytton, R. L., and Wray, W. K. (2001) “Suction Measurements by Filter Paper,” Expansive Clay Soils and Vegetative Influence on Shallow Foundations, ASCE Geotechnical Special Publication No. 115 (eds. C. Vipulanandan, M. B. Addison, and M. Hasen), ASCE, Reston, Virginia, pp. 243-261.

Chen, F. H. (1965a) “The Use of Piers to Prevent the Uplifting of Lightly Loaded Structures founded on Expansive Soil.” Concluding Proc. Eng. Effects of Moisture Changes in Soils Int. Res. Eng. Conf. Expansive Clay Soils, Supplementing the Symposium in Print, Texas A&M Press, pp. 152-171.

Chen, F. H. (1988b) “Foundations on Expansive Soils” American Elsevier Science Publ., New York.

Coduto (1998). Geotechnical Engineering - Principles and Practices. Prentice Hall, NJ.

Drumm, E.C., Madgett, M.R. (1997) “Subgrade Resilient Modulus Correction for Saturation Effects”, Journal of Geotechnical and Geoenvironmental Engineering, Vol. 123, No. 7, pp.663-670.

EI-Sohby, M. A., and Mazen, S. O. (1987) “The Prediction of Swelling Pressure and Deformational Behavior of Expansive Soils.” Regional Conference for Africa on Soil Mechanics and Foundation Engineering, 1, 129–133.

Elliot, R. P., Dennis, N. D., and Qiu, Y.(1998) “Permanent Deformation of Subgrade Soils.” Mack-Blackwell Rural Transportation Study Center, University of Arkansas, Fayetteville.

Elliott, R. P., and Thompson, M. R. (1985) “ILLI-PAVE Mechanistic Analysis of AASHO Road Test Flexible Pavements”, TRR 1043, TRB, Washington D. C. 39-49

Engineering Manual (1984) “Pavement Design for Seasonal Frost Conditions Mobilization Construction.” US Army Corps of Engineers, 1110, 3-138.

Holtz, R. D., and Kovacs, W. D. (1981) “An Introduction to Geotechnical Engineering,” Prentice Hall, Englewood Cliffs, NJ.

Holtz, W. G., and Gibbs, H.J. (1956) “Engineering Properties of Expansive Clays.” ASCE 121: 641-677

Hossain, D., Matsah, M. I., and Sadaqah, B. (1997) "Swelling Characteristics of Madinah Clays." Quarterly Journal of Engineering Geology, 30, 205-220.

Huang, Y. H. (1993). “Pavement Analysis and Design”, Prentice Hall

Komornik, A., and David, D. (1969) “Prediction of Swelling Pressure of Clays.” Journal of Soil Mechanics and Foundation Division, 95(SM1), 209–225.

Miller, G.A., The, S.Y., Li, D. and Zaman, M.M. (2000) “Cyclic Shear Strength of Soft Railroad Subgrade” Journal of Geotechnical and Geoenvironmental Engineering, pp.139-147

Mitchell, J. K. (1976) “Fundamentals of Soil Behavior.” John Wiley, New York.

Nayak, N. V., and Christensen, R. W. (1971) “Swelling Characteristics of Compacted Expansive Soils.” Clays and clay minerals, Pergamon press, (19), 251-261, Lawrence, KS.

Nazarian S., Yuan D., (2003) “Comprehensive Mechanistic-Based Quality Control of Flexible Pavements with NDT Methods.” Non-Destructive Testing in Civil Engineering 2003, Center for Highway Materials Research, The University of Texas at El Paso.

Nelson, J.D., and Miller D.J. (1992) “Expansive Soils: Problems and Practice in Foundation and Pavement Engineering” Wiley Professional Paperback Series.

Nwaiwu, C. M. O., and Nuhu, I. (2006) “Evaluation and Prediction of the Swelling Characteristics of Nigerian Black Clays.” Geotechnical and Geological Engineering, 1 (24), 45-56.

Puppala, A. J., Mohammad, L. N., and A. A. (1999a) “Permanent Deformation Characterization of Subgrade Soils from RLT Test.” Journal of Materials in Civil Engineering, ASCE, 11(4), 274-282.

Puppala, A.J., Katha, B. and Hoyos, L.R. (2004b) “Volumetric Shrinkage Strain Measurements in Expansive Soils Using Digital Imaging Technology” Geotechnical Testing Journal, Vol. 27, No. 6.

Raman, V. (1967) “Identification of Expansive Soils from the Plasticity Index and the Shrinkage Index Data”. Indian Eng., Calcutta 11 (1): 17-22.

Sabnis, A., Manosuthkij, T., Abdallah, I., Nazarian, S., and Puppala, A. (2008) “Impact of Moisture Variation on Strength and Deformation of Clays.” MS Thesis, Research Report 0-5430-1, The Center for Transportation Infrastructure Systems, The University of Texas at El Paso.

Shahu, J.T., Yudhbir, K.R. (1999) “Effective Stress Behavior of Quasi-Saturated Compacted Cohesive Soils” Journal of Geotechnical and Geoenvironemtal Engineering, Vol. 125, pp.322-329

Skempton, A. W. (1953) “The Colloidal Activity of Clays.” Proc. 3rd Int. Conf. Soil Mech, Found. Eng., Switzerland. V.1: 57-61.

Snethen, D. R., Johnson, L. D., and Patrick, D. M. (1977) “An Evaluation of Expedient Methodology for Identification of Potentially Expansive Soils.” Soils and Pavements Lab., U.S. Army Eng. Waterway Exp. Sta., Vicksburg, MS, Rep. No. FHWA-RE-77-94, NTIS PB-289-164.

Thompson, M. R. and Elliott, R. P. (1985) “ILLI-PAVE-Based Response Algorithms for Design of Conventional Flexible Pavements.” Transportation Research Board, 1043, 50-57.

Walker Jr., Daniel D. (Henderson, NV) (1992) “Method for Improving the Characteristics of Sulfate Bearing Soils.” United States Patent 5122012.

Wanyan, Y., Manosuthkij, T., Abdallah, I., Nazarian, S. and Puppala, A. (2008) “Expert System Design Guide for Lower Classification Roads over High PI Clays.” Ph.D. Dissertation, Research Report 0-5430-2, The Center for Transportation Infrastructure Systems, The University of Texas at El Paso.

Xiao-ming, Y., and Sun Jing, (2000) ”Laboratory Experimental Study on Dynamic Shear Modulus Ratio and Damping Ratio of Soil.” Earthquake Engineering and Engineering Vibration, 4 (20), 133-139.

Yuan, D. and Nazarian, S. (2002) “Variation in Moduli of Base and Subgrade with Moisture”, Transportation Research Board, Center for Highway Materials Research, The University of Texas at El Paso.

APPENDIX A: LATERAL STRAIN PREDICTION MODELS

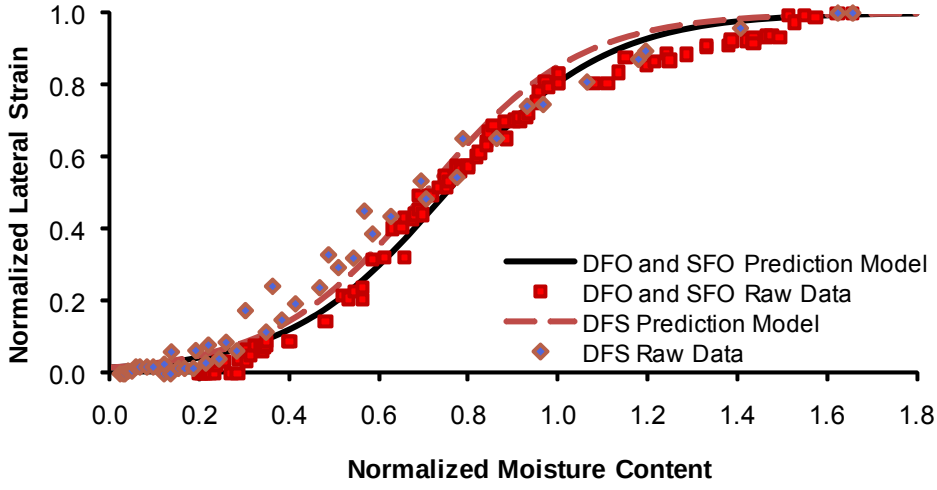

A.1: Lateral Strain Paris Prediction Model

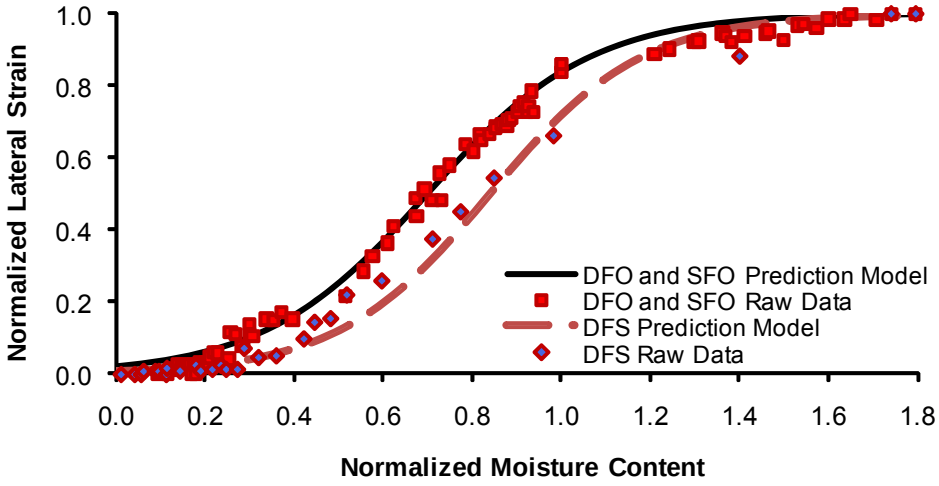

A.2: Lateral Strain San Antonio Prediction Model

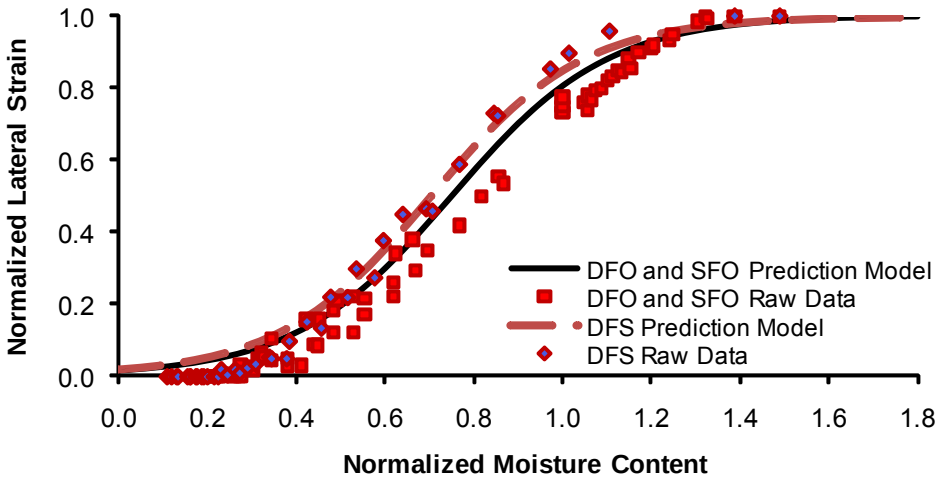

A.3: Lateral Strain Bryan Prediction Model

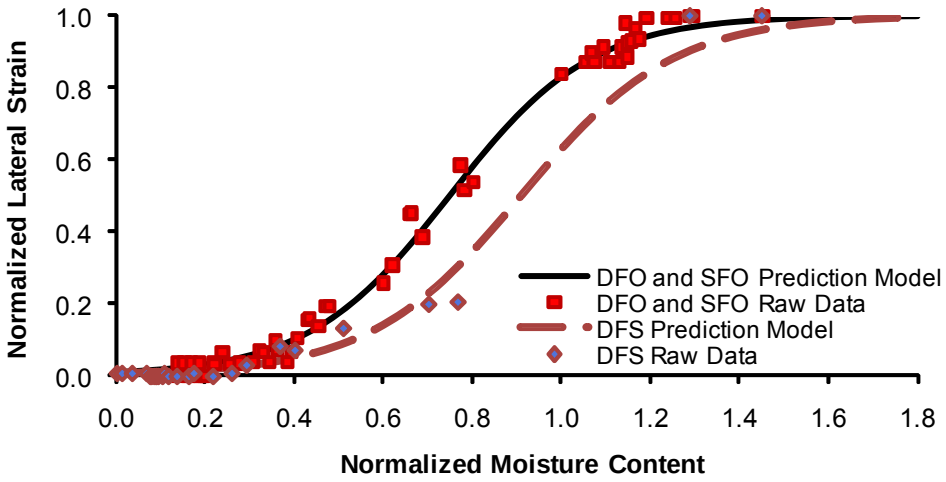

A.4: Lateral Strain El Paso Prediction Model

APPENDIX B: VERTICAL STRAIN PREDICTION MODELS

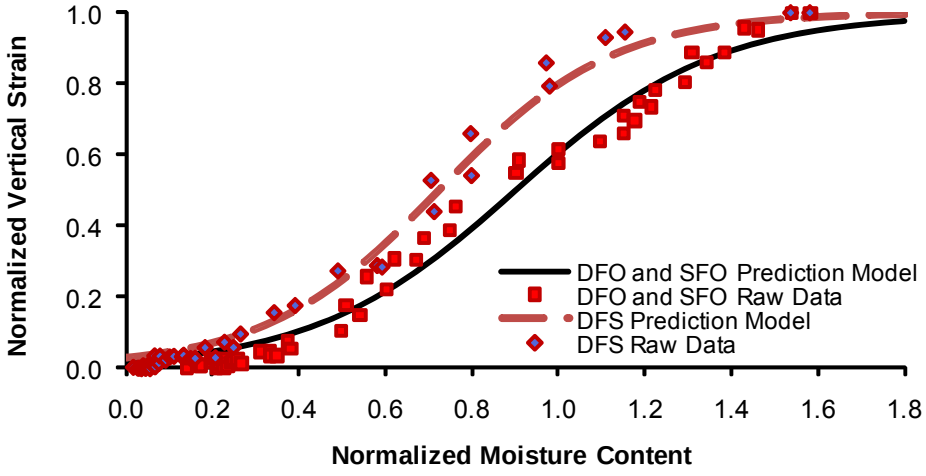

B.1: Vertical Strain Houston Prediction Model

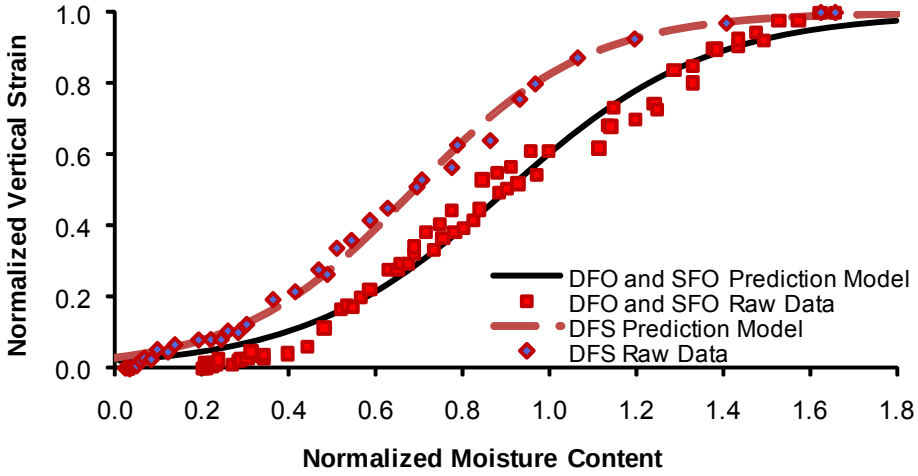

B.2: Vertical Strain Paris Prediction Model

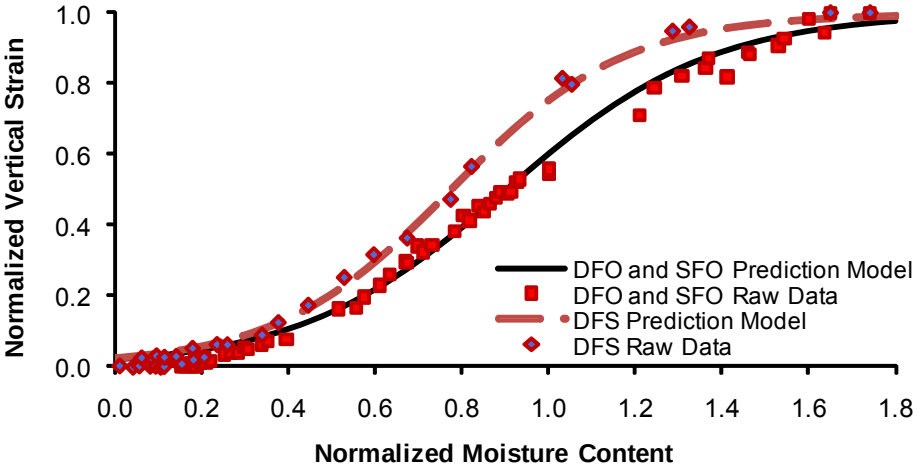

B.3: Vertical Strain San Antonio Prediction Model

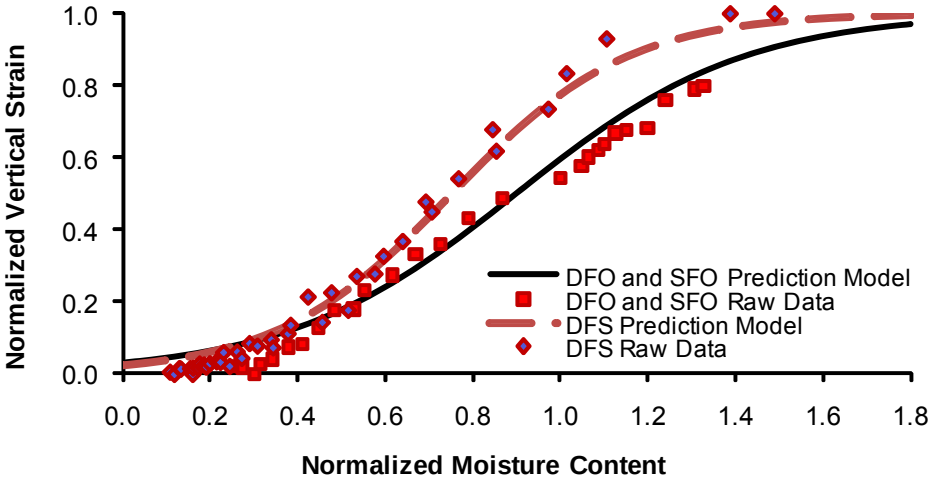

B.4: Vertical Strain Bryan Prediction Model

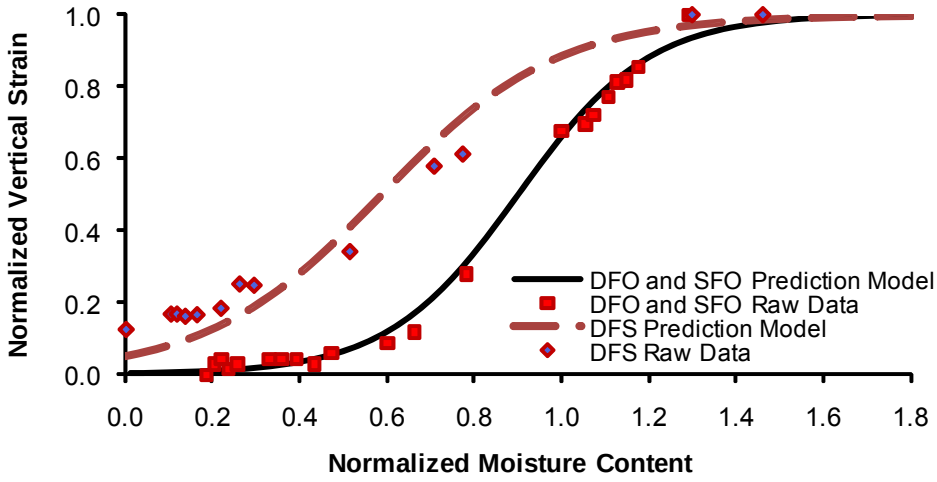

B.5: Vertical Strain El Paso Prediction Model

APPENDIX C: MODULUS PREDICTION MODELS

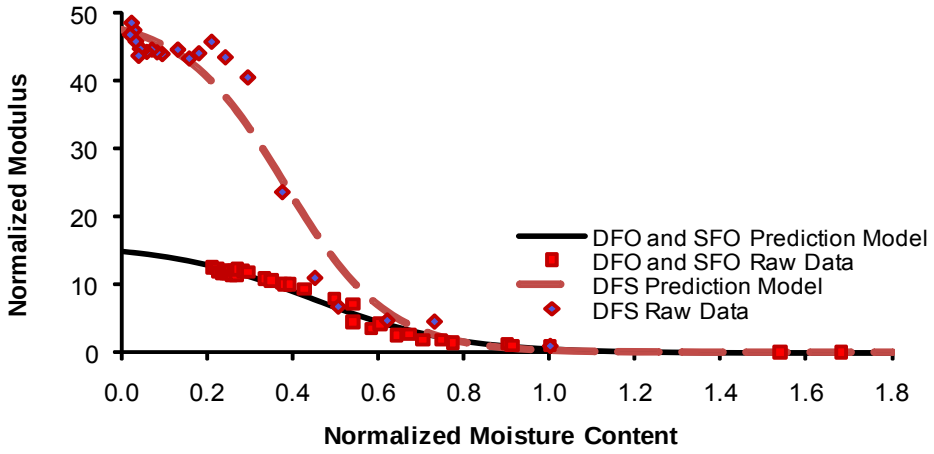

C.1: Modulus Houston Prediction Model

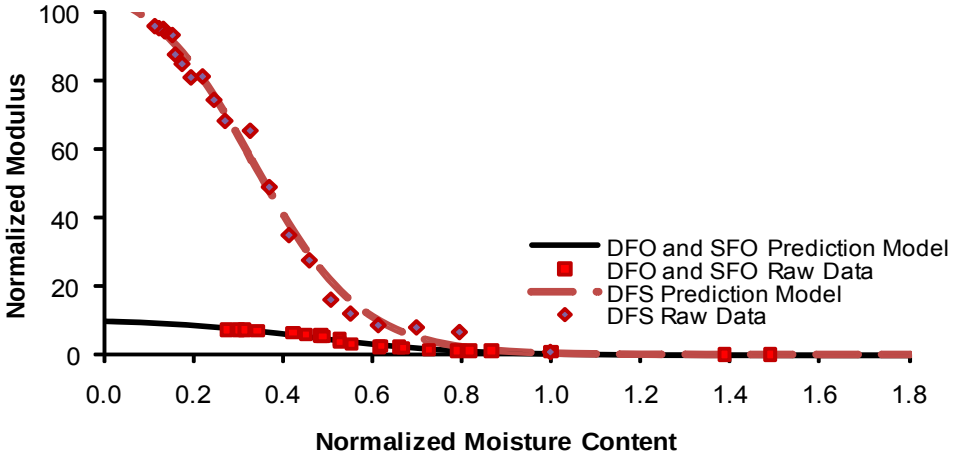

C.2: Modulus Bryan Prediction Model

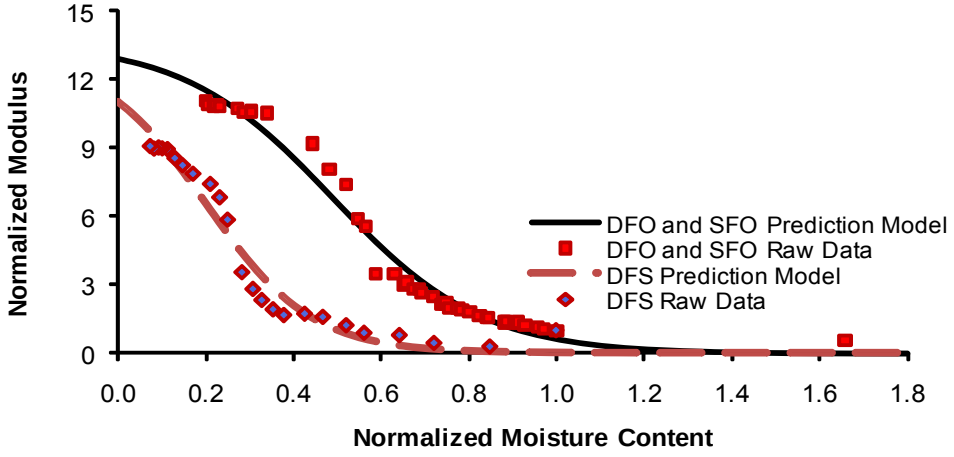

C.3: Modulus Paris Prediction Model

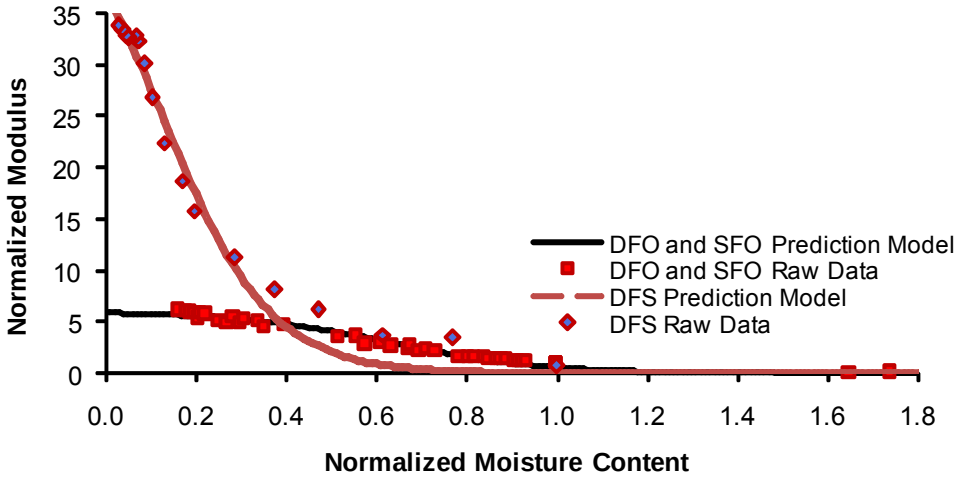

C.4: Modulus San Antonio Prediction Model

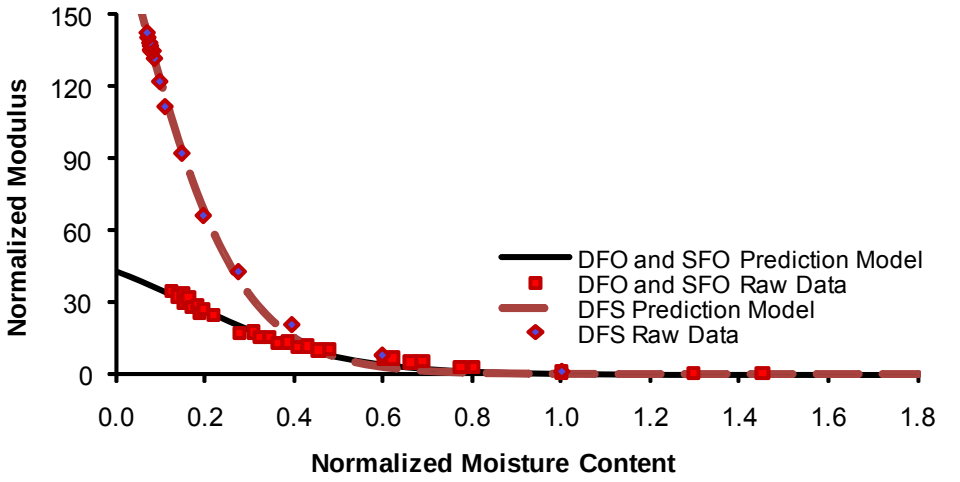

C.5: Modulus El Paso Prediction Model

APPENDIX D: SUMMARY OF FIT PARAMETERS AND INDEX PROPERTIES RELATIONSHIPS – LATERAL AND VERTICAL STRAINS

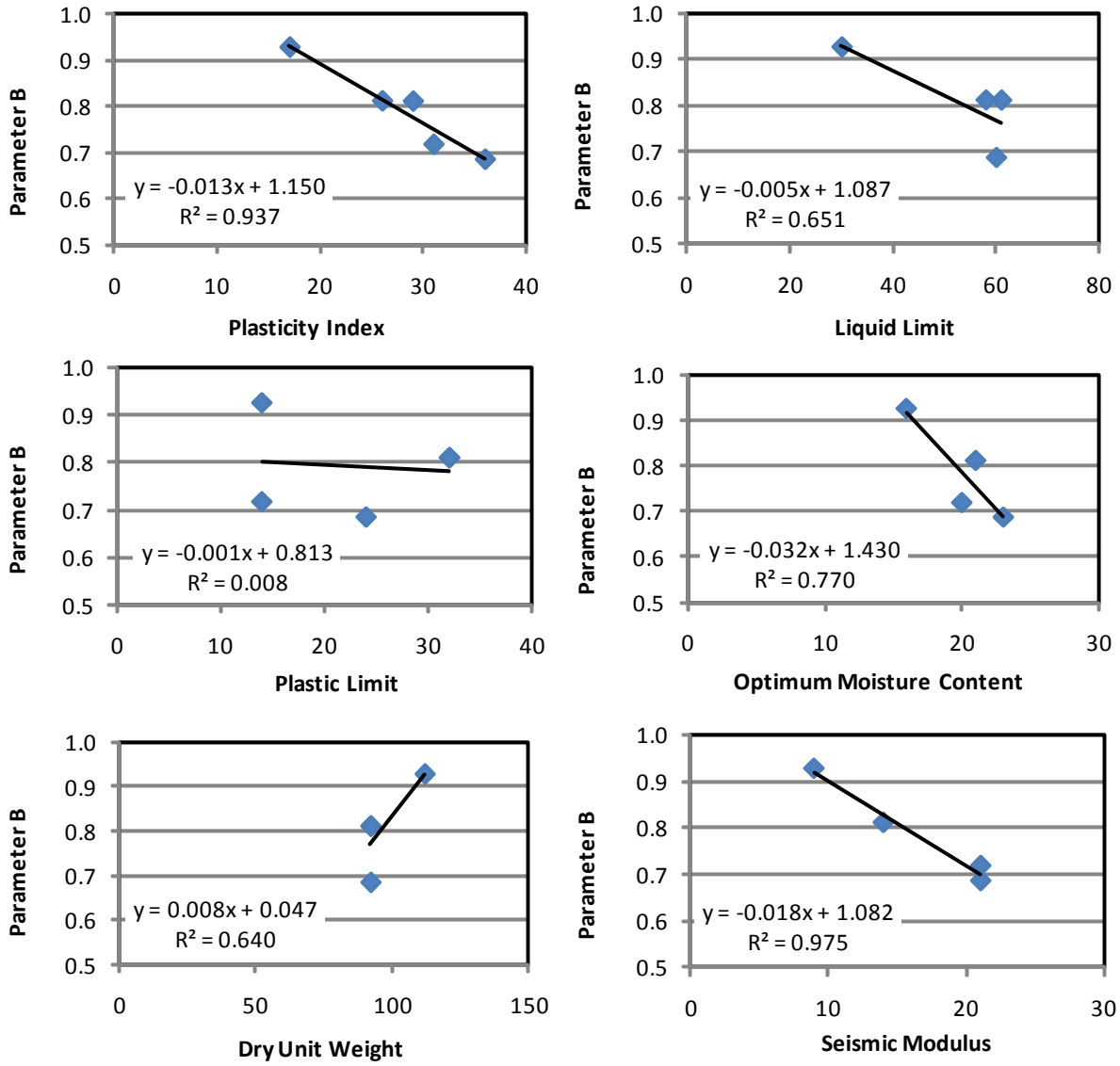

D.1: Correlations between Index Properties of Soils and Parameter B
(Lateral Strain, DFS Process)

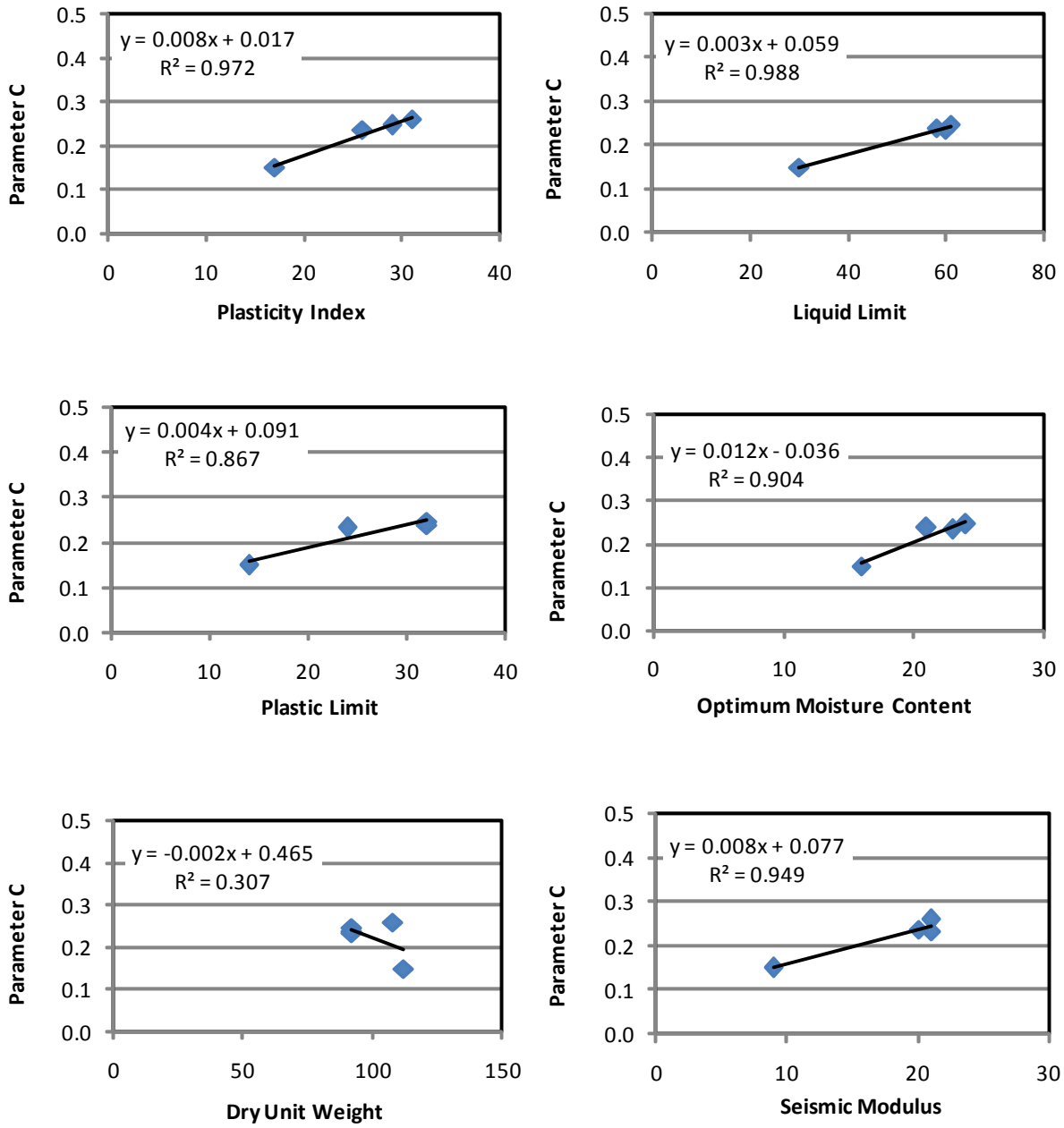

D.2: Correlations between Index Properties of Soils and Parameter C
(Vertical Strain, Combined DFO and SFO Process)

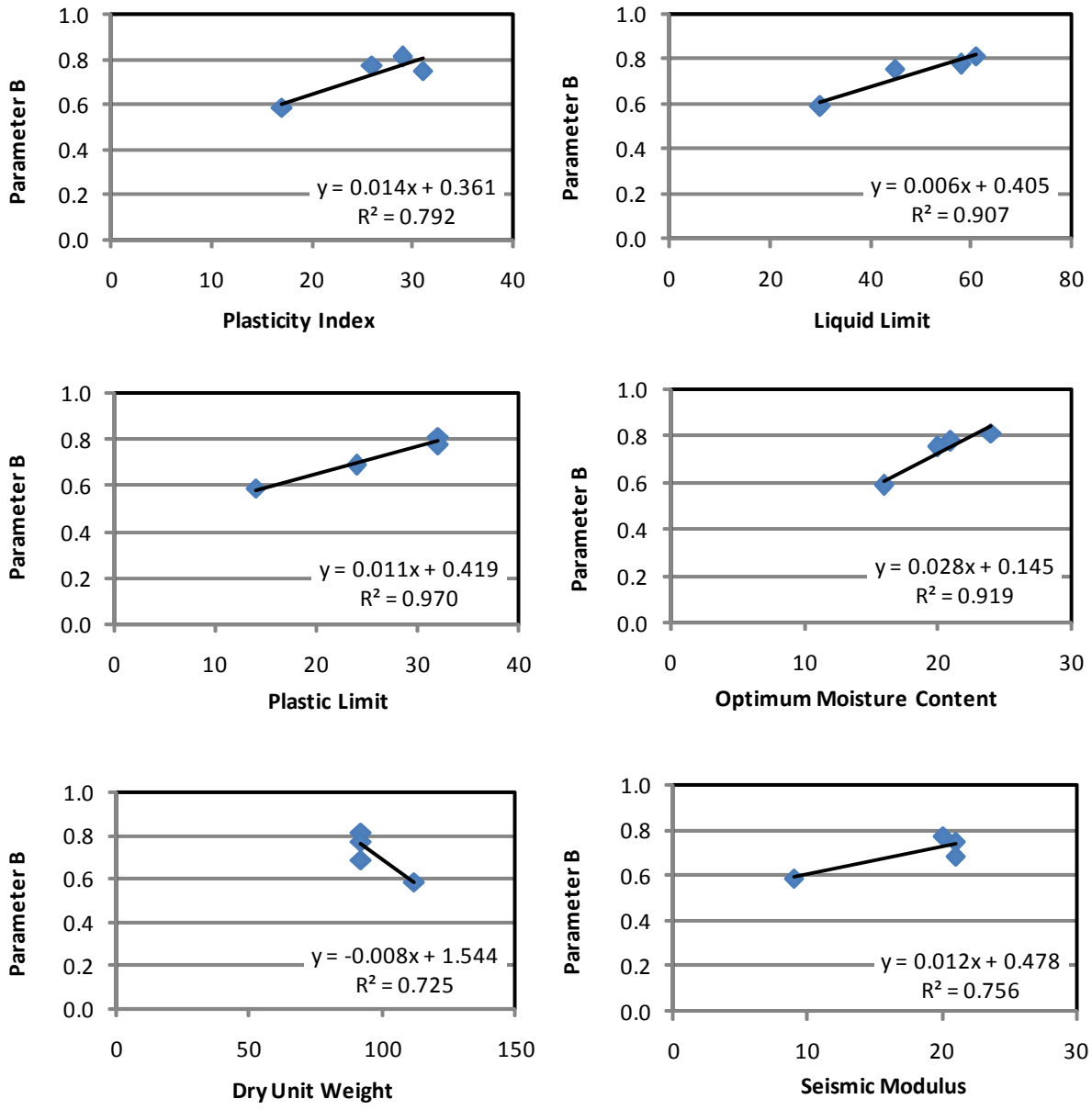

D.3: Correlations between Index Properties of Soils and Parameter B
(Vertical Strain, DFS Process)

APPENDIX E: SUMMARY OF FIT PARAMETERS AND INDEX PROPERTIES RELATIONSHIPS - MODULUS

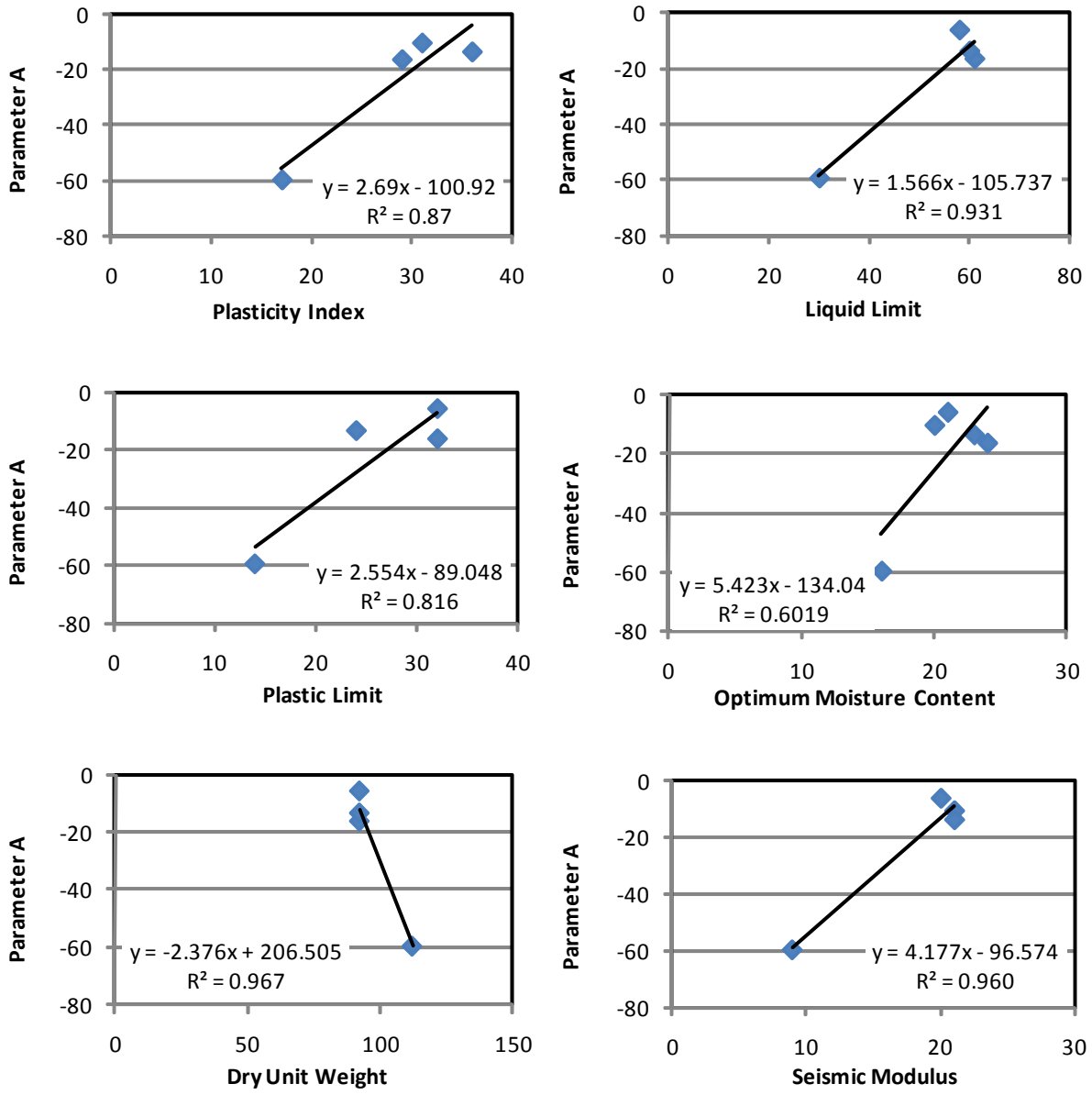

E.1: Correlations between Index Properties of Soils and Parameter A
(Modulus, Combined DFO and SFO Process)

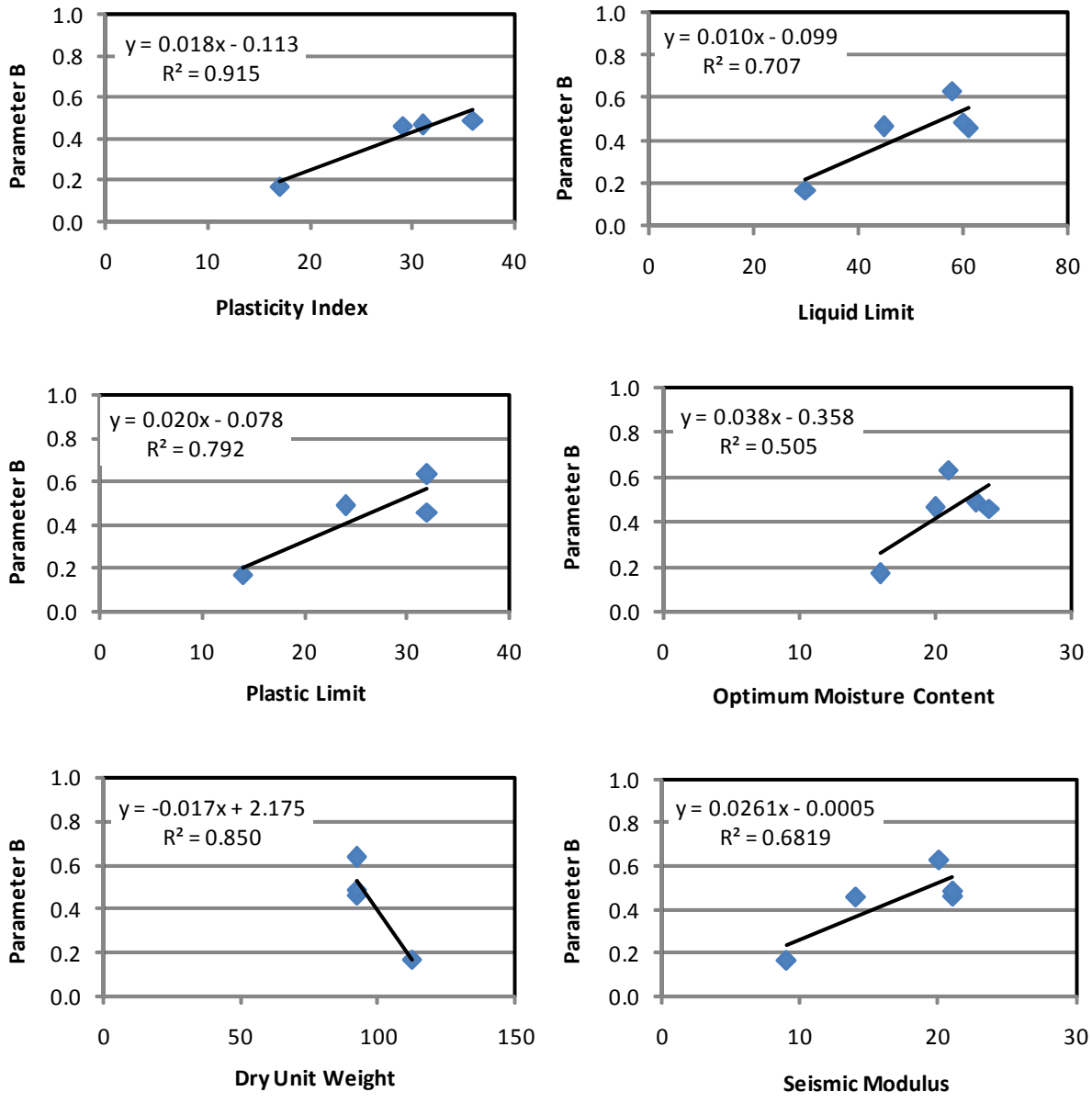

E.2: Correlations between Index Properties of Soils and Parameter B
(Modulus, Combined DFO and SFO Process)

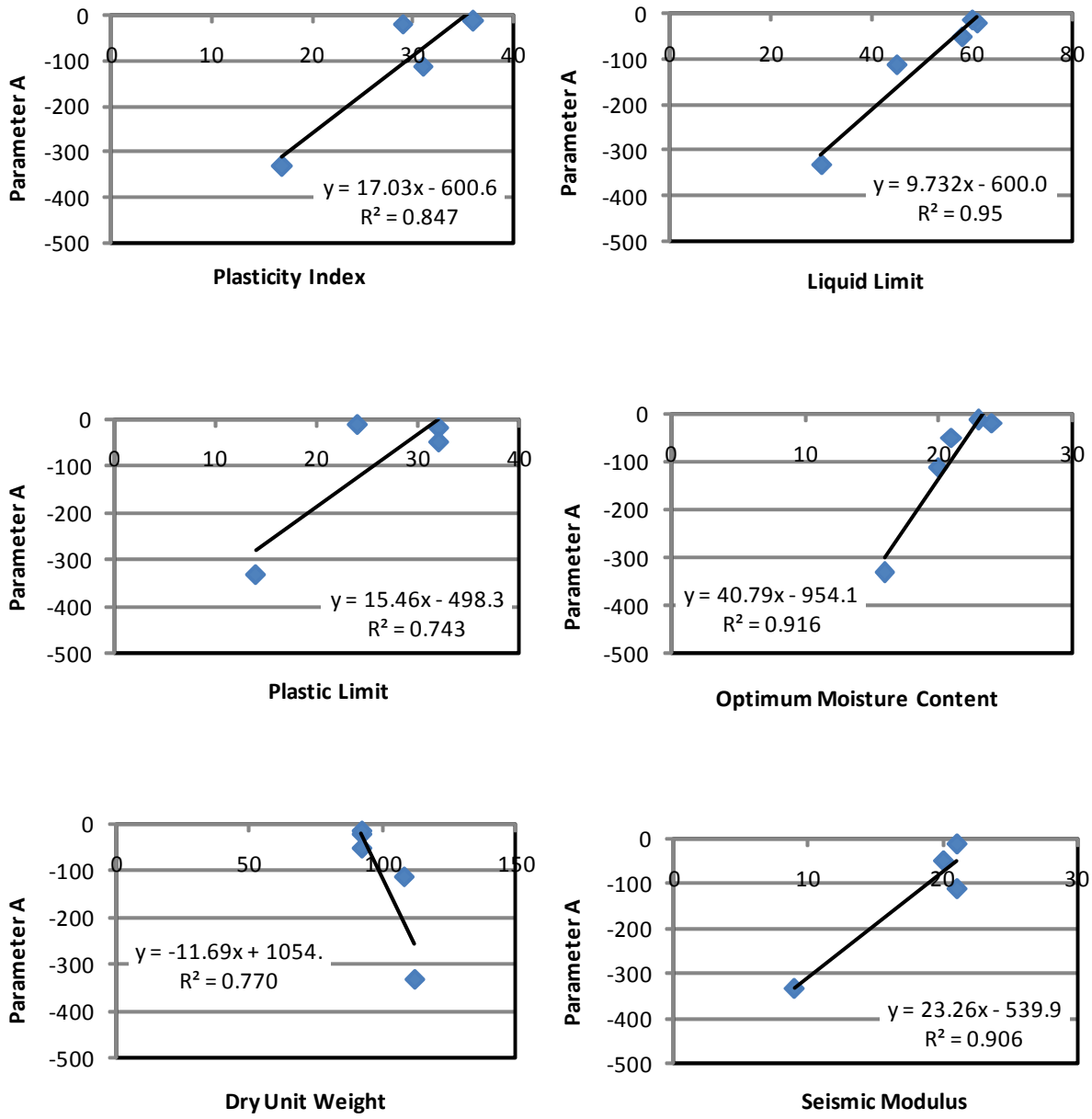

E.3: Correlations between Index Properties of Soils and Parameter A
(Modulus, DFS Process)

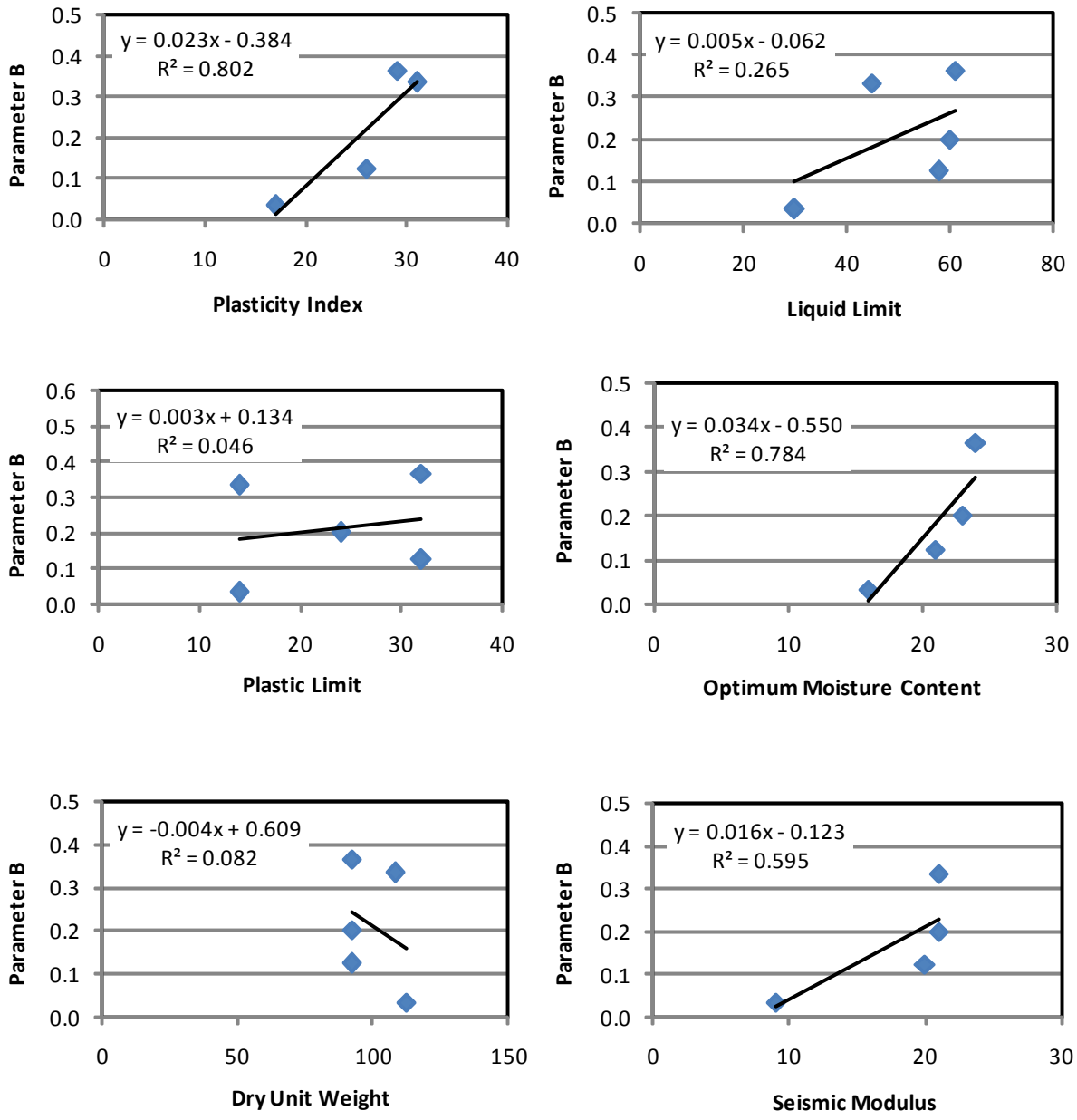

E.4: Correlations between Index Properties of Soils and Parameter B
(Modulus, DFS Process)

APPENDIX F: SUMMARY OF FIT PARAMETERS AND CHEMICAL-MINERALOGICAL PROPERTIES RELATIONSHIPS-STRAINS

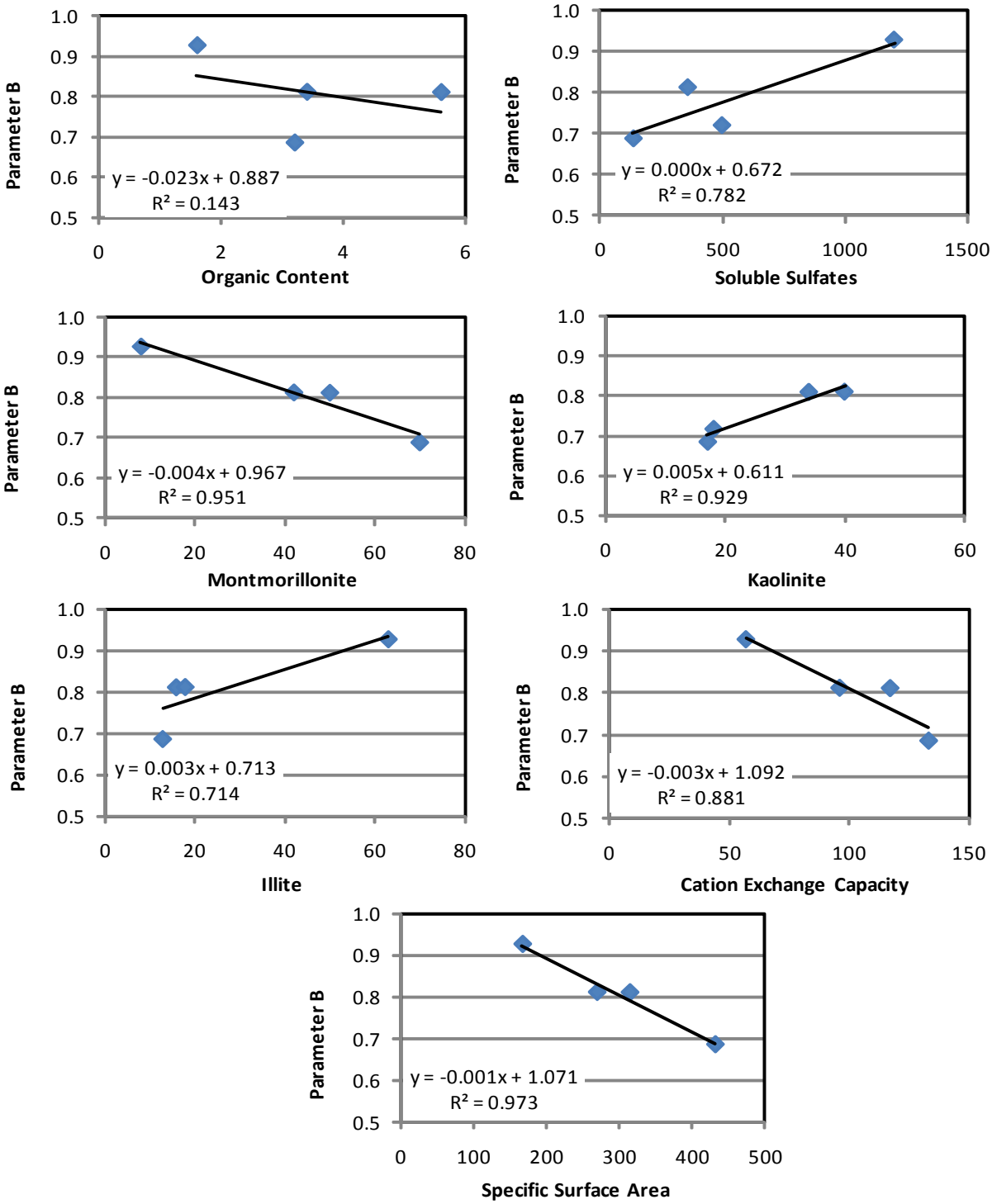

F.1 Correlations between Chemical-Mineralogical Properties and Parameter B (Lateral Strain, DFS Process)

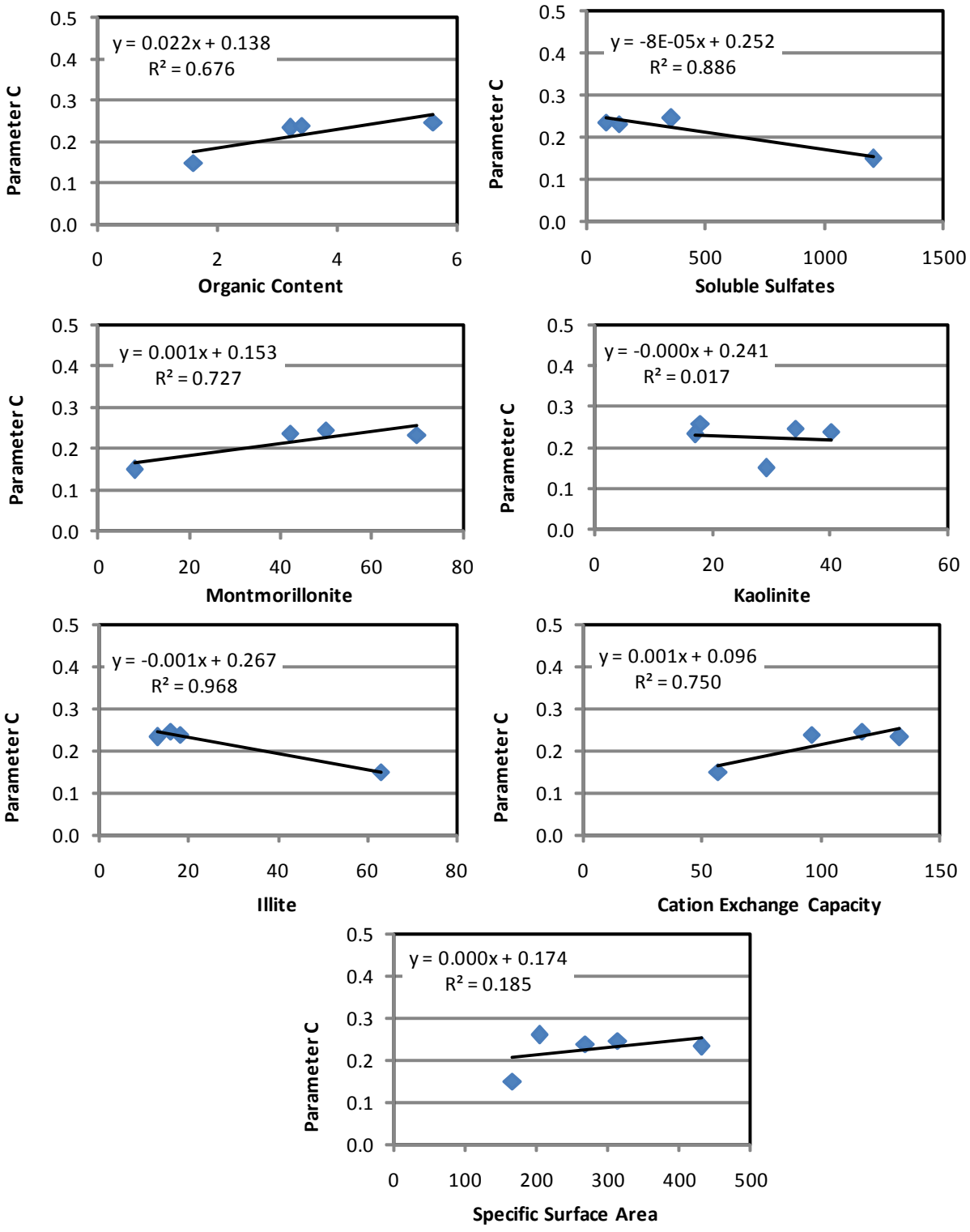

F.2: Correlations between Chemical-Mineralogical Properties and Parameter C (Vertical Strain, Combined DFO and SFO Process)

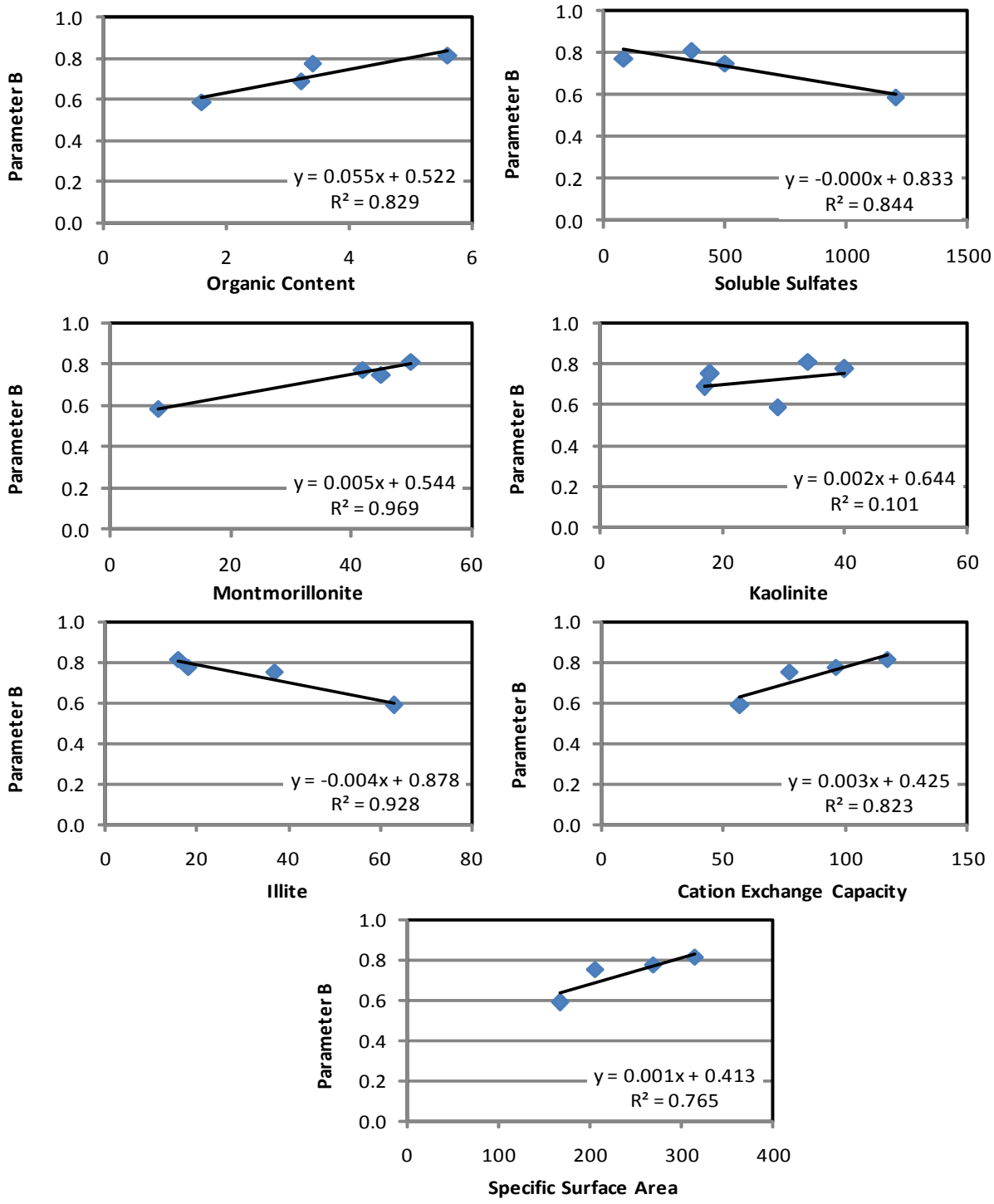

F.3: Correlations between Chemical-Mineralogical Properties of Soils and Parameter B (Vertical Strain, DFS Process)

APPENDIX G: SUMMARY OF FIT PARAMETERS AND CHEMICAL-MINERALOGICAL PROPERTIES RELATIONSHIPS - MODULUS

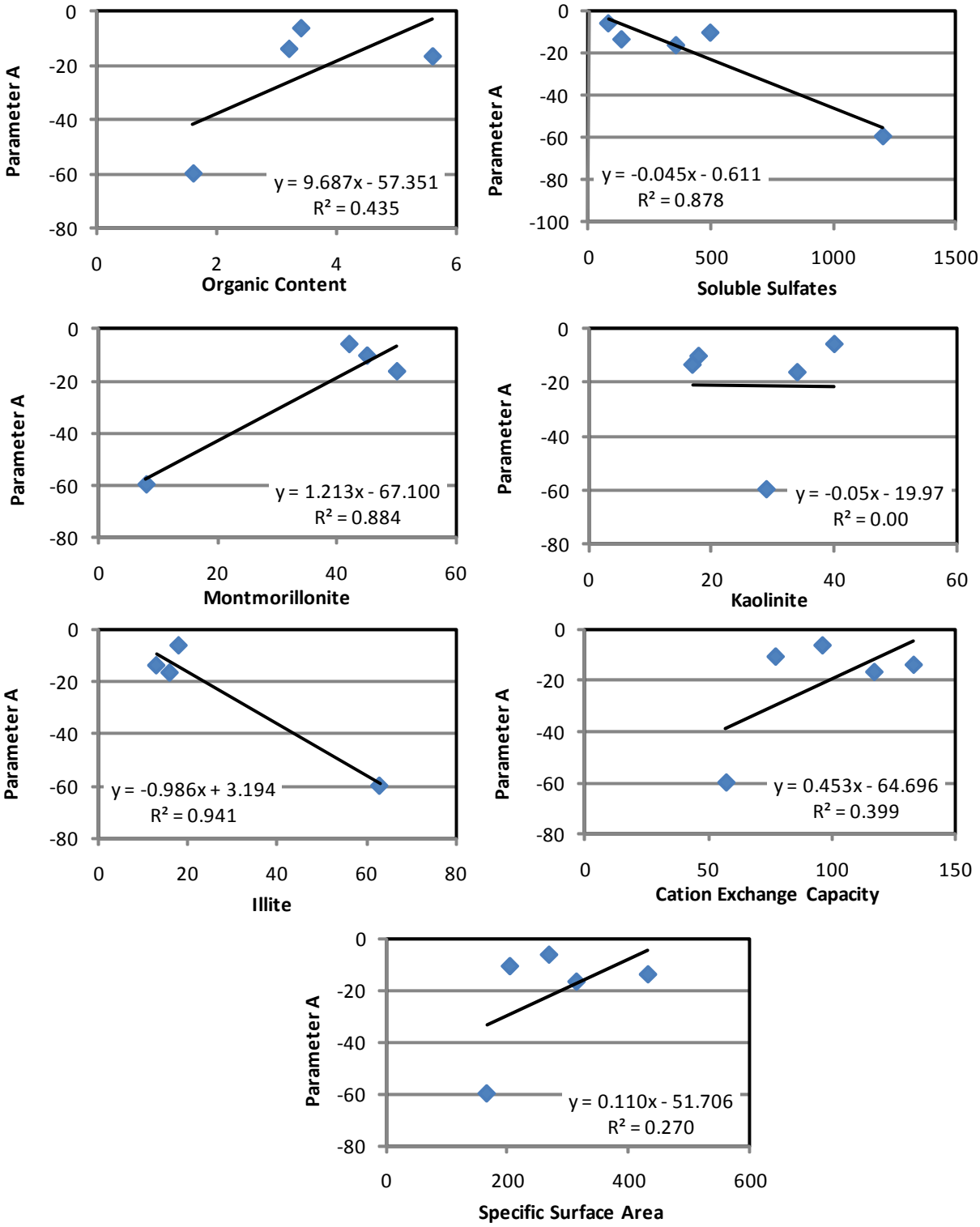

G.1: Correlations between Chemical-Mineralogical Properties of Soils and Parameter A (Modulus, Combined DFO and SFO Process)

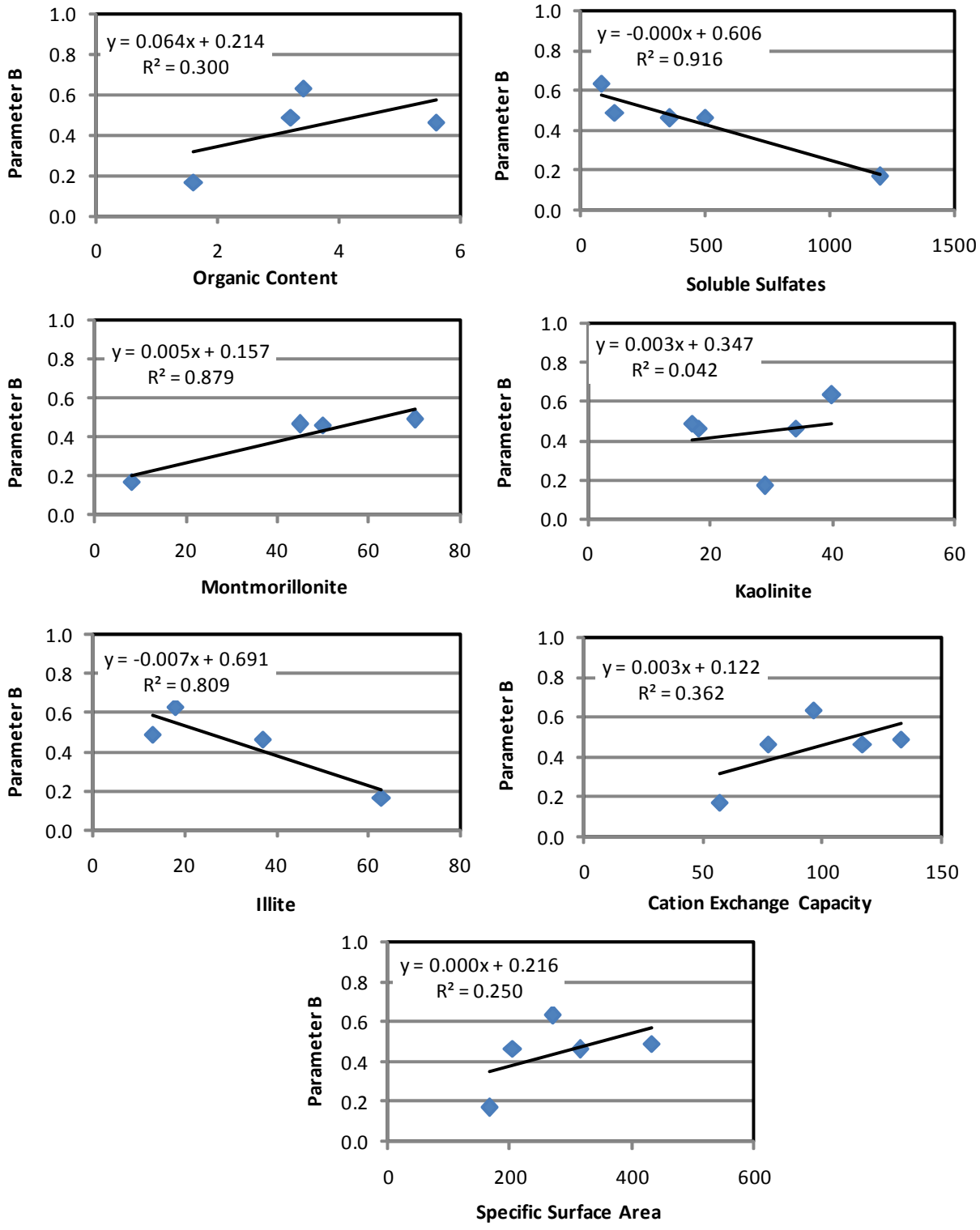

G.2: Correlations between Chemical-Mineralogical Properties and Parameter B (Modulus, Combined DFO and SFO Process)

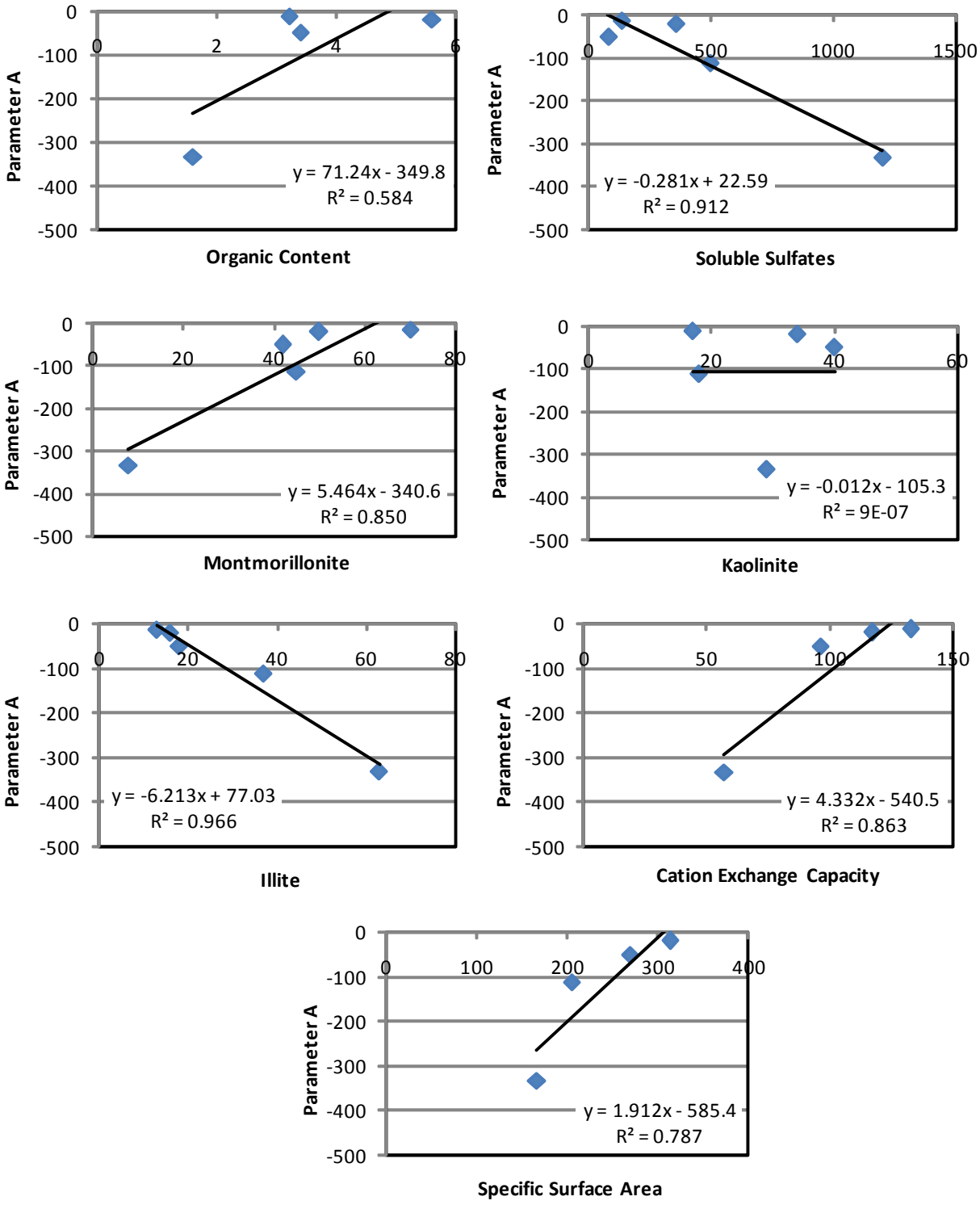

G.3: Correlations between Chemical-Mineralogical Properties and Parameter A (Modulus, DFS Process)

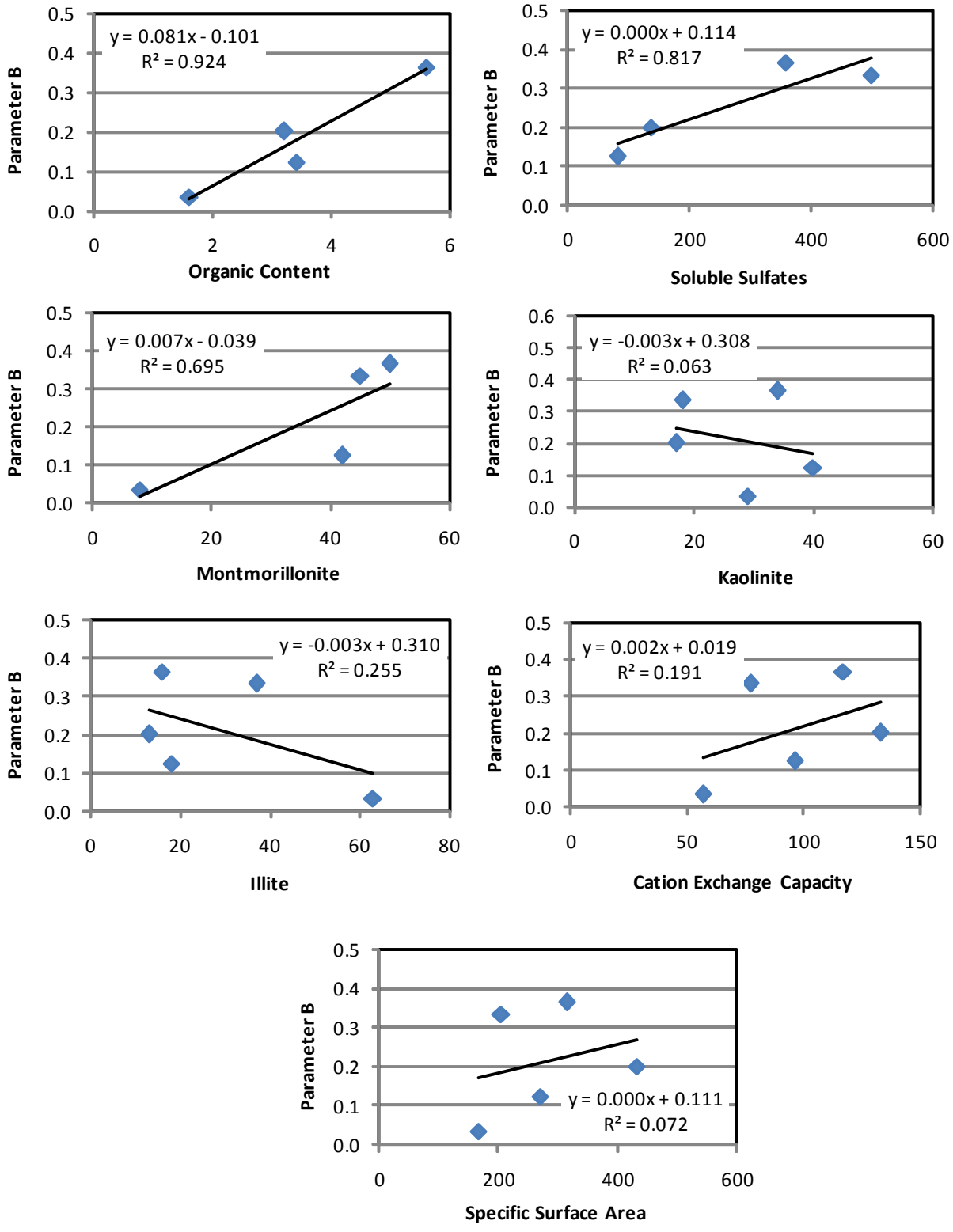

G.4: Correlations between Chemical-Mineralogical Properties and Parameter B (Modulus, DFS Process)

APPENDIX H: SUMMARY OF MINIMUM AND MAXIMUM STRAINS AND INDEX PROPERTIES RELATIONSHIPS

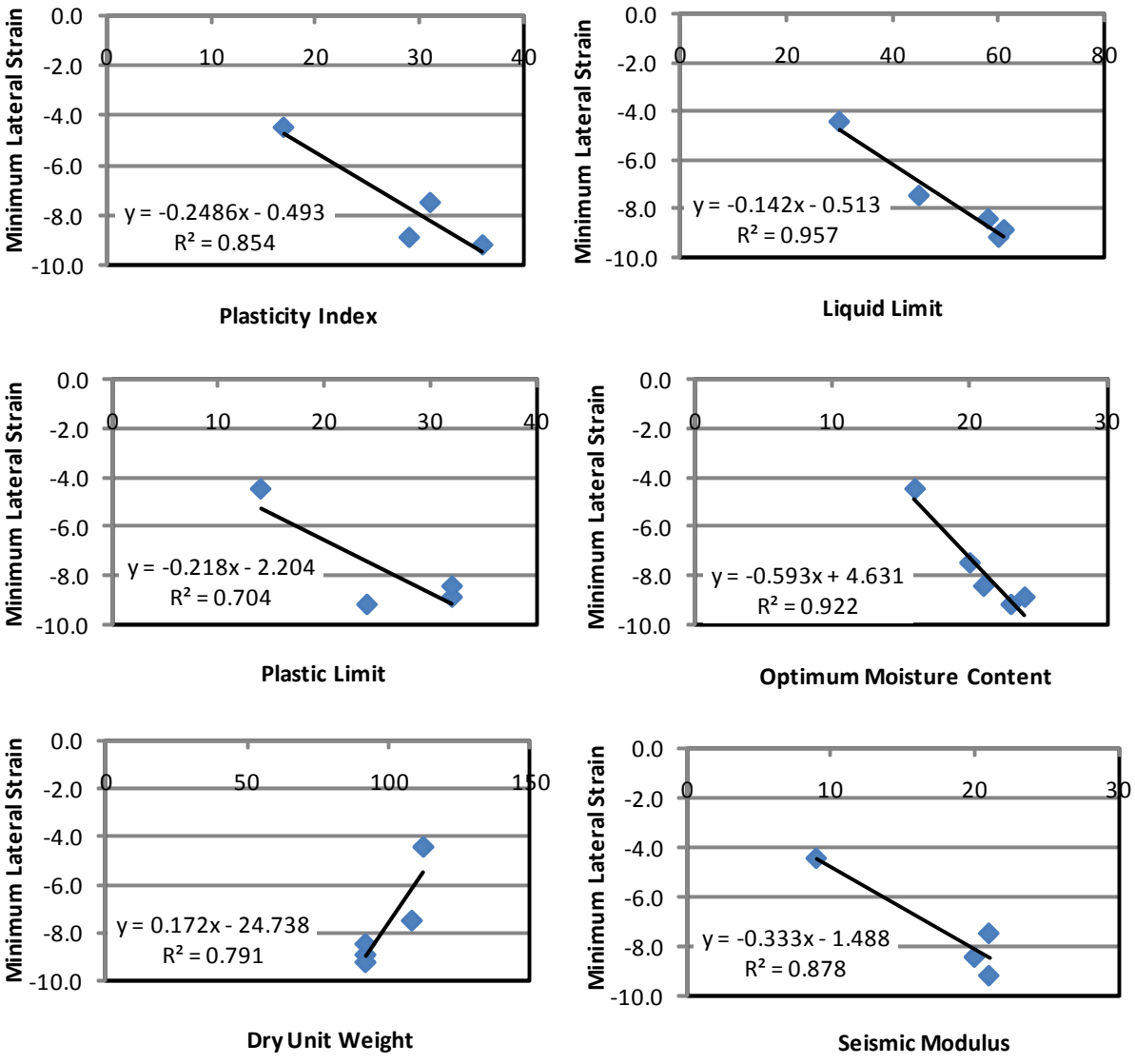

H.1: Summary of Correlations between Index Properties of Soils and Minimum Lateral Strain (DFS Process)

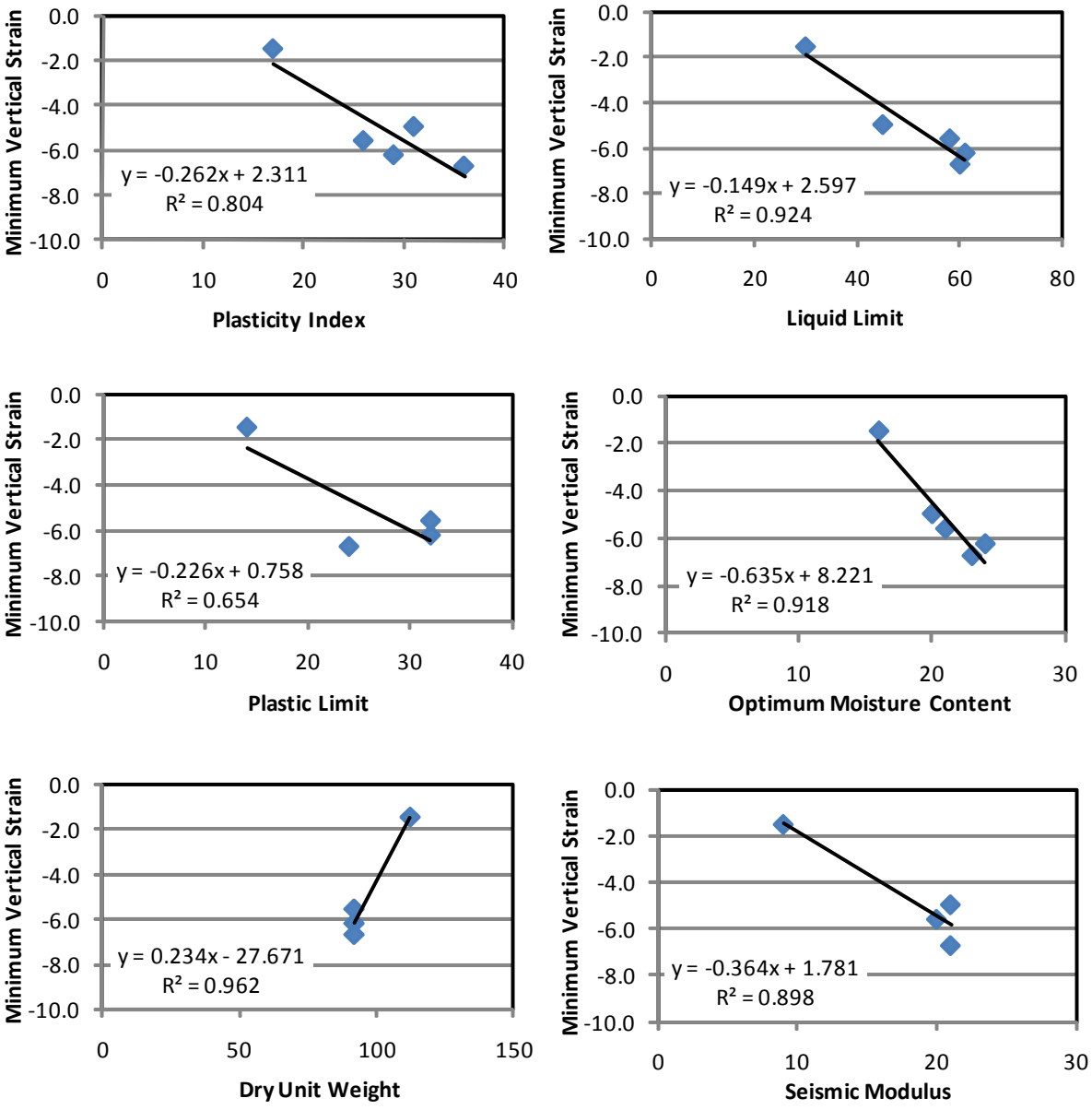

H.2: Summary of Correlations between Index Properties of Soils and Minimum Vertical Strain (Combined DFO and SFO Process)

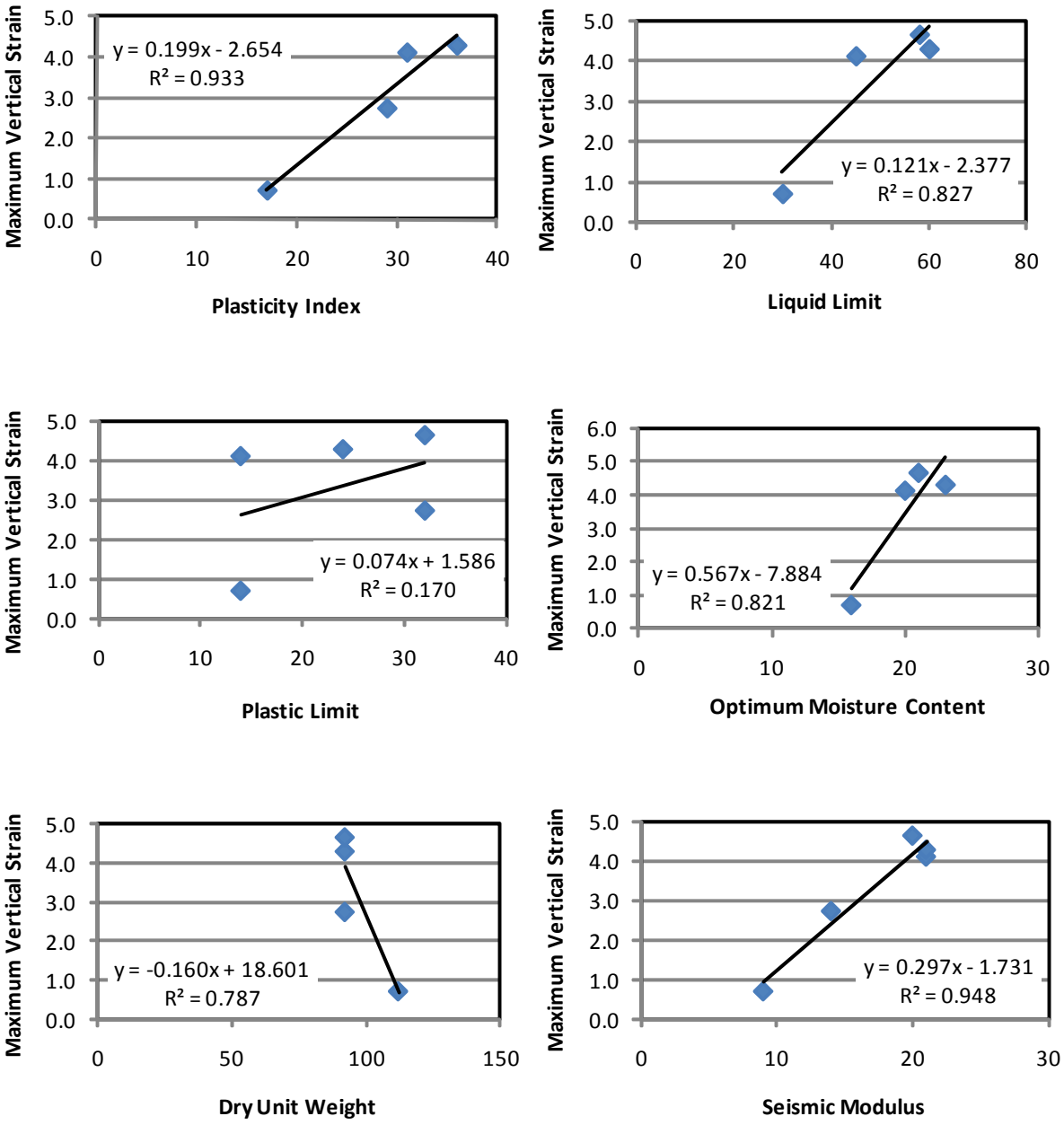

H.3: Summary of Correlations between Index Properties of Soils and Maximum Vertical Strain (Combined DFO and SFO Process, DFS Process)

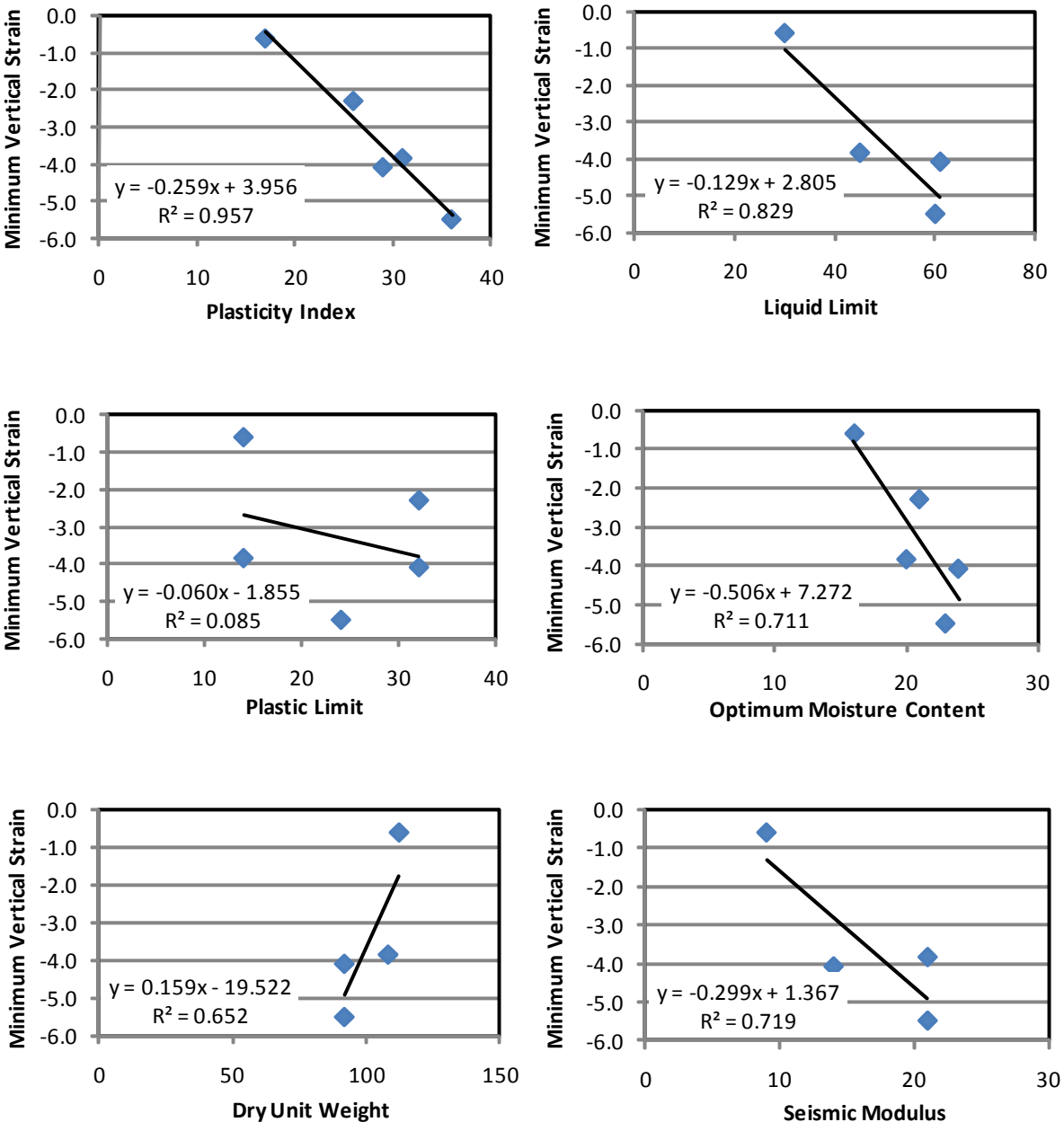

H.4: Summary of Correlations between Index Properties of Soils and Minimum Vertical Strain (DFS Process)

APPENDIX I: SUMMARY OF MINIMUM AND MAXIMUM STRAINS AND CHEMICAL-MINERALOGICAL PROPERTIES RELATIONSHIPS

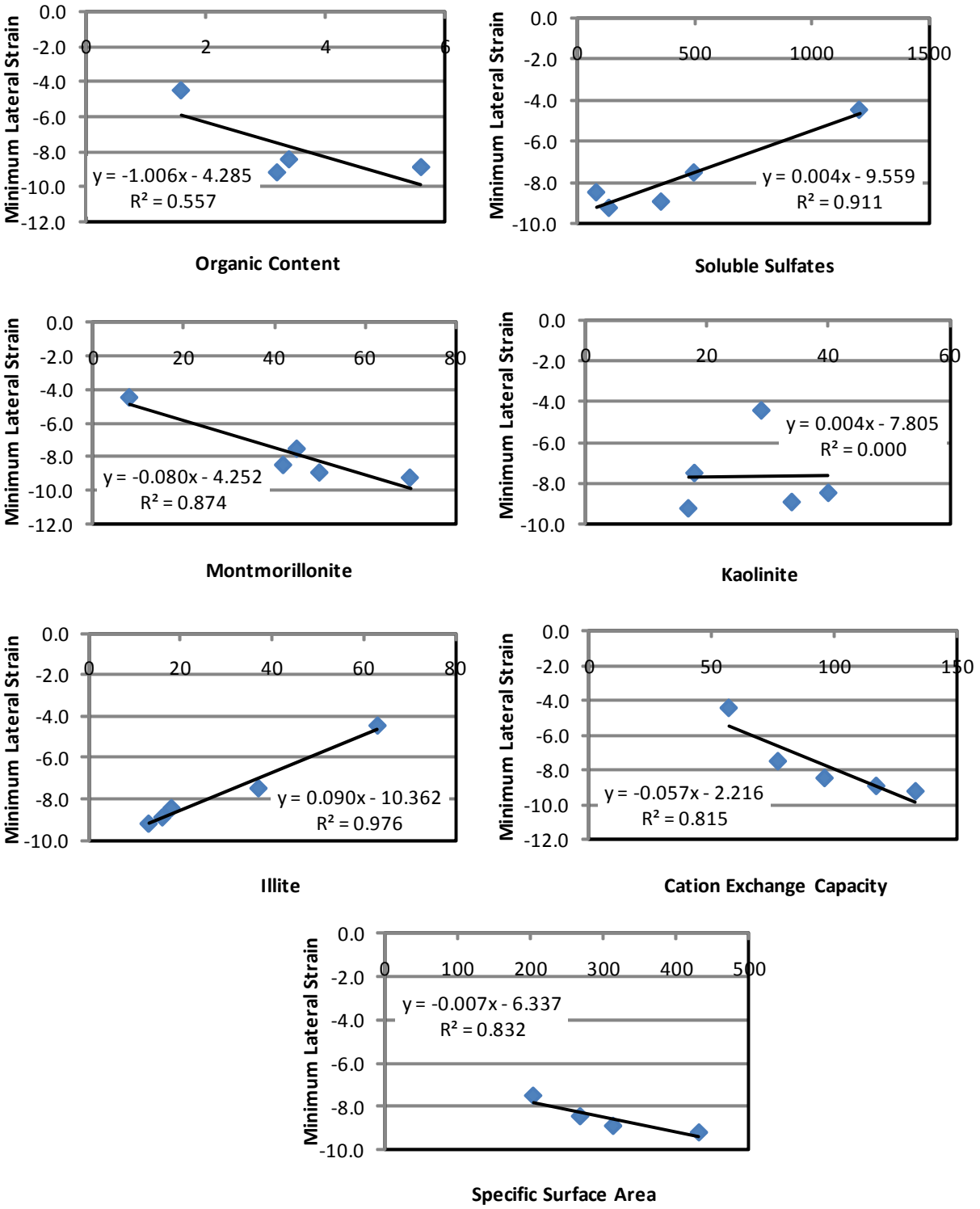

I.1: Summary of Correlations between Chemical-Mineralogical Properties and Minimum Strain (Lateral Strain, DFS Process)

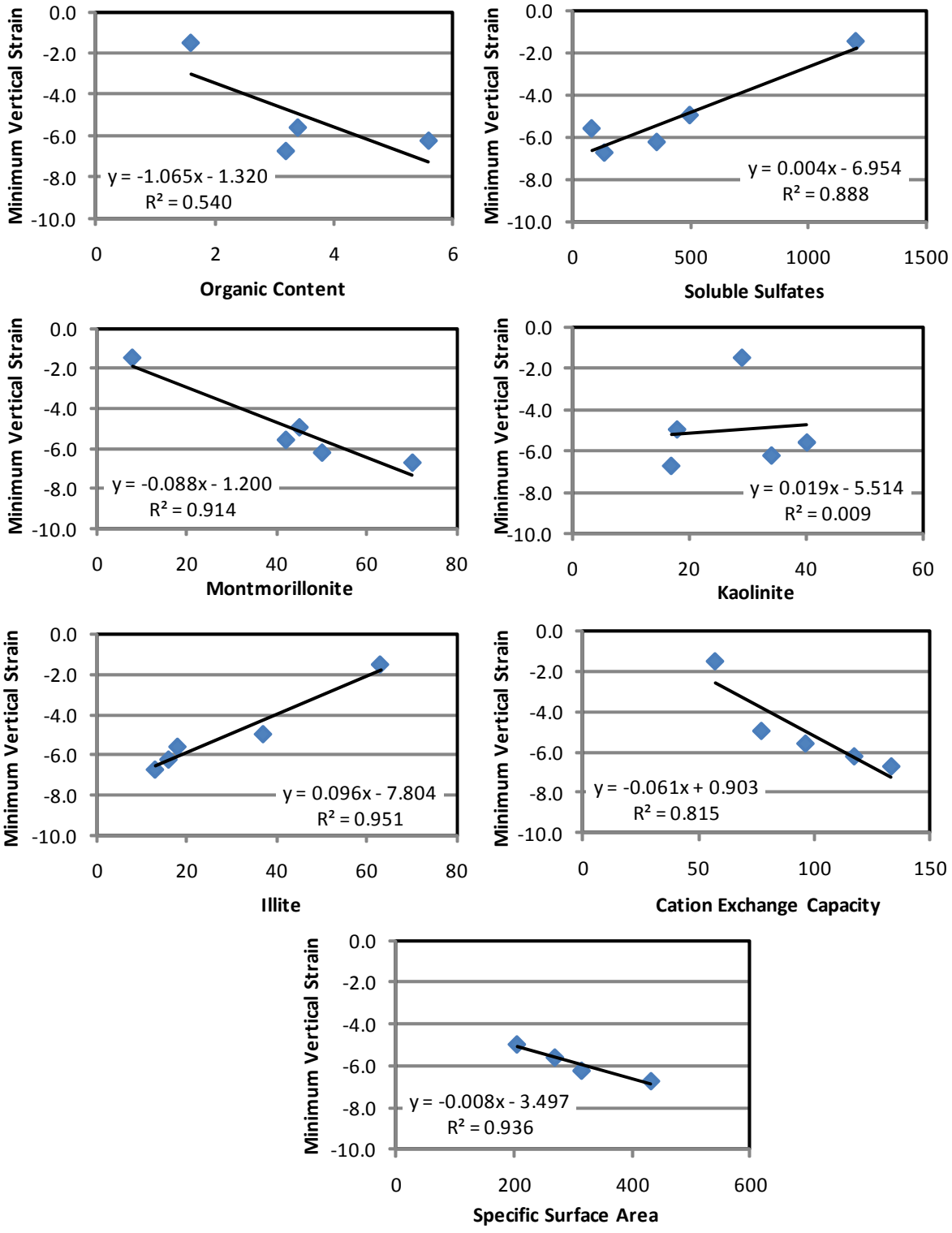

I.2: Summary of Correlations between Chemical-Mineralogical Properties and Minimum Vertical Strain (Combined DFO and SFO Process)

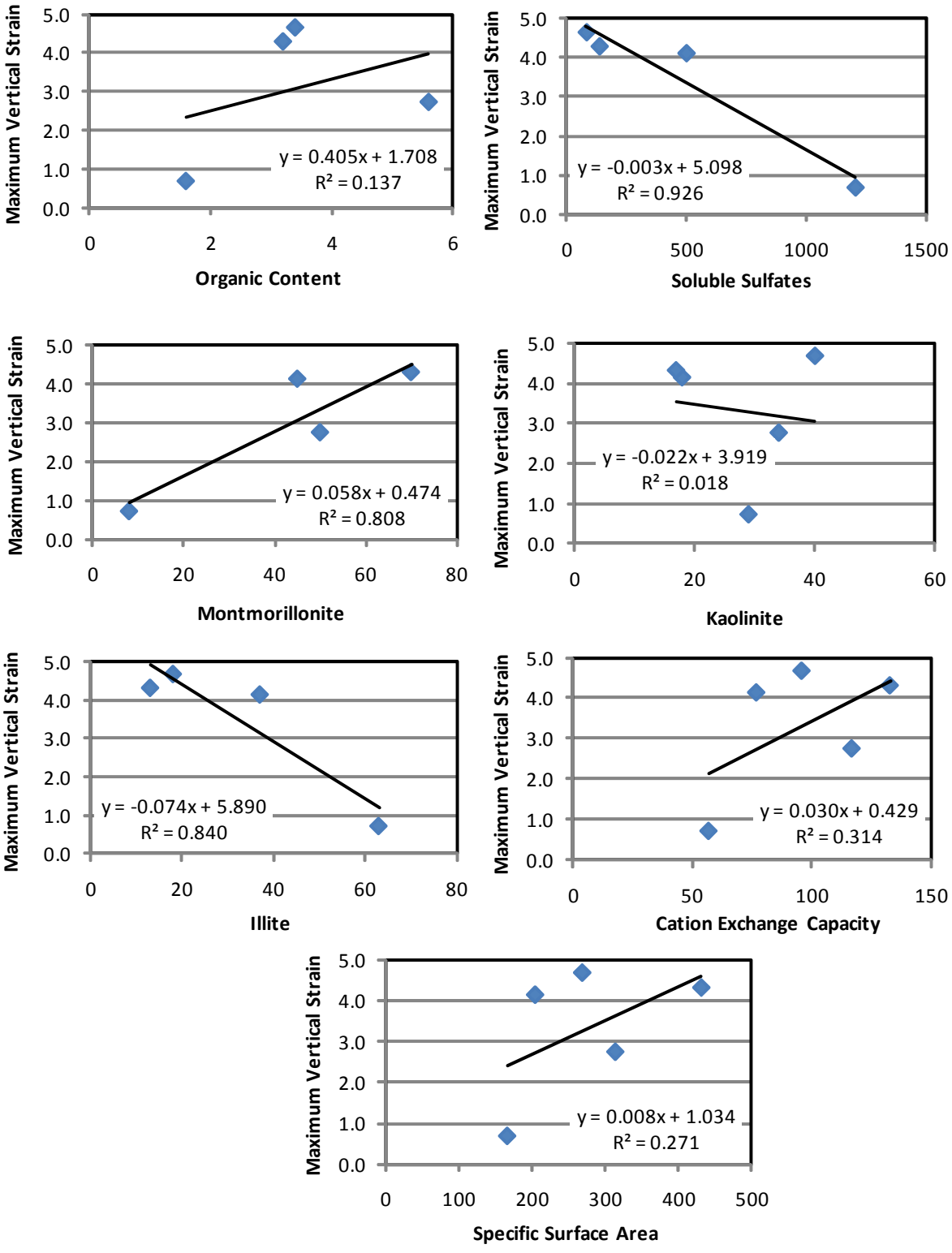

I.3: Summary of Correlations between Chemical-Mineralogical Properties and Maximum Vertical Strain (Combined DFO and SFO Process, DFS Process)

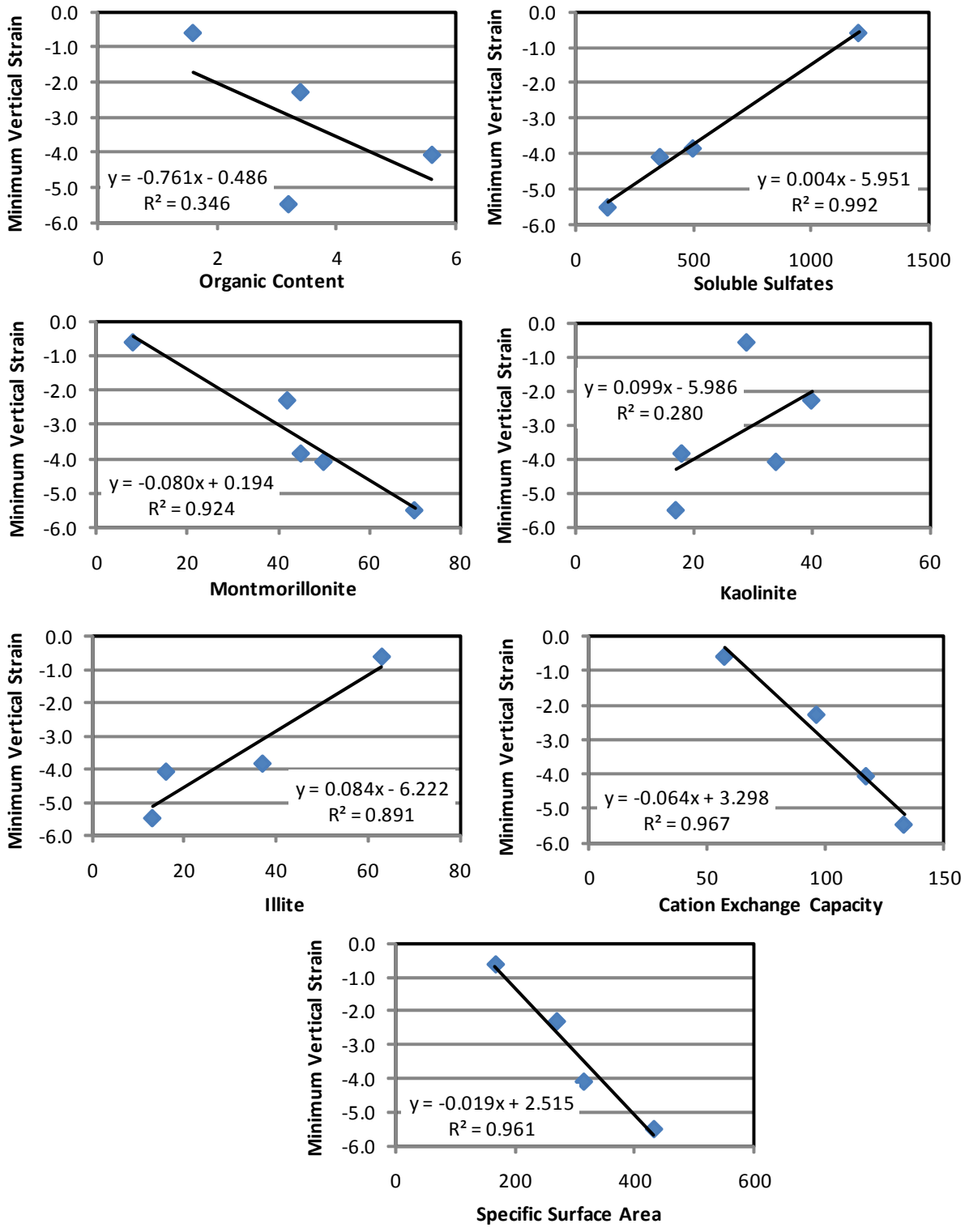

I.4: Summary of Correlations between Chemical-Mineralogical Properties and Minimum Vertical Strain (DFS Process)

VITA

Cynthia R. Zuniga was born in Cd. Juarez, Mexico. The third daughter of Jorge Zuniga and Yolanda Zuniga, she graduated from COBACH No. 5, Cd. Juarez, Mexico in the spring of 2000 and entered The University of Texas at El Paso in the fall of 2000. While pursuing a Bachelor's Degree in Civil Engineering, she worked at the Department of Political Sciences at the University of Texas at El Paso as an undergraduate research assistant, from 2001 to 2003. She later worked at White Sands Missile Range, White Sands, New Mexico, at the telemetry department, during the summer of 2003 and later worked at the Center for Transportation Infrastructure Systems (CTIS) from the fall of 2003 until receiving her Bachelor's of Science Degree from The University of Texas at El Paso in the spring of 2005. Immediately after receiving her Bachelor's Degree in the fall of 2005, she entered the Graduate School at The University of Texas at El Paso. While pursuing a Master's Degree in Civil Engineering, she worked with Professional Service Industries, Inc. (PSI) as a Graduate Engineer under the supervision of a Professional Engineer.

Permanent address: 10632-C Springwood Drive
El Paso, Texas 79935

This thesis was typed by Cynthia R. Zuniga